MANIPULATION OF ENDOGENOUS AND EXOGENOUS SOURCES OF CHOLESTEROL AND ITS EFFECTS ON BETA CELL FUNCTION

JOSEPH BACANI

A THESIS SUBMITTED TO

THE FACULTY OF GRADUATE STUDIES

IN PARTIAL FULFILLMENT OF THE REQUIREMENTS

FOR THE DEGREE OF

MASTER OF SCIENCE

GRADUATE PROGRAM IN BIOLOGY

YORK UNIVERSITY

TORONTO, ONTARIO

December 2013

Abstract

Type 2 diabetes mellitus (T2DM) prevalence continues to increase worldwide. Changes in β-cell function and mechanisms behind the aberrant insulin secretion found in T2DM patients are still poorly understood. Cholesterol is a vital molecule to all cellular systems, being an important factor regulating membrane fluidity and a number of signalling pathways. In this study, a series of experiments are conducted on the mouse insulinoma cell line, MIN6, limiting exogenous cholesterol through use of lipid free serum, as well as limiting endogenous cholesterol sources through the use of 3-hydroxy-3-methyl-glutaryl-CoA reductase and 7-dehydrocholesteral reductase inhibitors. The results show a marked decrease in both cholesterol content as well glucose stimulated insulin secretion in the drug-treated groups. A series of promoter assays, RT-PCR experiments and western blot analysis determined disruption in site-directed surface expression of important channel proteins involved in insulin secretion, and potentially a change in insulin degradation enzyme activity.

Acknowledgements

I would like to thank everyone who has supported me throughout my master's education, from my first day at orientation to the day of my defense. My family, close friends, and colleagues, all of them have made the journey not only one of academic growth, but personal growth as well. There are specific persons in the lab I would like to acknowledge for their contributions. Xiaodong Gao, our lab technician, has always gone well above expectations in the help she provides for each and every single student that enters the lab. Her patience and dedication to enriching all of our experiences is truly amazing. Adrian Kerr and Jagdeep Jassi, and Amir Koldorf, fellow master's students I have known since my first day in the lab have provided me with unforgettable advice, company, and comic relief. They played no small role in my ability to succeed, as they helped me when things were tough, in both my research and personal life. The undergraduate students I have taught have also had a very positive impact in my life. Steven Tran and Piru Parampalam have both been very important components to my research. Whether it was helping with western blots or patch-clamping, their company always made time fly and allowed me to get through many, many days of long hours in the lab. The newest students in the lab have also left an impression on me, Nikki and Andy, both of whom I'll never forget (for different reasons). Last, but not least, I would like to thank my mentor, supervisor, and guide throughout this long and arduous process. Dr. Robert Tsushima has been an incredible force in my life, extending advice not only to research, but also to personal life. His empathy, understanding, and consideration for each individual's unique situations and his unrelenting efforts to make sure all his students succeed in life, is truly awe-inspiring. There are so many things I've learned from him that the list might extend as long as this thesis itself. Without all these peoples' contributions I can confidently say I would not be where I am now in life, and I will always remember and cherish each and every one of them.

Table of Contents

List of Figures

List of Abbreviations

$[Ca^{2+}]_I$	intracellular concentration of Ca^{2+}
µg	microgram
µl	microliter
µM	micromolar
ABCA1	ATP-binding cassette transporter A1
ATP	adenosine triphosphate
BSA	bovine serum albumin
CDA	Canadian Diabetes Association
cDNA	complementary DNA
cAMP	cyclic adenosine monophosphate
Ca_V	voltage-gated Ca^{2+} channel
DMSO	dimethyl sulfoxide
FBS	fetal bovine serum
GK	glucokinase
GSIS	glucose-stimulated insulin secretion
HDL	high-density lipoproteins
HEPES	4-(-hydroxyethyl) piperazine-1-ethanesulfonic acid
HMG-CoA	3-hydroxy-3-methylglutaryl CoA
IR	insulin receptor
K_{ATP}	ATP-sensitive K^+ channel
KRB	Krebs-Ringer bicarbonate
K_V	voltage-dependent K^+ channel
LDL	low-density lipoprotein
LPS	lipid depleted serum
LXR	liver X receptor
mL	millilitre
µL	microlitre
mM	millimolar

mRNA	messenger RNA
ms	milliseconds
mV	millivolts
Na_V	voltage gated Na^+ channel
ng	nanograms
nm	nanometer
PAGE	polyacrylamide gel electrophoresis
PBS	phosphate buffered saline
PCR	polymerase chain reaction
RP	reserve pool
RRP	readily releasable pool
RT-PCR	reverse-transcriptase polymerase chain reaction
SNAP-25	synaptosomal-associated protein of 25 kilodaltons
SNARE	soluble N-ethylmaleimide-sensitive factor attachment protein receptor
SQS	squalene synthase
SREBP	SRE binding protein
SUR	sulphonylurea receptor
STX-1A	syntaxin 1A
t-SNARE	target-SNARE
TGN	trans-Golgi network
V	voltage
v-SNARE	vesicle-SNARE
VAMP	vesicle-associated membrane protein

1.0 Introduction

1.1 Diabetes Mellitus

Diabetes mellitus is a group of metabolic diseases that has shown a steady, and alarming, increase in prevalence over the past few years. In 2000 there was an estimated 171 million incidences of diabetes worldwide, and in 2011, the number almost doubled to 336 million cases (International Diabetes Federation, 2012; Diabetes Care, 2004). This growing pandemic has been closely linked to changes in lifestyle and the trend of increasing obesity in more developed countries. In North America alone, it is estimated that a child born in 2000 stands a one in three chance of being diagnosed with diabetes at some point within his or her lifespan (Canadian Diabetes Association, 2012). Diabetes mellitus comes in varying degrees of severity but is always characterized by chronic hyperglycemia and some sort of dysfunction in the pancreas. This disease comes in several forms, the two most common being type 1 (T1DM) and type 2 diabetes mellitus (T2DM), with gestational (GDM) being a fairly rare third type of diabetes mellitus, and finally monogenic/miscellaneous diabetes being the last and very uncommon 'form' of diabetes mellitus. As previously mentioned, the pathogenesis of diabetes mellitus is thought to revolve around the pancreas, specifically the islets found within the organ. The islets are comprised of a number of cells, but the focus of study has always been on the functionality of the β-cell, which is largely responsible for systemic fuel homeostasis (Ismail-Beigi, 2012; Ashcroft and Rorsman, 2012; Seino *et al*., 2011). As seen in figure 1, β-cells produce and secrete a hormone called insulin into the vascular system, which then helps to regulate blood-glucose levels. Diabetes arises at some point on this physiological control system, be it at the start (within the β-cells and pancreas), during delivery (within the vascular system), or in the uptake of the hormone (peripheral tissue resistance).

The current criteria for diagnosis revolve around the measurement of glycated hemoglobin in a patient's blood. Elevated glycated hemoglobin, or HbA_{1c} for short (typically termed A1C), is symptomatic of a diabetic condition. A1C values greater than 6.5% in the blood constitutes a patient with diabetes, and how chronically elevated it is will determine how aggressive a treatment regimen will be. The four types of diabetes mellitus will now be more thoroughly described.

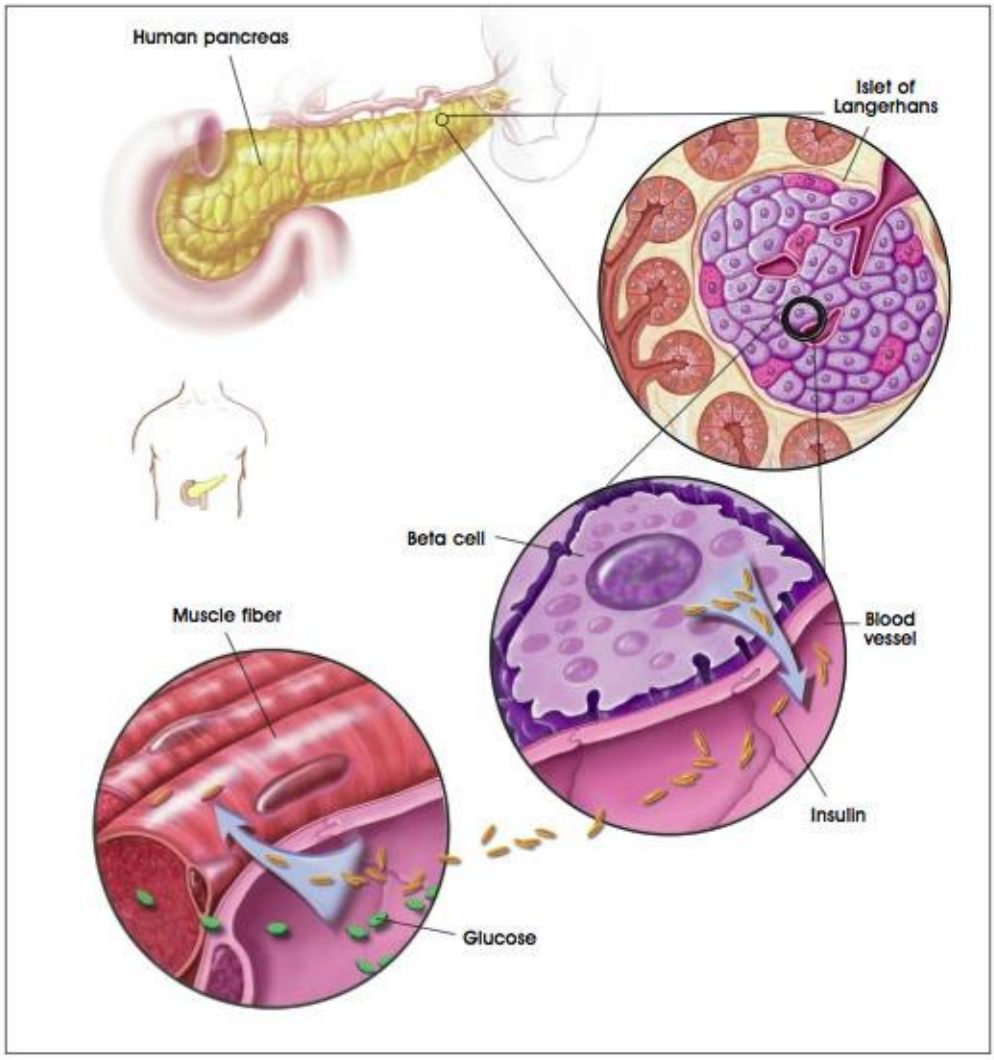

Figure 1. Insulin production and secretion from pancreatic β-cells. A simplified image showing the pancreas as well as organization of the β-cell containing islets of Langerhans. The islets are organized in small clusters, highly vascularized and distributed throughout the pancreas. As seen in the above image, β-cells secret insulin directly into blood vessels which then reach peripheral organs and tissues, such as the depicted muscle fiber. In healthy pancreases, this is done in response to elevated glucose in the circulatory system

Reprinted from National Institutes of Health, by T. Winslow, L. Kibuik, 2014, Retrieved from http://stemcells.nih.gov/info/scireport/pages/chapter7.aspx. ©2001. Reprinted with permission.

1.1.1 Type 1 diabetes mellitus

T1DM is the result of an autoimmune disorder that targets pancreatic β-cells leading to insufficient insulin synthesis and severely impaired glucose uptake by peripheral tissues (Rother, 2007). This form of diabetes mellitus accounts for approximately 5-10% of all cases of diabetes and is often developed during early childhood until about mid-adulthood. The high prevalence in pre-adult patients was the reason why T1DM was originally termed 'juvenile diabetes' (Ashcroft and Rorsman, 2012). As a result of the lack of insulin synthesis occurring in T1DM patients, the most common mode of treatment was by insulin injection, inhalation, or with the use of insulin pumps. Current technology has changed T1DM from being categorized as a fatal disease, to one where the patient can live a fairly normal life, as long as glucose levels were managed throughout the day with controlled administrations of insulin. Constant monitoring of A1C levels as well as diet and lifestyle changes, however, are still required to maintain a patient's health.

1.1.2 Type 2 diabetes mellitus

T2DM conversely, accounts for the vast majority of all diabetes cases, being exhibited in approximately 90% of all persons affected by this disease. It develops between early and late adulthood, and a large number of factors determine its onset. The cause of this form of diabetes mellitus is not due to a body's immune response to its own β-cells, but instead largely because of insulin resistance in peripheral tissues (Rother, 2007). Its higher incidence in adult patients as well as the presence of seemingly normal β-cell activity, gave this type of diabetes the names 'adult-onset diabetes' or 'non-insulin-dependent diabetes'. However, since those names were first coined, multiple advancements have been made that slightly disagree with them. Current research has found that T2DM often

manifests years before diagnosis, and there is now an emerging consensus that type 2 diabetes is a multifactorial disease, involving environmental, lifestyle, and perinatal risk factors, as well as genetic predisposition (DeFronzo and Abdul-Ghani, 2011; Portha *et al*., 2011; Rother, 2007). Additionally, there has been accumulating evidence that impaired insulin release may in fact play a large role in this disease's development, suggesting the possibility that β-cell dysfunction may precede the disease as opposed to being a result of it (Ashcroft and Rorsman, 2012). However, how the interaction between impaired β-cell activity and peripheral insulin resistance works, is still not fully understood. Additionally, the way we perceive the disease has also evolved, especially considering the fact that within recent years, many genes have been identified that significantly increase the risk of T2DM development. It has come to the point that many can regard T2DM as a "polygenic" type of diabetes with environmental factors that also play a significant role. Currently, there are more than forty genes identified that show some level of correlation with T2DM onset and susceptibility, the majority of which are important to insulin synthesis, secretion, and β-cell function (Bonne-fond *et al*., 2010).

Another significant advancement in the T2DM research front has been the growing trend of current treatment regimens becoming progressively specific for each unique case, as individual patient responses can vary greatly depending on the cause of their T2DM onset. Treatments range from a wide array of orally ingested drugs, depending on patient conditions (i.e. statins, metformin, sulphonylurea drugs, beta-blockers, aspirin therapy etc.), medical nutrition therapy (controlled diet with restricted caloric and fat intake as well as carbohydrate consumption), increased physical activity and exercise, and in some extraneous cases, even bariatric surgery (Ashcroft and Rorsman, 2012; Diabetes Care, 2010; Buchwald *et al*., 2009). Although this thesis will not focus on T2DM therapy, the aforementioned treatments will be explained in further detail in section 1.2.

1.1.3 Gestational diabetes mellitus

Another, and fairly uncommon, type of diabetes is gestational diabetes mellitus (GDM). This type of diabetes mellitus develops when hyperglycemia occurs in women who are pregnant as a result of hormonal changes leading to decreased insulin sensitivity. Often the symptoms of elevated blood sugar levels subside upon giving birth, but women diagnosed with GDM remain at increased risk of developing T2DM within the following five to ten years (Portha *et al*., 2011). Thus, patients with GDM are closely monitored for several months after giving birth. The treatment approach to GDM is fairly standard and consists of blood glucose control and a combination of exercise and diet restrictions to hit target A1C levels. The target A1C for most pregnant women is about 6.0%. However, despite successfully controlling GDM, multiple birth giving issues may still arise. The baby may often be much larger than normal and might require a caesarean as opposed to traditional birthing methods. Additionally, the newborn baby often suffers from hypoglycemia and hyperinsulinemia, so these conditions must be taken into account during GDM treatment and birthing (Canadian Diabetes Association, 2012). There have been some correlational studies linking GDM and a positive family history, as well as incidences of GDM in families with multiple T2DM cases. However, why and how GDM develops is still largely unpredictable and not well understood.

1.1.4 Monogenic and miscellaneous diabetes

There remain a few other types of diabetes mellitus, but these are very uncommon and are often associated with genetic defects, other diseases and infections. Thus they are typically grouped into a ‘fourth’ type of diabetes mellitus (Public Health Agency of Canada, 2011). A large number of monogenic diabetes types have already been identified through genetic studies, with over forty genes

catalogued to date (Smith *et al*., 2010; Stoy *et al*., 2010; Temple and Shield, 2010; Flanagan *et al*., 2009; Osbak *et al*., 2009). Some monogenic forms of diabetes mellitus have actually been previously misdiagnosed as T2DM or T1DM, for example maturity-onset diabetes of the young (MODY) and neonatal diabetes (ND). MODY is most commonly caused by mutations in the *HNF1A* gene or the *GCK* gene, which code for a transcription factor homeobox and the enzyme glucokinase, respectively. It has been erroneously diagnosed as T1DM in the past, and it was not until more recent research revealed that the causes were quite different. ND, on the other hand, is characterized by gain of function mutations in genes coding for the ATP-sensitive potassium- channel, which greatly reduced depolarization probability of β-cells. In the past, it was also often misdiagnosed, but as T1DM. With advancements in research and technology as well as a greater understanding of diabetes mellitus, it was later distinguished from T1DM since no anti-β-cell antibodies were found in patients with ND. Some viruses also have the ability to cause diabetes through auto-reactivity. The coxsackie virus is one example, and infection leads to insulin-dependent diabetes mellitus (Horwitz *et al*., 1998). After entry and inflammation of wounds, the coxsackie virus can cause an auto-immune response to islet cells within the patient's body. These are just some examples of monogenic and miscellaneous diabetes, and since the main focus of my research is specifically T2DM and how cholesterol acts in the development of T2DM symptoms, the rest of my thesis will focus on that.

1.2 Current Research on T2DM

Within the last two decades, a great deal of progress has been made in elucidating the nature of this growing pandemic and the contributing factors involved in its development (Andreassi *et al*., 2011; Ashcroft and Rorsman, 2012). T2DM has become an extremely well-researched pathology, not only because of its high prevalence, but also because T2DM has been linked to a variety of other diseases such as cardiovascular and periodontal disease, as well as some cancers (Anderson et al., 2012; Castillo *et al*., 2012; Lakschevitz *et al*., 2012; Narne *et al*., 2012). Even with this recent flurry of research, there remains much about T2DM etiology that is disagreed upon or unclear. Before addressing these however, some well-established characteristics about T2DM, which are generally accepted as fact in the scientific community will first be described.

First, it is known that insulin resistance is a core defect in T2DM (Ashcroft and Rorsman, 2012; Bajaj and DeFronzo, 2003; DeFronzo, 2009), as well as that a decrease in β-cell mass can often be seen in the diabetic pancreas (Butler *et al*., 2003; Rahier *et al*., 2008). Additionally, it has been found that lifestyle as well as a positive family history greatly influences the probability of developing T2DM (Bergman, 2005; Kayshap *et al*., 2003). But how exactly do these factors influence T2DM onset, how significant of a role do they play, and how best to treat T2DM patients? These have been the questions that have created much debate between great researchers throughout the world and will be explored in this section.

The questions being debated in the scientific community have fuelled current research on T2DM and have afforded us with a clearer and more accurate understanding of the disease and its etiology. Some findings have even greatly changed our perception of T2DM, proving previous definitions of the disease insufficient. For example, it was recently believed that T2DM's symptoms were attributed solely

to peripheral tissue resistance to insulin, which in turn caused β-cells to become exhausted from over-production and become dysfunctional over time. This would suggest that β-cells mass and function change as a result of T2DM, but do not play a significant role in its development. However, now there is growing evidence that it may be in fact impaired β-cell function and reduced β-cell mass that precedes and contributes to T2DM onset (Ashcroft and Rorsman, 2012; Walker *et al*., 2011). But which factor is more important in T2DM etiology and why? Like previous findings, this remains in heated debate.

1.2.1 Pancreatic islets: β-cell mass and function

The pancreas is integral to glycemic control in the body, as it is not only the site of insulin production and secretion, but also where glucagon is stored and secreted. Islets are the functional units in the pancreas, and they are scattered throughout the organ and play a central role in fuel homeostasis. As previously mentioned, β-cells are the insulin producing cells found in the pancreatic islets. Insulin plays an important role in reducing blood-glucose levels by signalling peripheral tissues to increase uptake of glucose from the blood. Glucagon, however, possess a reciprocal role, where it acts to stimulate a number of catabolic processes and mobilize glucose and free fatty acids, ultimately increasing blood-glucose levels. Glucagon is synthesized and secreted from the α-cells of pancreatic islets. When speaking of T2DM, β-cells are often referred to exclusively, and the role of α-cells often overlooked or ignored since it is thought that α-cell activity is regulated by insulin (Ismail-Beigi F, 2012). In patients with T2DM, it is consistently found that they possess a significant, but varying reduction, in β-cell mass. Up to a 60% reduction has been found in some T2DM patients when comparing persons of similar weight and age that have T2DM or are healthy. Additionally, it was not decreased β-cell cytoplasmic volume that was found in diabetic patients, but instead a decreased number of total cells,

hinting at the possibility of uncontrolled cell apoptosis being a contributing factor to T2DM development (Butler *et al*., 2003). However, it remains to be determined whether the decrease in number of β-cells occurred before T2DM onset and contributed to its development, or was the result of the disease. To shed a little light on the subject, a different group led by Bjoern Menge (2008) carried out a series of studies on patients that had undergone hemi-pancreatectomies. This group was researching the regenerative capabilities of human pancreases versus rodent pancreases, and if regeneration played any part in recovering a non-diabetic phenotype after partial pancreatectomy. The findings from their research showed that of the seven healthy donors to have undergone a hemi-pancreatectomy, six developed some degree of impaired fasting glucose (IFG). Thus even with half of the pancreas gone, progressed T2DM was not a resultant disease despite IFG occurring. However, it should be noted that the aim of the study was to assess regeneration of β-cells, so no longitudinal studies were carried out to see whether these patients eventually developed T2DM as a result of losing ~50% of their pancreases. Menge suggested that a steady deterioration of glycemic control would likely occur as a result of patients undergoing hemi-pancreatectomies in the long-term. So it seems that there still exists the possibility that reduced β-cell mass may indeed cause IFG, and perhaps lead to T2DM. But as previously stated, this is not definitive and hardly conclusive.

There have been multiple other groups that have conducted studies to find the relationship between β-cell mass and T2DM development. Rahier *et al*. (2008) has found much only slight decrements in patients with T2DM, whereas Del Guerra et al. (2005) have found a difference of ~10% in β-cell mass between diabetic and non-diabetic patients. Although there is much disagreement in the importance of β-cell mass in T2DM etiology, one consistent finding is that of the cell's function being severely impaired in all T2DM patients, most notably glucose stimulated insulin secretion (Ashcroft and Rorsman, 2012; Walker *et al*., 2011; DeFronzo and Abdul-Ghani, 2011). One group has found that the decreased functionality of the β-cell stems from a number of genetic alterations, from the glucose

transporter 2 (Glut-2) to glucokinase (GK) (Del Guerra *et al*., 2005). The findings that show insulin secretion from T2DM islet cells is severely impaired, even when accounting for decreased β-cell mass, strongly suggest that function may potentially hold a more significant role in T2DM etiology than mass. This is also mirrored in my own results, showing that under restricted cholesterol conditions attempting to mimic T2DM, glucose stimulated insulin secretion (GSIS) is significantly reduced.

1.2.2 T2DM Risk Factors

As previously mentioned, β-cell mass and function are not the only factors involved in T2DM onset and susceptibility. Important genes involved with the GSIS response (such as Glut-2 and GK) have already been implicated in the diminishing of T2DM patients' ability to carry out normal glycemic control. There have also been a multitude of meta-studies that link several polymorphisms in high risk loci with the development of T2DM, genes important in insulin sensitivity, secretion, and even proinsulin conversion to insulin (Kirchhooff *et al*., 2008; Staiger *et al*., 2007). In addition to that, it has been found that positive family history plays a significant role in T2DM onset, shown in the dramatic experiments conducted by Kashyap *et al*. (2003) where it was demonstrated that persons with first-degree relatives possessing T2DM displayed significantly decreased insulin secretion when challenged with infusion of triglyceride emulsions. Correlational studies linking fetal birth-weight and T2DM risk have also been carried out, with low birth weight showing increased incidence of T2DM development when compared to high birth weight (Harder *et al*., 2007). Thus, it becomes very apparent that a multitude of factors can affect the T2DM etiology; however the strongest and most reliable predictor of T2DM remains obesity.

1.2.3 Obesity and Diabetes Mellitus

There are some who believe that obesity is the single most relevant risk factor to the development of T2DM. This assumption may not be too far off, as somewhere between 60% to 90% of all known T2DM cases appear to be related to obesity or weight gain (Anderson *et al*., 2003). Additionally, the marked increase in T2DM prevalence is highly correlated with a comparably steep increase in obesity prevalence (Flegal *et al*., 1998). According to Masato Kasuga (2006), T2DM develops, in general, when pancreatic β-cells are unable to produce and secrete enough insulin to meet the metabolic demands of a patient. As seen in figure 2, obese patients have increased free fatty acids (FFAs) throughout their body, and in turn this increased weight and stress on the patient causes a cascade of hormone as well as inflammation responses (Prentki and Madiraju, 2011). These factors are thought to lead to insulin resistance, and in turn, compensation by β-cells via increased insulin synthesis and secretion. Eventually, it is thought that β-cells become exhausted, and then ultimately cease being fully functional.

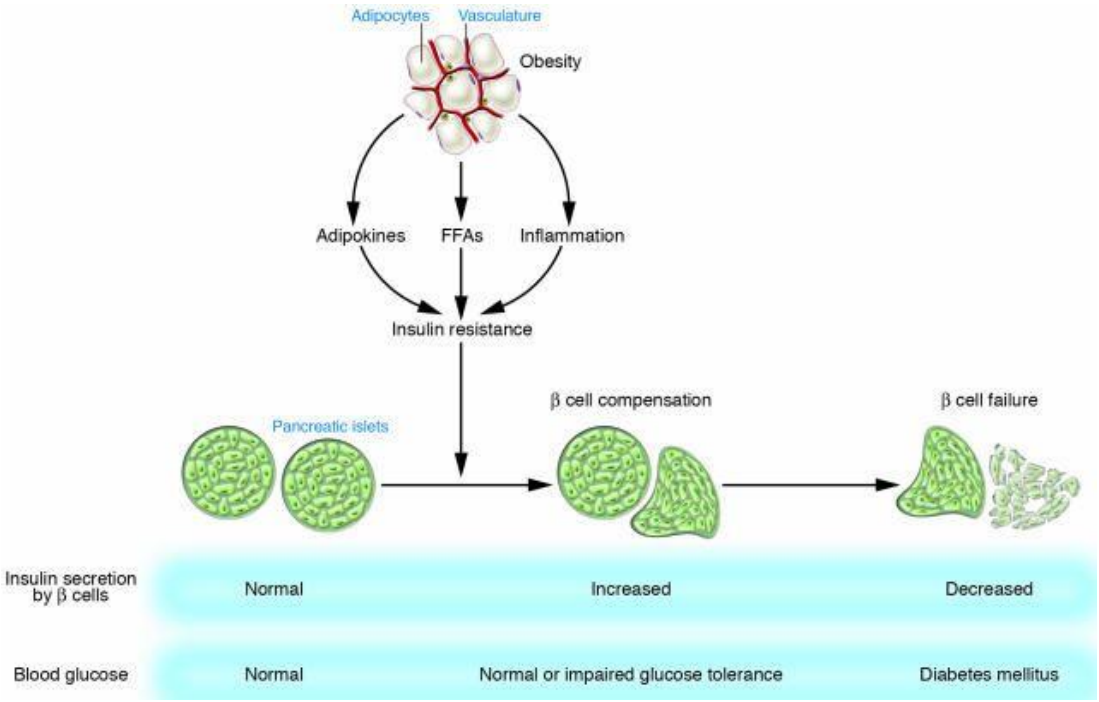

Figure 2. Development of type 2 diabetes due to obesity. Depicted above is the proposed relationship of increased fatty intake and the outcomes of a fat-rich diet. Adipokines, free fatty acids (FFAs) and inflammatory elements are released due to increased adipocytes. These factors all contribute to Insulin resistance, and ultimately, failure and even death of β-cells.

Reprinted from "Insulin resistance and pancreatic Beta cell failure," by M Kasuga, 2006, J Clin Invest. 116(7):1756-1760. ©2006. Reprinted with permission.

The risk involved with being obese is well demonstrated in an excellent longitudinal study carried out by Colditz and colleagues. The study looked at incidences of diabetes in age adjusted weight groups, measured as body mass index (BMI), as well as positive family history and what the relative risk of developing diabetes was when those factors were independent, and when they were together. For these studies, BMI was calculated for an individual as [mass (in kilograms)] / [height (in meters)]^2. Colditz *et al*. (1995) wanted to assess the impact of BMI at age 18, weight gain after age 18, and attained BMI at age 30 to 55, on the risk of developing diabetes in women. Over 100,000 female registered nurses were part of the study which was launched in 1976, at which point participants were also screened ensuring that none had diabetes at the time of the study. Follow up examinations were conducted every two years and the study was concluded 14 years later in 1990. At this point it was obvious to Colditz and and colleagues that very startling results were obtained. A BMI of <22kg/m^2 was standardized to a relative risk (RR) of 1 and adjusted for age 18. When comparing the RR for participants with a BMI >35.0 at ages 30 to 55, the difference was extremely elevated, sitting at 93.2. Additionally, when correlating the impact of weight gain and family history on the risk of developing T2DM, the risk was constantly doubled in participants that encountered moderate weight gain and had at least 1 parent or sibling with a known case of diabetes mellitus. The risk was exponentially increased if both parents had cases of diabetes or if a parent and a sibling had diabetes. In more current studies, these trends were verified when it was found that an inverse relationship existed between the amount of fat content in the pancreas and the efficiency of GSIS responses. Additionally, in the same study it was determined that reducing pancreatic fat saw a significant increase in glucose tolerance and GSIS (Tushuizen *et al*., 2007). It has long been established that a real and alarming relationship exists between diabetes and obesity, and current approaches to treating diabetes often address both pathologies.

1.2.4 Current therapies for T2DM

As T2DM progresses in patients, blood-glucose levels continually rise and the functionality of pancreatic β-cells further diminish. Despite all the recent advances in clinical research, there remains some debate on how to best approach the general treatment of diabetic patients. A group led by Ralph A. DeFronzo (2011) believes that the key to T2DM treatment lies within early detection and treatment of impaired glucose tolerance (IGT), a symptom that often precedes a T2DM diagnosis. His group has found that pharmacological approaches decrease IGT conversion to T2DM uniformly, and at a much higher incidence than any lifestyle changes do (i.e. weight loss, exercise etc.). Thus the emphasis on T2DM treatment is prevention and with aggressive drug administration during IGT. However, many of the T2DM cases today go largely undetected until it has fully progressed. Although prevention would be fairly ideal, it is not always feasible. Most other groups approach T2DM from a curative perspective, and attempt to find the most successful treatment regimen for the most common causes. Contrary to DeFronzo's view, many tend to lean towards the argument that lifestyle changes are the best way to both prevent, and treat, T2DM (Seino *et al*., 2011; Anderson, 2003). Schwartz and Kohl (2010) suggests that even a modest reduction in weight improves glycemic control, blood pressure, and other cardiovascular risk factors significantly. However, they also emphasize the great influence that delaying treatment has on diabetic patients. Patients with a longer duration of untreated or improperly treated diabetes mellitus do not experience the benefits of intensive therapies to the same extent as those who receive treatment in a timely manner. This is even despite the fact that target A1C levels are reached in both groups.

Most treatments currently in practice make use of pharmacological agents that mimic insulin (or is synthesized insulin), take advantage of the glucose lowering effects of certain receptor or channel inhibitors and agonists (i.e. glucagon-like peptide-1 (GLP-1), sulfonylureas) or attempt to slow glucose

biosynthesis and reduce its storage (i.e. metformin). Some drugs work so effectively that hypoglycemia and other adverse side effects of drug administration may cause more harm than benefit at times. The oldest and most notorious class of drugs that falls under this category are sulfonylureas. They have been in use for many decades now, employed shortly after its discovery in 1942 by chemist Marcel Janbon. This compound acts on ATP-dependent potassium channels in the β-cell and prevents its opening, causing hyperpolarization and ultimately, increased insulin secretion (Davis and Granner, 2001). The actual binding site for this drug is found on a protein complex called SUR1, or sulfonylurea receptor-1, which is closely linked to the potassium channel. The significantly increased probability and duration of insulin release greatly reduces blood glucose levels, but also has a very high risk of hypoglycemia incidence associated with it. Sulfonylurea induced hypoglycemia (SIH) is a well-known serious side effect of sulfonylurea usage, and is attributed to the fact that there is a lack of regulation in its activity. It has been recently estimated that sulfonylureas carry with them up to a 10-fold increased risk of causing hypoglycemia when compared to other drugs, which is the leading cause of hospital complications when treating diabetic patients (Holstein *et al*., 2010).

Around the same time that sulfonylureas became popularly used to treat T2DM, another class of drug was also discovered. Metformin was introduced after the first set of successful clinical trials in 1957, although it did not become popularly prescribed in Canada until over a decade after. Metformin lowers blood glucose levels by inhibiting hepatic gluconeogenesis as opposed to increasing circulating insulin. Additionally, it helps sensitize peripheral tissue glucose uptake by increasing insulin receptor activity on these cells, allowing for a reduction in blood glucose even during fasting (Kirpichnikov *et al*., 2002). There are much fewer incidences of hypoglycemia as well as less overall adverse side effects, when comparing this class of drugs to sulfonylureas. These are the reasons why metformin is typically used as the standard drug for base line T2DM blood glucose control, and works well as both a monotherapy and part of a combination therapy approach (International Diabetes Federation, 2005).

More recently, another class of drugs have been discovered and developed that helps potentiate insulin secretion similarly to sulfonylureas, but without the adverse side effects. Glucagon-like peptide-1 (GLP-1) was discovered in the mid-1970s and was determined to be a very effective insulinotropic hormone that carried out important functions in food digestion, feelings of satiety, insulin secretion, glucose disposal, as well as suppression of plasma glucagon levels (Kieffer and Habener, 1999). Since then, a lot of effort has gone into creating stable GLP-1 analogs for oral consumption. Current GLP-1 mimetics and analogs have been found to greatly improve systemic fuel homeostasis by affecting glucose metabolism at various sites and in multiple cell types. In addition to greatly increasing insulin secretion and circulation, an important difference between GLP-1 analogs and sulfonylureas is that GLP-1 will only lower blood glucose levels in the presence of glucose. Hypoglycemia as a result is rarely, if ever, a side effect of GLP-1 drug administration (Leech *et al*., 2011).

One of the most remarkable findings to date, however, has come about only within the past two decades. As previously mentioned, obesity and diabetes are strongly correlated and in up to 90% of T2DM cases, the patients are also obese (Buchwald *et al*., 2009). Bariatric surgery had been in practice since the early 1990s to aid with weight loss in obese diabetic patients (Shimizu *et al*., 2012). However, there have been stunning beneficial effects seen in bariatric patients that exceeded even the results obtained through strict dieting, weight management, and exercise. In one meta-analysis conducted by Shimizu and colleagues (2012), remission of T2DM occurred in up to 86.8% of diabetic patients that had undergone bariatric surgery, with the rest of the patients enjoying some degree of improved glycemic control. Additionally, following bariatric surgery, Shimizu pointed out that more stable long-term weight loss and no serious excessive weight loss was experienced by the 477 patients included in his analysis. Similar statistics were found in 2009 by a group led by Henry Buchwald. He found that 79.3% of all patients undergoing some form of bariatric surgery enjoyed complete resolution of T2DM, with 98.9% enjoying either resolution or great glycemic control improvements. Bariatric surgery has also been

recently declared by the International Diabetes Federation as an accepted form of treatment of T2DM for patients with a BMI of 35 kg/m^2 or more (Buchwald *et al*., 2005). However, there are still a significant proportion of T2DM patients that are not good candidates for bariatric surgery, as they are neither obese nor overweight. So although there is currently a treatment that allows for complete resolution of this disease, much progress can still be made in finding a cure for all cases of T2DM.

1.3 Glucose Stimulated Insulin Secretion

Glucose stimulated insulin secretion (GSIS) is the primary mechanism involved in maintaining systemic fuel homeostasis. Insulin secretion occurs in response to elevated blood glucose concentrations and regulates when energy, in the form of glucose, is mobilized and when it is stored (Rorsman, 2005). During the last few years, breakthroughs in genetics have afforded ways of identifying genes that carry with them a high risk of T2DM susceptibility. With the advent of genome-wide association (GWA) studies, multiple gene mutations could be identified that T2DM patients often possess. One of the most striking findings from these studies was that the vast majority of T2DM risk genes were involved in GSIS and β-cell function in some way, as opposed to insulin sensitivity or adiposity (Schäfer *et al*., 2011). Because of this, not only is the study of GSIS important in the understanding of T2DM development, but it is also the main focus of my thesis work.

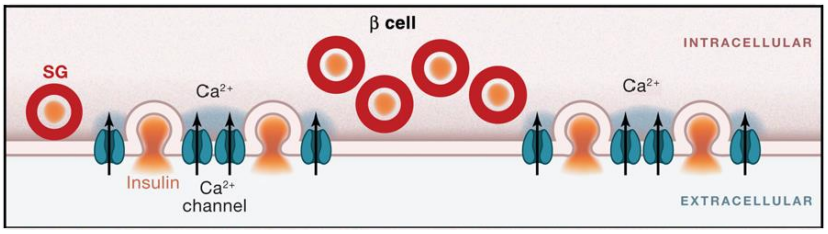

Figure 3a. Secretion due to localized calcium influx. A schematic showing the relative location of Ca^{2+} channels to secretory granules (SG) containing insulin. This organization emphasizes the need for localized increases of Ca^{2+} ions into the β-cell to allow for successful fusion of SGs and subsequent release of insulin into the blood vessels surround the islets of Langerhans.

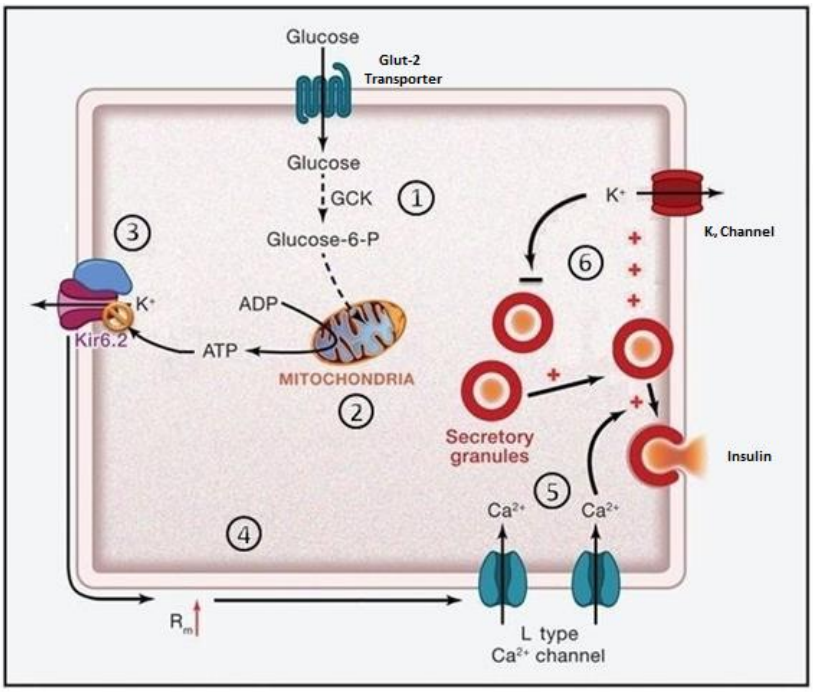

Figure 3b. Glucose stimulated insulin secretion. Simplified diagram of a glucose stimulated insulin secretion event in the pancreatic β-cell of a mouse:

1. Glucose in the bloodstream is taken up into the β-cell via Glut-2 transporter and quickly phosphorylated by glucose kinase (GCK).
2. Through glycolysis as well as Kreb's cycle, ADP is converted to ATP.
3. Increased ATP will bind the ATP-sensitive potassium (K_{atp}) channel, inhibiting it and preventing K^+ ion efflux.
4. Membrane resistance increases as K^+ ions build up in the cytoplasmic face of the plasma membrane.
5. This depolarization of the membrane reaches L-type voltage-gated Ca^{2+} channels, opening them and allowing for a quick and large influx of Ca^{2+} ions into the cell. This triggers the fusion of insulin granules and subsequent release of insulin into the circulatory system.
6. A persistent depolarization due to Ca^{2+} influx and K^+ ion accumulation will cause the membrane to reach positive values, triggering the opening of voltage-gated K^+ channels (K_V) and efflux of K^+ ions. This allows the cell to return to resting membrane potentials and also stops insulin secretion.

Figures adapted from "Diabetes Mellitus and the B-Cell: The Last Ten Years," by FM. Ashcroft and P. Rorsman, 2011. Cell Press. 148(6):1160-1171. ©2013. Reprinted with permission.

1.3.1 Glucose, Glycolysis, and GSIS

As previously mentioned GSIS occurs as a result of elevated blood glucose, which is due to the recent consumption of a meal or to energy mobilization in the body. Because of the β-cell's important role in regulating glucose uptake, the cell itself can catabolize glucose at a much higher threshold than peripheral cells. That is to say the β-cell has more glucose transporters than any other cell type, and can take up glucose beyond the physiological K_m that other cell types stay beneath (German, 1992). The primary method by which the pancreatic β-cells can regulate how much insulin must be secreted and synthesized is by sensing the catabolic intermediates and products of glucose metabolism, but most notably, the concentration of glucose-6-phosphate (Macdonald *et al*., 2005).

The process of GSIS begins when glucose is first taken up by the β-cell from the vascular system via the Glut-2 transporter. Once in the cell cytoplasm, glucose is quickly converted to glucose-6-phosphate by the enzyme glucokinase. At this point, glucose has been primed and can undergo glycolysis to create multiple metabolic products, including pyruvate and adenosine triphosphate (ATP). The quantity of ATP, other catabolic intermediates, and even glucose itself, serve as indicators to the β-cell of the quantity of glucose in the blood stream and will 'tailor' how much insulin is secreted and synthesized as a result (Crobett, 2006). For GSIS specifically to occur, ATP-dependent potassium channels sense the increase in ATP by binding with it at the Kir subunit of the channel. This results in the closing of their pores, preventing any potassium ions from escaping out of the β-cell. The localized increase in membrane resistance (R_m) causes voltage-gated calcium channels to open, allowing for a strong acute influx of calcium ions into the cell (refer to **figure 3a**). Calcium influx is the trigger for both mobilization as well as fusion of secretory granules that house insulin and proinsulin. Once the membrane reaches a critical threshold of depolarization, voltage-dependent potassium channels open and allow for potassium ion efflux to resume, repolarizing the cell and bringing the membrane

resistance back down to resting levels. This decrease in membrane resistance also closes voltage-gated calcium channels and ceases insulin secretion (Rorsman, 2005; Olofsson *et al*., 2002). This was a brief summary of the events that comprise GSIS, however prior to exploring the more detailed aspects of insulin secretion the three main channels involved will be further explored.

1.3.2 Ion Channels in the β-cell

The β-cell's ability to secrete insulin is wholly dependent on electrochemical changes that occur in localized sites within the cell. These changes are mediated by a series of ion channels, all of which play an important part in action potential generation and membrane resistance (Rorsman *et al*., 2011; Drews *et al*., 2010; Yang and Berggren, 2004). In this section, three channels will be briefly described, exploring their structure, function, as well as specific roles in glucose stimulated insulin secretion.

ATP-Sensitive Potassium Channels (K_{ATP})

K_{ATP} channels are responsible for the coupling of cell metabolism to electrical activity along the β-cell membrane. When the β-cell is exposed to low concentrations of glucose, the K_{ATP} channels remain open and continue producing K^+ ion efflux (Clark and Proks, 2010). This ion efflux suppresses electrical activity by allowing membrane resistance to remain very low, essentially determining the β-cell's resting membrane potential of approximately -60 mV (Ashcroft *et al*., 1984). This low electrical resistance persists during fasted states when glucose is not abundant enough in the blood to elicit an electrical response. However, when the concentration of glucose in the blood reaches approximately 7 mM or greater, this decreases the open probability of K_{ATP} channels. This decreased potassium ion efflux is in

fact caused by a large gain in ATP to ADP ratio due to increased glucose metabolism. The more glucose taken up by the β-cell, the larger the increase in ATP and the more K_{ATP} channels become closed at one time (Rorsman, 2008). When K_{ATP} channels are inhibited, a large membrane resistance is generated as positive ions accumulate along the cell membrane. This membrane resistance is what regulates if a GSIS response occurs and how strong it will be (Ashcroft, 2005). It should be noted that K_{ATP} channels are not only limited to the β-cell, but can be found also in other pancreatic islet cells as well as throughout the body (Gopel *et al*., 2000; Rorsman *et al*., 2008). K_{ATP} channels are abundant at the synapses of neurons to regulate neurotransmitter secretion, they help modulate glucose uptake into skeletal muscle, regulate hepatic glucose output as well as play a regulatory role in appetite (McTaggart *et al*., 2010).

The molecular structure of this channel protein is that of a hetero-octameric complex, with four Kir6.x and four SUR subunits. Kir6.x subunits are considered 'inwardly rectifying' channels and exist in four isoforms, numbered 1 through 4. The fact they are called inward rectifiers is because they conduct positive charges (potassium ions) in the inward direction of a cell (Inagaki *et al*., 1995). The K_{ATP} channel found within pancreatic β-cell contains the Kir6.2 isoform from the Kir6.x family of channel proteins. The physical binding site for ATP is at the large C-terminus of the Kir6.2 subunit, and binding causes the channel to close (Tanabe *et al*., 1999). The other half of the K_{ATP} channel is comprised of four SUR subunits, which as previously mentioned, stands for 'sulfonylurea receptor'. This is because sulfonylureas bind with high affinity to these sites and exact a similar response to that of ATP on the Kir6.2 subunit. SUR subunits are part of the ABC class of channel proteins (ATP Binding Cassettes) and serve a regulatory role in K_{ATP} channel activity (Inagaki *et al*., 1995; Aguilar-Bryan *et al*., 1995). SUR subunits exist in three isoforms, named SUR1, SUR2A, and SUR2B, and the β-cell contains solely the SUR1 type (Aguilar-Bryan *et al*., 1995). It is also worth noting that sulfonylureas have long been used to treat T2DM because of its ability to elicit a strong stimulatory response from the β-cell. Loss of function K_{ATP} channel mutations are the most common cause of congenital hyperinsulinism (HI) and conversely,

mutations that reduce K_{ATP} sensitivity to ATP lead to severe forms of neonatal diabetes, and in some cases, neurological complications (Thomas *et al*., 1996). These examples serve to highlight the importance of K_{ATP} channels' regulatory action in the β-cell, and the devastating effects that occur when its ability as metabolic sensors become compromised (McTaggart *et al*., 2010).

Voltage-Gated Calcium Channels (Ca_v)

Voltage-gated calcium channels mediate a wide variety of critical cellular processes throughout the human body. They are important in exocytotic events, cell proliferation, signalling pathways, gene expression, and cell cycle regulation (Drews *et al*., 2010). Within the β-cell, voltage-gated calcium channels are distributed in very organized microdomains along the plasma membrane. They are situated in clusters and are co-localized with secretory granules containing insulin, allowing for highly concentrated increases in Ca^{2+} ions to occur near the vesicles (Barg *et al*., 2001). Ca_v channel activity is extremely important in regulating insulin secretion, as Ca^{2+} ion influx is a necessity for fusion events to occur (Yang and Berggren, 2006). As the name implies, Ca_v activity is dependent on the electrical state of the cell. Once the β-cell has depolarized to approximately -50 mV due to K_{ATP} channel closing, Ca_v channels open allowing for a strong influx of Ca^{2+} ions into the cell (Ashcroft *et al*., 1989). This increased Ca_v activity has also been shown to plateau at approximately -20 mV, at which point it may potentially start to pump Ca^{2+} ions out of the cell. A very interesting observation was made in 2008 that implicated a loss of localization of Ca_v with SNARE proteins potentially playing a large part in the development of a diabetic phenotype (Xia *et al*., 2008). One proposed explanation of this result is based on the understanding that the organization of Ca_v into microdomains are found in cholesterol-rich membrane rafts, and thus a reduction in cholesterol could potentially explain an abnormality in insulin secretion (Xia *et al*., 2004).

The Ca_v is comprised of multiple subunits: A pore-forming α_1 subunit that contains a voltage sensor, and auxiliary β, γ, and $\alpha_2\delta$ subunits, which modulate channel activity (Catterall, 2000; Davies *et al*., 2007). There are in fact three closely related families of Ca_v proteins that are determined by the nature of their α_1 subunits, and thus, how the pore acts when electrical activity occurs in the cell. The first is the Ca_v1, numbered 1.1-1.4, the second being Ca_v2, numbered 2.1-2.3, and last, Ca_v3, numbered 3.1-3.3. All four isoforms of the Ca_v1 family of channel proteins are said to be of an L-type, or "long-lasting", form of the channel. The Ca_v2 family fall under the category of P/Q-type ($Ca_V2.1$), N-type ($Ca_V2.2$), and R-type ($Ca_V2.3$), which all have a very high-voltage requirement for activity. $Ca_v3.1$-3.3 channels are all considered to be T-type channels, which require very small depolarizations to activate, but are also 'transient' with their opening (Catterall *et al*., 2005). Since persistent changes in Ca^{2+} ion concentrations are required for glucose stimulated insulin secretion, it is generally agreed upon that Ca_v1 channels are the most significant contributors to the Ca^{2+} ion influx required for insulin secretory granule fusion (Satin *et al*., 1995). Although many of the other isoforms of Ca_v channels are present, experiments have found that when L-type Ca^{2+} channel activity is blocked, glucose stimulated insulin secretion is almost completely diminished, again emphasizing the Ca^{2+} ion influx contribution of Ca_v1 channels over the other isoforms in the β-cell (Braun *et al*., 2008).

Voltage-Gated Potassium Channels (K_v)

The pancreatic β-cell expresses multiple types of voltage-gated potassium channels (K_v channels), all of which have been known to contribute to its K^+ ion flux in varying degrees (Yan *et al*., 2004). There have been five subfamilies of K_v channels (K_v1, 2, 3, 6, and 9) detected so far in primary β-cells, which can be further split into two groups based on their distinct electrophysiological profiles. The first, consisting of $K_v1.4$, 3.3, and 3.4, are active at more negative values than the other groups of K_v

channels and have a self-inactivating current called A-currents. Channels with A-currents have activity starting at approximately -40 mV, with maximal channel inactivation at around +30 mV. The ion flux in these channels become progressively smaller as membrane potential becomes more positive, thus contributing less to K^+ ion flux as the β-cell becomes more depolarized (Smith *et al*., 1989). The second group of K_v channels are without inactivation, and possess a delayed rectifier current (Macdonald *et al*., 2001). The most predominant form of this K_v delayed rectifier channel in both human and rodent β-cells is K_v2.1. K_v2.1 channels were found to be the most significant contributor to potassium currents during Ca_v action potentials, allowing the β-cells to return back to resting voltage. Also, these channels are often co-localized in cholesterol-rich lipid rafts with Ca_v, SNARE proteins required for fusion, and insulin secretory granules, emphasizing their importance in the β-cell's glucose response (Xia *et al*., 2004).

This family of protein channels is characterized by six transmembrane regions with multiple subunits coming together to create functional pores. K_v1, 2, and 3 bind together as homo- or hetero-tetramers whereas K_v6 and 9 often play modulatory roles in K_v2 and 3 channels by co-assembly with them (Kerschensteiner and Stocker, 1999). K_v channels play a critical role in the repolarization of the β-cell after glucose stimulated insulin secretion, and because of this, heavily influences serum insulin levels. They are often the target of hormones and neurotransmitters, such as glucose-dependent insulinotropic polypeptide (GIP) and glucagon-like peptide-1 (GLP-1), which modify the rate of repolarization by diminishing K_v currents (MacDonald *et al*., 2002; Kim *et al*., 2005). As previously mentioned, K_v channel activity is required to repolarize the β-cell, which essentially stops fusion of secretory granules by closing Ca_v channels. Thus, K_v channel activity is only present when the cell is significantly depolarized, and absent when the cell is at rest. Because of this, K_v channels possess a fairly unique role in that they can be manipulated to exert an effect specifically when high glucose concentrations are found in the serum. As a result it has been the focus of multiple pharmacological studies in order to find more ways to treat diabetes mellitus.

1.3.3 SNAREs and their Role in Glucose Stimulated Insulin Secretion

SNARE proteins (soluble *N*-ethyl-maleimide-sensitive fusion protein attachment protein receptor) are strongly believed to mediate all intracellular fusion events between vesicles and target phospholipid membranes (Chen and Scheller, 2001). Because of this role, SNAREs play a very important part in allowing normal cellular functions and even membrane growth, to occur. For example, SNAREs and their associated proteins allow the trafficking of essential cellular materials between organelles as well as the secretion and uptake of a wide variety of important molecules into, or from, the extracellular space. Additionally, because of fusion events, cell and organelle membranes can change and shift in size, and the transfer, secretion, or uptake of molecules never compromise cellular or organelle compartmentalization (Ramakrishnan *et al*., 2012). Every fusion event involves a series of very coordinated cellular activities and is often triggered by a change in Ca^{+} ion concentrations (Heidelberger *et al*., 1994). The β-cell's high rate of insulin secretion and vesicle trafficking make it a very good cell model candidate to study SNARE activity. Conversely, any changes in the normal expression and function of SNAREs and associated proteins can have a very large impact on β-cell function and insulin secretion.

Before vesicles can fuse with membranes, they must first be recognized, tethered and docked. In order for this to occur correctly, vesicles are "targeted" and will fuse only to the correct membrane and location for which its contents should be released into (Pfeffer, 1999). In order for tethering and docking to be specific, specialized proteins that can interact with each other exist on both the vesicle as well as the pre-synaptic membrane region. The proteins involved in this process are syntaxin 1A (STX1A), synaptosomal-associated protein of 25 kDa (SNAP-25) and vesicle-associated membrane protein (VAMP, or synaptobrevin), all of which are members of the SNARE superfamily (Jahn and Fasshauer, 2012). The

defining features of these proteins are their extended coiled-coil domains that associate together to form a strong SNARE complex between the vesicle and pre-synaptic membrane (Weber et al., 1998). This complex is integral in the cell's ability to bring two membranes together and to overcome the high energy requiring process of fusion pore formation (Li *et al*., 2007). The structure of a SNARE core complex is that of two coils of SNAP-25 intertwined with one coil of each STX1A and VAMP, forming a "zippered" four α-helix stranded coiled-coil super structure (Sutton *et al*., 1998). VAMP is a synaptic vesicle protein whereas STX1A and SNAP-25 are localized in the pre-synaptic membrane. As the SNARE complex 'zippers', it pulls both vesicle and pre-synaptic membrane closer together, with the assembly of the complex being associated with a significant release of energy as membrane fusion begins (Wiederhold and Fassahauer, 2009). Synaptotagmins are a family of membrane-trafficking proteins that are also a very important in exocytosis (Gustavsson *et al*., 2009). They are proteins found on a pre-synaptic vesicle's membrane and have been determined to play an important role in Ca^{2+}-triggered fusion. Although not a primary contributor to the SNARE complex structure, synaptotagmins have been found to bind to pre-synaptic membranes in the presence of Ca^{2+} ions. Most believe that this interaction allows synaptotagmin to bridge itself between the phospholipid heads of each bilayer and induce fusion (Jeremic *et al*., 2004). Additionally, it has been established by numerous groups that Ca_V bind directly to the core SNARE complex which ensures that Ca^{2+} ions can quickly induce the exocytotic machinery in a localized area along the β-cell membrane (Atlas, 2001; Wiser *et al*., 1997). In addition, SNARES and their associated proteins have also been found to interact with K_v channels, serving as a site of modulation for electrical activity (Xia *et al*., 2004). This relationship emphasizes the interplay between various membrane proteins as well as the importance of SNAREs not only in the actual fusion of vesicles containing insulin, but also in the regulation and modulation of glucose stimulated insulin secretion.

1.3.4 Biphasic Insulin Secretion and Secretory Granule Mobilization

Up to this point, it has become apparent that insulin secretion is a very complex and multi-faceted process. It involves a vast array of proteins to work cohesively for a successful glucose response to occur. In addition to requiring functional ion channels, SNARE proteins, and proper localization of exocytotic machinery via lipid rafts, the actual response itself employs two different pools of insulin containing secretory granules (Yang and Berggren, 2006). These two pools of granules are what give insulin secretion a biphasic profile, with the first wave of secretion coming from the 'readily releasable pool', or RRP, and the second the 'reserve pool', or RP. The first phase of insulin secretion occurs as a fast immediate response to an increase in glucose from basal concentrations of 5 mM to approximately 10 mM (Rorsman *et al*., 2000). Roughly 95% of secretory granules in a β-cell exist in the RP, whereas less than 5% are members of the RRP pool. To elicit the first wave of insulin secretion, the β-cell does not necessarily need to be stimulated using metabolites of glucose; instead it can begin as a result of membrane depolarization from other factors such as sulfonylureas or an elevated extracellular concentration of K^+ ions (Henquin, 2000; Rorsman *et al*., 2000). Oddly enough, one of the first indicators of T2DM development is an impaired first phase insulin secretion and precedes other manifestations of this disease (Cerasi, 1992). The RRP pool of granules has been proposed to exist very close to the membrane and already 'primed' for quick release. Total internal reflective fluorescence microscopy (TIRFm) has helped to validate this theory by providing direct evidence that the initial phase of a glucose response involves granules that are already docked at the membrane (Ohara-Imaizumi *et al*., 2007). This is what gives glucose stimulated insulin secretion a very strong, but quick, initial burst of insulin in this characteristic first phase. The second phase of insulin secretion involves the mobilization of the RP of granules towards the membrane, where they can then be primed, docked, and its contents released. A series of ATP, Ca^{2+} ions, vesicle mobilization and temperature-dependent processes precedes the

secretion of insulin in this second phase. These processes are widely believed to account for the small delay seen between first and second phase insulin secretion, and since the pool is comprised of many more granules, this second phase can persist for far longer than the first phase (Rorsman and Renstrom, 2003).

1.4 Cholesterol

Cholesterol has long been established as a tightly regulated and essential molecule to virtually all cellular systems (Goedeke and Fernandez-Hernando, 2012). Any disturbances in cholesterol homeostasis result in a wide variety of pathologies including a number of cardiovascular diseases and metabolic syndromes, including diabetes. Cholesterol is vital in modulating membrane fluidity and permeability, in addition to being the precursor of all known steroid hormones and bile acids. It has also been found to play important roles in cellular trafficking, signalling pathways, and cell proliferation and growth (Fernandez *et al*., 2004; Fernandez *et al*., 2005). Because of all these important cholesterol-dependent processes, it is of little wonder that cholesterol content and homeostasis has been a central focus in the research carried out in this thesis. In order to fully appreciate the impact of cholesterol content on glucose stimulated insulin secretion, the fundamentals of cholesterol and its regulation will first be explored.

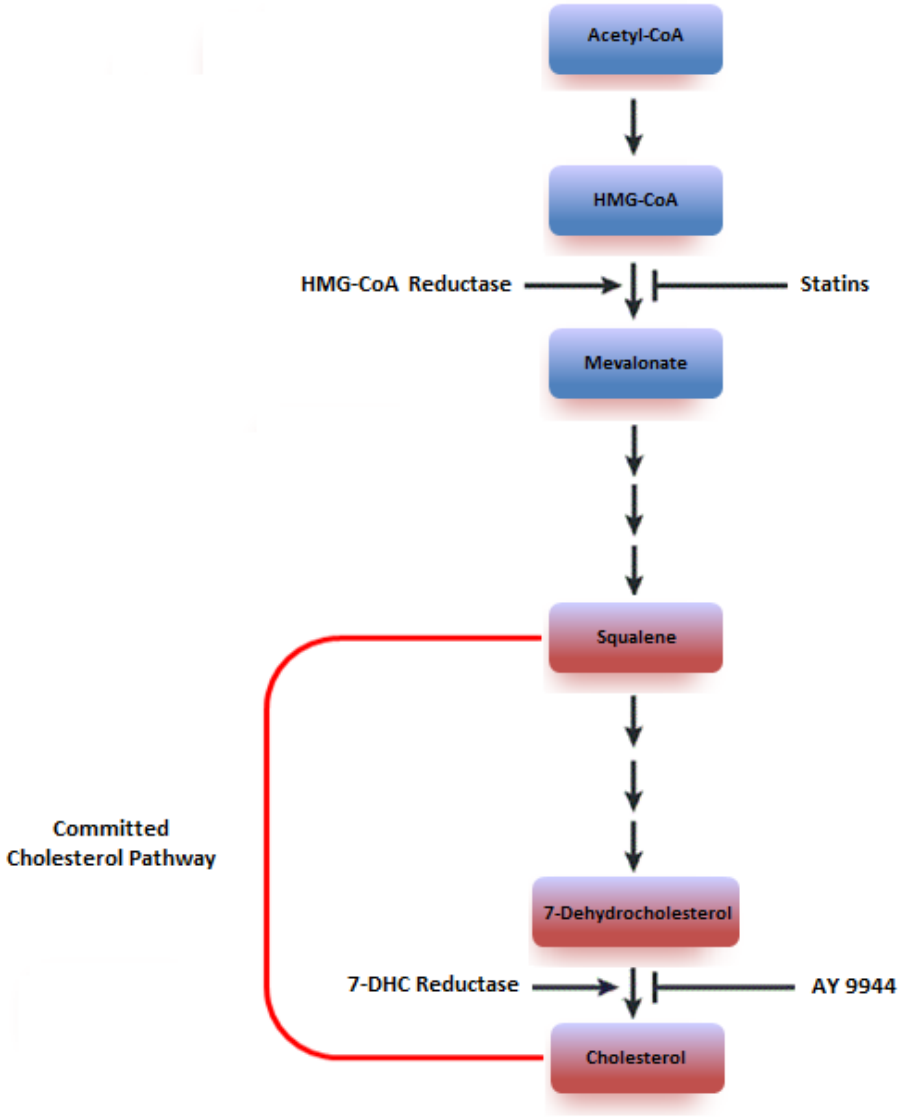

Figure 4. Cholesterol biosynthetic pathway beginning with Acetyl-CoA. In this simplified diagram, the intermediates and enzymes of interest to this thesis have been included. As seen in the top of the diagram, statins are responsible for the inhibition of HMG-CoA reductase, the enzyme which converts HMG-CoA to mevalonate. In red are the steps in the committed cholesterol pathway, which starts with squalene. It is in this portion of the cholesterol pathway that all intermediates lead up to only cholesterol. As seen in the bottom of the diagram, AY 9944 inhibits the last step prior to completing cholesterol, and acts on the enzyme 7-dehydrocholesterol (DHC) reductase.

1.4.1 Cholesterol Biosynthesis, Trafficking, and Homeostasis

There are two ways by which an animal cell can acquire cholesterol. The first is through exogenous uptake of circulating cholesterol in the form of apolipoprotein B-containing lipoproteins (i.e. low-density lipoprotein, or LDL), and the second is through a tightly regulated biosynthetic pathway available to almost all animal cell-types (Bloch, 1992; Brown and Goldstein, 1986). Extracellular sources of cholesterol require LDL particles to be delivered via the blood stream at which point they are taken into the cell through receptor-mediated endocytosis (Brown and Goldstein, 1986). Endogenous synthesis of cholesterol is also a very significant source of cholesterol, and at times virtually the only source for certain cell types such as neurons. A series of transcriptional and post-transcriptional feedback mechanisms are in place to help regulate intracellular levels of cholesterol and maintain homeostatic concentrations, emphasizing the importance this molecule to cellular function and growth (Brown and Goldstein, 1997).

Cholesterol Biosynthesis and Nuclear Regulation

Since cholesterol obtained through diet is for the most part limited, cholesterol biosynthesis makes up the large majority of cholesterol content in mammalian cells. Approximately 50% of the body's endogenous cholesterol is synthesized strictly in the liver, with the other half occurring in all the other extra-hepatic cells (Dietschy *et al*., 1993). Cholesterol biosynthesis occurs at the endoplasmic reticulum (ER) and undergoes a 19-step process involving 9 different enzymes, starting with the conversion of acetyl-CoA to HMG-CoA (refer to **figure 4**). The rate-limiting step of this synthetic pathway is where HMG-CoA is reduced to mevalonate, which also happens to be the target of the class of clinically-used drugs called statins (Jasinka *et al*., 2007). The entire process is much more complex than what is shown

in **figure 4**, with multiple branching pathways occurring from various cholesterol biosynthesis intermediates; however the focus of this thesis will be on the direct pathway to cholesterol formation. Following the synthesis of cholesterol in the ER, the newly made cholesterol is targeted for transport to the plasma membrane as well as alternate membranes such as endosomes (Bauman *et al*., 2005). Cholesterol concentrations are kept at homeostasis in part through the conversion of cholesterol into cholesterol esters, carried out by acyl-CoA acyl-transferases. These esters are stored in the cell's cytoplasm as lipid droplets and are easily accessed by the cell using cholesterol ester hydrolases (Chang *et al*., 1997). This ester conversion is a rapid and reversible reaction, allowing for the storage as well as access to free cholesterol as the cell requires it (Brown and Goldstein, 1980). Cholesterol accounts for approximately 20%-25% of lipid content in plasma membranes, but the ER contains roughly 1% of cholesterol in terms of lipid content (Lange, 1991). This is in large part due to the immediate trafficking of cholesterol from the ER to the Golgi for further use by the cell.

Cholesterol content in the ER membrane is a very important biomarker that controls one of two main nuclear receptor mechanisms regulating cholesterol biosynthesis. Sterol regulatory binding proteins (SREBPs) are important for the transcription of gene products required for cholesterol biosynthesis. SREBPs only become active when low sterol levels exist in the ER membrane. Two chaperone proteins are essential for the transport of SREBP to the Golgi, where SREBP can be cleaved and released to act as a nuclear signal. One protein is called SREBP cleavage-activating protein (SCAP), which is an escort protein that aids in the transport of SREBP to the Golgi, and the other is insulin-induced gene (INSIG), which is an anchor protein found on the ER membrane (Goldstein *et al.*, 2006). Binding of cholesterol to SCAP and the binding of 25-hydroxycholesterol to INSIG causes these two chaperone proteins to form a strong complex with each other, preventing them from interacting with SREBP (Sun *et al.*, 2007). If both cholesterol and 25-hydroxycholesterol are found in low levels in the ER, SCAP and INSIG dissociate from each other and activate SREBP. At this point, SREBP is released from the

ER and processed in the Golgi, where it can then act as a nuclear signal to stimulate the transcription of genes such as HMG-CoA reductase and LDL receptor (Goldstein *et al.*, 2006).

The other major form of transcriptional regulation of cholesterol involves oxysterols and receptors in the cell, namely the liver X receptor (LXR) (Goldstein *et al.*, 2006; Schropfer Jr., 2000). Oxysterols are a class of cholesterol derivatives that have multiple actions in a cell including the down regulation of HMG-CoA reductase activity and activation of LXRs. LXRs are important receptors that activate genes involved in the reduction of excess cellular cholesterol concentrations (Beaven and Tontonoz, 2006). One of these gene groups belongs to the reverse cholesterol transport pathway, which helps remove cholesterol from peripheral cells and also increases biliary cholesterol secretion (Tontonoz and Mangelsdorf, 2003).

Cholesterol Uptake, Secretion and Trafficking

Dietary intake of cholesterol is also a very important source of this valuable lipid and as a result, the uptake of exogenous cholesterol is a very well regulated and complex process. Cholesterol from food is initially absorbed by the enterocytes of the small intestine and then transported to the liver for further processing and packaging. To describe this process briefly, enterocytes will package dietary cholesterol along with triglycerides into particles called chylomicrons. These chylomicrons reach hepatic tissue via the lymph and are taken up by the hepatocytes. The liver will then further process the chylomicrons and package them into very low density lipoproteins (VLDL), which get processed further in the circulatory system into low density lipoproteins (LDL) (Grundy, 1983). LDL particles are then taken up by the cell via receptor-mediated endocytosis using LDL receptors (LDLr). Once the LDL particle is inside, cholesterol molecules are liberated from the LDL complex within a lysosome and become readily useable by the cell. This is the pathway that is most commonly used by peripheral cells to obtain

exogenous sources of cholesterol when cellular concentrations are low. It should be noted however, that because most cells possess the ability to synthesize cholesterol as well as have a ready supply of circulating cholesterol typically being available, there are many cases where cholesterol can over-accumulate in a cell. As previously mentioned, cholesterol efflux is a very important aspect of cholesterol homeostasis that allows the removal of excess cholesterol in bulk. Cholesterol is a very difficult molecule to break down and there is a limited quantity of cholesterol esters a cell is capable of keeping within its cytoplasm. Similar to dietary intake of cholesterol, cholesterol removed from cells must re-enter the liver in order to be expelled or eventually re-used. This process is referred to as reverse cholesterol transport (RCT) and greatly aids in the homeostatic control of physiological concentrations of cholesterol (Glomset and Norum, 1973).

High density lipoproteins (HDL) is the main particle associated with cholesterol exchange and is the only acceptor of cholesterol released from extra-hepatic cells. HDL serves important roles in the two pathways that mediate cholesterol efflux. The first method of cholesterol removal is through passive diffusion. This pathway involves the removal of cholesterol from a cell's plasma membrane and the diffusion of it directly into a nearby HDL particle. Many factors are required for this diffusion to occur, such as compartments on the plasma membrane's extracellular face as well as enzymes attached directly to HDL (Yokoyama, 2000). The enzyme lecithin-cholesterol acyltransferase (LCAT) has been implicated in this process and exists on the surface of lipoproteins such as HDL. The proposed mechanism by which LCAT facilitates the transfer of membrane cholesterol into HDL particles is by the conversion of free cholesterol into cholesterol esters. These esterified cholesterol molecules are then sequestered into the HDL particle and delivered to the liver (Jonas, 2000). The second method of reverse cholesterol transport is mediated by ApoA-I, the major apoprotein found in HDL particles, and ATP-Binding Cassete-1 (ABCA1), a very important transporter protein required for the formation of HDL. ABCA1 is essential for both methods of cholesterol efflux, and this is exemplified with Tangiers disease, a

condition in which a person possesses low plasma HDL. The mutation was mapped back to the *Abca1* gene and when ABCA1 was reduced, over-abundance in cellular cholesterol became a characteristic phenotype (Brooks-Wilson *et al.*, 1999). In this pathway, the HDL particle itself is internalized into the target cell via phospholipids and cholesterol complexes formed at the cell surface. Once in the cell cytoplasm, the HDL particle reforms and is then targeted to intracellular membranes, where the ApoA-I becomes lapidated. The HDL particle then undergoes re-secretion back into the circulation where it is targeted to the liver (Neufeld *et al.*, 2004; Takahashi and Smith, 1999).

1.4.2 Lipid Rafts and Caveolae

The cell membrane is best characterized as a fluid bilayer containing well over 2000 species of lipids with distinct properties (Barenholz, 2000). Some of these lipids prefer to interact with hydrophobic protein regions, others prefer to associate with each other and some even act in an exclusionary manner. Because of these diverse properties, formations of distinct lipid structures arise and create what are referred to as phase separations (Binder *et al*., 2003). Cholesterol, along with sphingolipids, is a very important component in the formation of liquid-ordered (Lo) phases along the cell membrane which are otherwise known as lipid rafts. Lo phases are organized structures or domains that exist within a sea of more fluid membrane regions, which are referred to as liquid-disordered phases (Ld). These cholesterol-sphingolipid interactions are so strong that they are resistant to most detergents used to disrupt cell membranes. Because of this stability, lipid rafts commonly associate with protein structures that require close proximity with other proteins for functionality or to serve as targets for regulation. These roles were determined using the fact that lipid rafts participate actively in signal transduction pathways in the cell as well as having been implicated in the structural organization of ion

channels and SNARE proteins in the β-cell and cardiomyocyte membranes (Maguy *et al.*, 2006; Xia *et al.*, 2008).

Caveolae are small invaginations within a cell membrane that are rich in sphingolipids, cholesterol, and caveolin (Helms and Zurzolo, 2004). They have the distinct property of also being detergent resistant and are considered a sub-type or specialized form of lipid rafts. As seen in **figure 5**, caveolae possess a static flask-shaped form which arises from the coalescence of smaller rafts. Caveolin-1 makes this specialized structure possible by oligmerizing with itself and forming the cytoplasmic face's caveolin coat (refer to **fig. 5 B**) (Rothberg *et al*, 1992). Many receptors and channel proteins involved in the insulin secretion response have been found to colocalize with lipid rafts or caveolae, such as GLUT transporters, insulin receptors and voltage-gated potassium and calcium channels (Bickel, 2002; Xia *et al*., 2008). Caveolin knockout mice have also been shown to confer a degree of insulin resistance, as well as further studies that propose a regulatory relationship between caveolin and insulin receptors (Capozza *et al*., 2005; Karlsson *et al*., 2002; Yamamoto *et al.*, 1998).

1.4.3 Cholesterol and Lipid Rafts in β-cell Dysfunction

There have been numerous studies conducted looking at the effects of increasing, as well as decreasing, lipid content in the β-cell and how it affects function. More recently, a study conducted by Bogan and his colleagues (2012) determined that across a variety of β-cell lines, the insulin granule possesses the highest concentration of cholesterol when compared to all other cellular and organelle membranes.

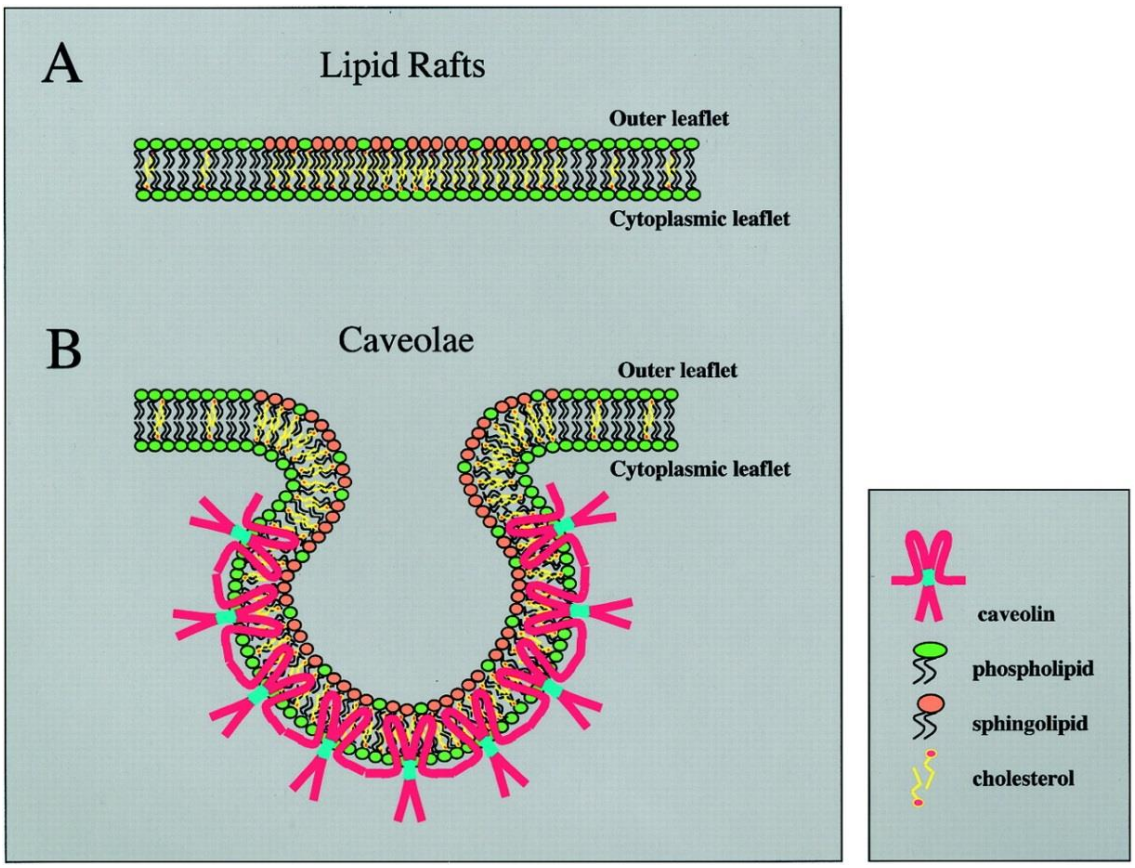

Figure 5. Common lipid raft and caveolae structural organization in mammalian cells. In A) the lipid raft is seen with a high concentration of sphingolipids and cholesterol when compared to the rest of the membrane. In B) the caveolae is seen also with high sphingolipid and cholesterol content, in addition to caveolin organized throughout the cytoplasmic face of the caveolae.

Reprinted from "Caveolae: From Cell Biology to Animal Physiology," by B. Razani, SE. Woodman, MP. Lisanti, 2002, Pharm. Rev. 54 (3):431-467. ©2002. Reprinted with permission.

Thus, when lipids like cholesterol were increased or even decreased in the β-cell, the most obvious effects were found to be in mechanisms involving the insulin granule, from trafficking, maturation, as well as secretion. Bogan suggested that an increase in cholesterol caused an increase in granular size, which in turn prevented normal docking and fusion of insulin granules (Bogan *et al.*, 2012). Oddly, a decrease in β-cell function was also witnessed when cholesterol was significantly reduced in the β-cell (Tsuchiya *et al.*, 2010), and in one instance, the reduction in cholesterol was also associated with increased granular size resulting in decreased secretion (Sturek *et al*., 2010). Although some findings do appear to potentially contradict each other, the foundation on which the conclusion was built on remains the same; a disruption in cholesterol homeostasis bears severe adverse effects on β-cell function and insulin secretion.

Recent findings have also established a strong connection between necessary machinery required for a GSIS response and lipid rafts. As with the case of voltage-gated calcium channels, many proteins involved in signal transduction have a localization requirement for a stimulus to become effective (Yang and Berggren, 2006). Numerous other studies have proven repeatedly that channels are targeted to lipid rafts, and that the loss of these rafts is associated with diminished effects of the target protein. For example, lipid raft studies in HEK293 cells showed that when cholesterol was reduced in the cell, a loss of colocalization of voltage gated potassium channels with their associated receptors occurred (Oldfield *et al.*, 2009). Additionally, in the case of β-cells in particular, voltage-gated calcium ion channels were found to colocalize with SNARE proteins required for exocytosis, and when this colocalization was disturbed, secretion was notably diminished (Xia *et al*., 2007; Xia *et al*., 2008). This relationship between reduced cholesterol and impaired glucose secretion is the basis of the many meta-studies conducted that explore the connection between statin usage and the development of diabetic phenotypes. In the next section, the results of vast meta-studies conducted on clinical trials involving

statin use and diabetes risk will be explored, allowing us a practical and applicable perspective on the relationship of cholesterol reduction and T2DM.

1.5 Statins and Diabetes

Although it has been well over a century since high cholesterol was first discovered to increase risk of cardiovascular disease, it was not until the mid-1900s that a cholesterol biosynthesis pathway inhibitor was found. However, the first naturally occurring inhibitors were far too toxic to be used in a clinical setting and it took almost three decades after that to find a usable alternative. In 1978, a team working at the Merck laboratories discovered a compound they could isolate from fermented *Aspergillus terreus* broth. They called this compound mevinolin, and it proved to be a potent inhibitor of 3-hydroxy-3-methyl-glutaryl-CoA reductase (HMG-CoA), a vital enzyme in the cholesterol biosynthetic pathway. Later, the official market name of this compound became lovastatin, creating the general term 'statin' for all future HMG-CoA inhibitors (Tobert, 2003). Shortly after the last stages of clinical trials, statins have grown to become the most widely prescribed cardiovascular disease medication around the world (Mills *et al.*, 2011). Originally thought of as a wonder drug with no negative side-effects, statin therapy has recently been looked at from a much more critical light. Oddly enough, the criticism started shortly after statins were thought to have additional benefits that went beyond fighting cardiovascular disease. One of the earliest reports to assess the risk and benefits associated with long term statin use had actually found statins to not only effectively decrease incidences of cardiovascular injury, but also to decrease the risk of developing T2DM (Freeman *et al.*, 2001). The West of Scotland Coronary Prevention Study, or WOSCOPS, suggested that there existed a protective effect with pravastatin usage in preventing new onset diabetes. To further support this theory, research conducted on Zucker rats also

found a significant reduction in diabetes susceptibility (Wong *et al.*, 2006). This triggered a multitude of further research and meta-analyses to verify this protective effect. However, virtually all studies after WOSCOPS had in fact found the opposite to be true; statin usage was associated with a small, but significant risk, of developing T2DM.

1.5.1 Meta-Analyses Linking Statin Use and New Onset Diabetes

Since the turn of the century, there have been well over a dozen major randomized clinical trials assessing both the benefits and risks of statin use. In light of the immense amount of data collected from all these studies, a series of meta-analyses were conducted to determine what all the results meant from a clinical standpoint. From the perspective of how well statins performed to reduce cardiovascular event rates, all studies were unanimous in agreeing that the benefit statins provided was significant (Colbert *et al.*, 2012; Goldfine, 2012; Preiss *et al.*, 2011; Preiss and Sattar, 2011; Sattar *et al*., 2010). However, when looking at the risk to the development of new onset diabetes, the studies were in slight disagreement as to what the severity of the risk was. Despite the differences in perceived risk, almost all the meta-analyses did agree at the end that the benefit to cardiovascular disease did outweigh the overall risk of developing diabetes. The existence of a connection between statin treatment and new onset diabetes has repeatedly been established however, and much can be learned about the nature of diabetes by considering the findings of both statin trials as well as the meta-analyses that arise from them.

In 2010, a major collaborative analysis of statin trials was carried out by Naveed Sattar and a multitude of other prominent researchers. What they determined across 13 trials involving 91,140 participants, was that patients using statin therapy experienced an overall 9% increased risk in

developing new onset diabetes incidences (Sattar *et al.*, 2010), with some of the studies reporting values as high as a 25% increased incidence of physician diagnosed diabetes (Ridker *et al.*, 2008). As if to reinforce this relationship between statins and diabetes, a follow up analysis of new statin trials that surveyed specifically for diabetes risk was conducted. In that study, Sattar and colleagues confirmed a dose-dependent effect with statin usage as well as differences in the risk of new onset diabetes when different statins with higher potencies were used (Preiss and Sattar, 2011). They found that the overall risk increased from 9% to 12% when patients were prescribed intensive-dose statin therapy. However, when assessing the only placebo-controlled trials using statins, the rate was much higher. There are two major clinical trials to date that involve a placebo group. The first is the Stroke Prevention by Aggressive Reduction in Cholesterol Levels (SPARCL) investigation which was conducted in 2006. This statin trial randomly assigned 4,721 patients who had experienced a cardiovascular complication within one to six months prior to the study to either an intensive statin dose or placebo group (Amarenco *et al.*, 2006). After the trial was concluded, 3803 patients that did not possess diabetes at baseline were examined to see if any symptoms had arisen. 166 patients on an 80 mg atorvastatin dose developed diabetes, whereas only 115 did that were in the placebo group. This translated to a 44% increase in new onset diabetes incidence in the high dose statin group, indicating that the use of statins significantly increased risk (Waters *et al.*, 2011). The conclusion of this study was that for every 10 patients protected from a cardiovascular complication event, 7 additional cases of diabetes occurred. The second trial to include a placebo group had found even more compelling values of statin's risk in developing diabetes. The Justification for the Use of Statins in Primary Prevention: An Intervention Trial Evaluating Rosuvastatin (JUPITER) trial was conducted in 2010 and involved almost 17,000 participants (Mora *et al.*, 2010). This trial had been conducted to see if there were any gender specific outcomes from undergoing statin therapy, of which none were found. However, the final conclusion of the trial was that for every 10 patients protected from a cardiovascular complication event (either male of female), 9 patients

developed diabetes (Preiss and Sattar, 2011). As previously mentioned, another point of interest was that of the differences between certain statins. Rosuvastatin, the most powerful type of statin, showed an 18% increase in overall risk of developing new onset diabetes, whereas a modest strength statin, pravastatin, yielded only a 3% increased risk (Preiss and Sattar, 2011). Additionally, the drastically different risk assessments found in the JUPITER trial versus the other statin trials could partially be attributed to an assessment made exclusively on rosuvastatin use. Regardless of the outcomes, the meta-analyses conducted on recent major statin trials all point to a significant and real relationship between statin use and new onset diabetes.

1.5.2 Other Cholesterol Biosynthesis Inhibitors: AY 9944

Within this thesis more than just statins were used to see the effects of restricting endogenous sources of cholesterol. The drug AY 9944 was also employed and showed very strong results that appeared to be even more drastic than the results obtained with statin usage. Unlike statins which inhibit the initial step of cholesterol biosynthesis, AY 9944 targets the enzyme 7-dehydrocholesterol reductase (DHCR7) which catalyzes the last step of cholesterol biosynthesis; the conversion of 7-dehydrocholesterol to cholesterol (refer to **figure 4**). Understanding the implications of using AY 9944 versus statins then became a very important task. There have been noted mutations of the DHCR7 enzyme in humans manifesting into the disease called Smith-Lemli-Opitz syndrome (SLOS), an autosomal recessively inherited disorder. SLOS is a severe defect that leads to very low plasma cholesterol levels and elevated levels of 7-dehydrocholesterol (Gedam *et al.*, 2012). Associated symptoms are mental retardation, facial dysmorphism, cardiac and renal complications, polydactyly and oligodactyly, with an overall failure to thrive and develop. Patients with homozygous mutations in the DHCR7 gene die during

early childhood (Gedam *et al.*, 2012). These devastating symptoms emphasize the importance of cholesterol in cellular structure, essential mechanisms, and signalling pathways. However, it also demonstrates how accumulation of 7-dehydrocholesterol in the cell can be very toxic. Fairly recently, a group conducted a series of experiments on DHCR7 knockout mice and assayed for cellular and physiological effects of 7-dehdryocholesterol accumulation as well as the reduction of available cholesterol. One interesting finding was that 7-dehydrocholesterol accumulation appeared to trigger increased proteolysis of HMG-CoA reductase, which further exacerbated the effects of inhibiting or knocking out DHCR7 (Fitzky *et al*., 2001).

1.6 Experimental Aims and Hypothesis

If current research is any indication of the state of a β-cell after disturbing cholesterol homeostasis, it is evident that either cholesterol overloading or inhibition plays a part in the development of diabetic-like symptoms. The aims of my research are first to establish a base line reference from which I can assess the degree of cholesterol reduction in the MIN6 mouse pancreatic β-cell under varying experimental conditions. Afterward, the effects of the reduction on glucose stimulated insulin secretion as well as overall β-cell function and health were assayed. Using a variety of techniques, from ELISA, patch-clamp, and RT-PCR, a deeper understanding of the impact that cholesterol reduction has on the development of T2DM-like symptoms using the MIN6 cells was determined.

1.6.1 General Hypothesis

Cholesterol plays a number of important roles in the cell, including being a vital component to membrane integrity, localization of proteins, cell trafficking, signaling, and gene transcription. Xia *et al.* (2004) have proposed that reducing cholesterol, which is a key component in lipid raft formation, will compromise the structural stability of microdomains within the plasma membrane dedicated to insulin secretion. Additionally, it has been suggested that integral to these microdomains are lipid-protein interactions that allow for proper signaling between protein complexes within the cell that help fusion events occur (Helsm and Zurzolo, 2004; Seino *et al.*, 2011). My hypothesis is cholesterol reduction will have over-arching effects on β-cell electrical activity, specifically by affecting the mRNA profiles of important SNARE proteins, insulin, and ion channels, all contributing to the reduction of glucose stimulated insulin secretion.

2.0 Methods

2.1 Cell Culture

Mouse insulinoma cell line 6 (MIN6) cells were maintained in Dulbecco's Modified Eagle Media (DMEM; 25 mM glucose) from Wisent, QC, enriched with 10% v/v fetal bovine serum (Invitrogen, Burlington, ON), 1X penicillin/streptomycin (Invitrogen), and 4.86 x 10^{-5} M β-mercaptoethanol (Sigma-Aldrich, Oakville ON) in 500 ml DMEM. A volume of 10 ml enriched DMEM per 10 cm dish was kept standard for cell maintenance, in a 5.0% CO_2 incubator.

2.2 Cell Passage

Cells were passaged when cell confluency was high (~85%). Cells were removed from the dish with the use of 1.5 ml of 0.5% v/v trypsin (Invitrogen) per 10 cm dish, and then collected in 3 ml enriched DMEM and centrifuged at 1600 g in a Thermo Scientific 4600 RPM Sorvall centrifuge (Thermo Scientific, Rockford IL, USA) for 2 minutes. Afterwards, each dish of cells collected was passed into fresh 10 cm dishes or 6-well plates. The number of dishes and plates depended on pellet size.

2.3 Trypan Blue Cell Viability Assay

After cells were treated in 6-well dishes for 24-48 hours, the media was aspirated then the cells washed once with 1X PBS to minimize serum staining. After the wash, 400 µl of fresh sterile 1X PBS was added to the well, followed by 200 µl of 0.4% trypan blue (Invitrogen). This mixture was allowed to incubate for 3 minutes. One field of vision was counted at a time, with cells that possessed a blue cytoplasm indicating a dead cell versus one that excluded the blue color. Five fields of vision per well per treatment was averaged to give the mean cell viability per treatment sample group. There were 3 wells per treatment group.

2.4 Western Blot

After MIN6 cells were plated into 6-well dishes and treated with statins or AY 9944 for 48 hours, they were then washed once with 1X PBS and 1 ml of clean 1X PBS added to each well. Cells were then scraped off using a rubber scraper and dispensed into sterile Eppendorf tubes. The tubes were then centrifuged for 5 minutes at 3000 g, and the supernatant removed. 50 µl of immune-precipitation (IP) buffer (150 mM NaCl, 20 mM Tris-HCl pH 7.4, 1 mM EDTA, 1mM EGTA with 1% Triton-X100) was then added to the pellets. Samples underwent Bradford assay to determine protein content and 20 µg of protein, along with a protein ladder, was loaded into a 1X sodium dodecyl (lauryl) sulfate-polyacrylamide gel (SDS-PAGE). Gel electrophoresis was then carried out and proteins were transferred onto a polyvinylidene difluoride-plus (PVDF) membrane (Fisher Scientific Ltd., Nepean ON). Primary antibodies were used to bind to the protein of interest on the membrane; K_v2.1 at 1:1000 dilution (Abcam, ON, Canada), Ca_v1.2 at 1:500 dilution (Alomone Labs Jerusalem, Israel), and β-actin at 1:5000

dilution (Cell Signalling Technology Inc., MA, USA). The secondary antibody used were anti-mouse or anti-rabbit HRP conjugated antibodies at the concentration of 1:20,000 (Jackson Immuno Research Laboratories, PA, USA). The proteins on the PVDF membranes were visualized via chemiluminescence using ECL (GE Healthcare, Mississauga ON) and captured on X-ray film (Eastman Kodak Co., Rochester NY, USA). Using ImageJ (NIH, United States), densitometry was performed on these films.

2.5 Cholesterol Isolation

MIN6 cells were treated for 48 hours with specified drug (i.e. AY 9944, statins). After the 48 hour period, media was removed and cells washed twice with cold 1X PBS. 1 ml PBS was then added and the cells were scraped off and collected into an Eppendorf tube. 200 µl of the collected cells were then placed into a different tube to run a Bradford assay. All tubes were then centrifuged at 3000 rpm for 5 minutes, and the supernatant was discarded. Tubes for cholesterol assays had 50 µl 2:1 chloroform-methanol and 100 µl PBS added to them, while the tubes for Bradford assays had 50 µl IP buffer (150 mM NaCl, 20 mM Tris-HCl pH 7.4, 1 mM EDTA, 1mM EGTA with 1% Triton-X100), with protease inhibitor (Roche, Manheim, Germany) added to them. Bradford tubes were then set aside in at -70 °C for later use, and the cholesterol assay tubes mixed and set on ice for 10 minutes. Cholesterol samples were then centrifuged at 10,000 rpm for 5 minutes at 4°C. The top layer of the supernatant (PBS) was discarded, and the remaining 2:1 chloroform-methanol mixture was vacuum dried with a steady nitrogen stream. 200 µl cholesterol assay buffer (Cayman Chemical Company, Ann Arbor MI, USA) was then added to the dry cholesterol. This could be stored at -70 °C or used immediately.

2.6 Cholesterol Assay

A cholesterol standard was made from the provided cholesterol stock according to the manufacturer's protocol (Cayman Chemical Company). 50 µl of standard and samples (made from the protocol in 2.4 Cholesterol Collection) was loaded into each well of a 96-well plate. 50 µl of the assay cocktail was also added to each well and the plate covered. The plate was then incubated for 30 minutes at 37°C protected from light. After incubation the plate was read using a Fluoroscan Ascent plate reader (Thermo Scientific, Rockford IL, USA). The data was read using a fluorescence excitation wavelength of 560 nm and an emission wavelength of 590 nm, and analyzed using the Ascent Fluoroscan software.

2.7 Glucose-Stimulated Insulin Secretion (GSIS) Assay

Cells were seeded into multiple 6-well plates and grown to a confluency of approximately 60% prior to drug administration. Triplicates for each drug group were prepared (3 wells per drug) and cells washed once with 1X PBS after 24 hours prior to adding fresh treatment media. The cells were then incubated for 48 hours with FBS and LPS enriched media containing either 10 µM AY 9944 (Sigma-Aldrich), 10 µM pravastatin (Sigma-Aldrich), 10 µM Atorvastatin (Tocris Bioscience, Ellisville MO, USA), or no drug at all. After 48 hours, cells were washed with 1X PBS and incubated for 2 hours in 1 mM low glucose DMEM media (Sigma-Aldrich). During this time, KRB buffer was prepared (129 mM NaCl, 5 mM $NaHCO_3$, 4.8 mM KCl, 2.5 mM $CaCl_2$, 1.2 mM KH_2PO_4, 2.4 mM $MgSO_4$, 10 mM HEPES, and 0.1% BSA). A volume of 50 ml low glucose KRB (1 mM glucose) and 50 ml high glucose KRB (16.7 mM glucose) were prepared in separate tubes. After the 2 hour incubation, the cells were then washed once with 1X PBS and 500 µl low glucose KRB added to each well. The plates were then incubated for 30 minutes. After 30

minutes, the media was aspirated from each well and 1 ml of low glucose KRB added, this was then incubated for 1 hour. The media was then collected and spun down at 3000 rpm for 5 minutes. 500 µl of the supernatant was kept and stored at -20°C for later analysis. 1 ml of high glucose KRB was then added to each well and incubated again for 1 hour, then collected and spun down at 3000 rpm for 5 minutes. Again, 500 µl of the supernatant was kept and stored at -20°C. The plates were then washed once with cold 1X PBS then 1 ml of sterile 1X PBS was added. Each well was then scraped and collected into two tubes filled with 500 µl each of the cell lysate. One tube would be kept for a Bradford assay, which was spun down for 5 minutes at 3000 rpm, supernatant removed, and 50 µl of IP buffer added (150 mM NaCl, 20 mM Tris-HCl pH 7.4, 1 mM EDTA, 1mM EGTA with 1% Triton-X100). The other set of tubes were then sonicated at 15% amplitude for 20 seconds to homogenize the sample, using a Fisher Scientific Sonic Dismembrator 500 (Fisher Scientific Company, Ottawa ON). These samples were used to quantitate the amount of total insulin content in the cells and stored at -20°C.

2.8 ELISA Assay

ELISA was performed using the samples obtained from the GSIS assays. 96 well plates were coated using 100 µl/well of D6C4 insulin-proinsulin, rat-mouse antibody (Hy-Test Ltd., Turku, Finland) diluted in 1X PBS for a working concentration of 2 µg/ml. The plate was then stored overnight at 4 °C. The contents were discarded and the plate was then tap-dried. Afterward, 300 µl of blocking buffer (1% BSA, 5% sucrose in 1X PBS) was added to each well and the plate incubated for 2 hours at room temperature. The blocking buffer was then discarded and the plate tap-dried, and then placed in a ventilation hood for 1 hour. The coated 96 well plate was then wrapped in foil and kept at 4 °C overnight for storage.

A stock sample of insulin was diluted in ELISA dilution buffer (1% BSA in 1X PBS) to create a standard. Collected samples of cell supernatant and whole cells were diluted in dilution buffer for readings within the standard curve. The samples and standards were then loaded into a 96 well plate for a final volume of 100 µl/well. This was then incubated on a rocker for 1 hour at room temperature. After incubation, the wells were emptied and tap-dried. Wash buffer (0.1% Tween-20 in 1X PBS) was then added at a volume of 200 µl/well, placed on an orbital rocker for 2 minutes, then dried. This was repeated 3 times. D3E7-HRP secondary antibody (Hy-Test Ltd., Turku, Finland) was then loaded at a volume of 100 µl/well with a concentration of 0.5 µg/ml in ELISA dilution buffer. The plate was then incubated again at room temperature for 1 hour on a rocker. After incubation, 100 µl of ready to use Pierce TMB-ELISA (Thermo Scientific) was added to each well and incubated at room temperature for 10-15 minutes, or until a significant color change was detected. The plates were then read using a DTX 880 Beckman Coulter 96-well plate multimode detector for absorbance at 450 nm (Beckman Coulter, Mississauga ON). The data was then analyzed using Beckman Coulter's multimode analysis software.

2.9 DNA Amplification

An Eppendorf tube containing approximately 50 µl of competent DH5α bacterial cells were thawed and 1 µl of the plasmid DNA to be amplified was added (see sections 2.10 and 2.11 below for plasmid details). The tube was then gently mixed and placed on ice for 30 minutes. The bacteria was heat shocked by being placed in a 37°C water bath for 30 seconds then back on ice for 2 minutes. 200 µl LB medium (1% w/v tryptone, .5% w/v yeast extract, 1% w/v NaCl, pH to 7.0) was then added to the tube and incubated at 37 °C for 1 hour with vigorous shaking (250 rpm). 50 µl was pipetted onto antibiotic treated LB plates (3 g agar, 200 ml LB medium, 20 mg kanamycin or ampicillin) and incubated

at 37 °C overnight. A single colony was picked and allowed to grow for 8 hours in a tube containing 5 ml of selective LB medium at 37°C with vigorous shaking (250 rpm). The tube was then transferred into a pre-weighed 50 ml tube containing 45 ml of selective LB medium and allowed to grow overnight (12-16 hours). After the incubation time, the tube was weighed again to obtain the pellet wet weight. If the contents of the tube weighed ~3 g/liter, the tube was centrifuged at 6000g for 15 minutes at 4 °C. The supernatant was then removed, keeping only the pellet.

A Promega PureYield Plasmid Midiprep system (Promega Corporation, Madison WI, USA) was then used to isolate the plasmid DNA from the pellet obtained from the previous steps. 3 ml Cell Resuspension Solution was added to the harvested pellet followed by 3 ml Cell Lysis Solution. The tube was then inverted 4 times to mix. 5 ml Neutralization Solution was then added to stop the lysis reaction. The lysate was centrifuged at 15000g for 15 minutes and then the supernatant carefully decanted into a PureYield clearing column. The lysate was then vacuumed through the clearing column and into a binding column which captured the DNA. Afterward, 5 ml Endotoxin Removal Wash was added and vacuumed through the column, followed by 20 ml Column Wash Solution. The DNA was then eluted into a sterile Eppendorf tube using 500 µl Nuclease-Free water and the concentration measured using a NanoDrop system (Thermo Scientific).

2.10 Luciferase Promoter Assay

MIN6 cells were passed into 6-well plates and incubated overnight in regular FBS enriched media. Once the confluency reached approximately 60% per well, the cells could be used for transfection. A mixture of 2 µl Lipofectamine-2000 (Invitrogen), 1 µg plasmid DNA and 0.1 µg *Renilla* DNA (details below), was added for every 1 ml of total Opti-Mem media (Invitrogen). This mixture was

allowed to incubate at room temperature for 30 minutes prior to adding to the cells. After the incubation time, the plated cells were aspirated and washed once with 1X PBS before adding 1 ml of the DNA containing Opti-Mem mixture to each well. The plates were then incubated overnight in a 37°C incubator. After this period, the transfection mixture was aspirated from the plates and appropriate treatment media was added to the wells. The cells were then incubated for 48 hours, changing the treated media after 24 hours. After the treatment period, the cells were washed twice with cold 1X PBS and then 300 µl of lysis buffer was added to each well (20 mM Tris at pH 7.4 with 0.1% Triton-X100). The cells were then collected using rubber scrapers into labeled Eppendorf tubes and vortexed for 10 seconds. The tubes were then centrifuged at 12,000 rpm in 4°C for 10 minutes. 20 µl of the supernatant was then added to 5 ml luminometer tubes to be used for both the luciferase and *Renilla* luciferase readings. A Promega Luciferase Assay System (Promega Corporation, Madison WI, USA) was used to determine luminescence of all the samples on an EG&G Berthold – Lumat LB 9507 luminometer (Berthold Technologies GmbH & Co. KG, Bad Wildbad, Germany).

Test Plasmids

The cells were transfected with one of three luciferase containing plasmids fused with either the rat insulin-1 promoter, L-type Ca^{2+} channel α_{1C} subunit promoter, or the $K_v2.1$ promoter. Ins715-Luc was the reporter plasmid used to assay for rat insulin-1 promoter activity. It contained the gene promoter fragment from -715 to +31 bp of the rat ins-1 gene, cloned into the *SmaI* site of a basic pGL2 vector from Promega (courtesy of Dr. Michiyo Amemiya-Kudo; Amemiya-Kudo *et al.,* 2005). The L-type Ca^{2+} channel α_{1C} subunit reporter plasmid was created by inserting the -1727 to +220 bp region of Isoform A of the CACNA1C gene into a pGL3 vector (Promega). The fragment was inserted into the poly-linker region using the *BamHI* restriction site (courtesy of Dr. Stanley Nattel; Pang *et al.*, 2003). Finally, the $K_V2.1$ reporter plasmid was generated using the KCNB1 gene from mouse which was 1601 bp in length. It was

inserted into the pGL2 vector (Promega) at the *KpnI* and *XhoI* restriction sites (courtesy of Dr. David McKinnon; Rosati *et al.*, 2008). Each sample was also transfected with a *Renilla* luciferase plasmid (phRL-SV40) at a 1,000 fold lower concentration than the test plasmids, to act as an internal control.

2.11 Secreted Alkaline Phosphatase (SeAP) Luciferase Assay

Cells were passed into 6-well plates and incubated overnight in regular FBS enriched media. Once the confluency reached approximately 60% per well, the cells could be used for transfection. A mixture of 2 µl Lipofectamine-2000, 1 µg plasmid DNA (Genecopoeia, Rockville MD, USA) was added for every 1 ml of total Opti-Mem media. This mixture was allowed to incubate at room temperature for 30 minutes prior to adding to the cells. After the incubation time, the plated cells were aspirated and washed once with 1X PBS before adding 1 ml of the DNA containing Opti-Mem mixture to each well. The plates were then incubated overnight in a 37°C incubator. After this period, the transfection mixture was aspirated from the plates and appropriate treatment media was added to the wells. The cells were then incubated for 48 hours, changing the treated media after 24 hours. The media was then collected and used in the Secrete-Pair Assay Kit protocol as provided by Genecopoeia. Briefly, a buffer mixture was prepared to cause fluorescence of the secreted Gaussia luciferase from the cell. 100 µl of this buffer mixture was then added to a luminometer tube holding 20 µl of the collected cell media. The tubes were then read on an EG&G Berthold – Lumat LB 9507 luminometer and the values recorded. Afterward, the collected cell media was heated to 65°C for 10 minutes then cooled on ice. A buffer mixture to detect secreted alkaline phosphate (SeAP) was then added at a volume of 100 µl to luminometer tubes containing 20 µl of heated cell media. These samples were then read on an EG&G Berthold – Lumat LB 9507 luminometer and again, recorded. The SEAP values were used to normalize the obtained Gaussia

luciferase luminescence readings. Gaussia luciferase was attached to the promoter sequence of interest, whereas SEAP was attached to a constitutively expressed promoter region on the same plasmid.

Test Plasmids

Cells were transfected with one of four different pEZX-PG04 (see appendix figure **A1**) vectors fused with promoter sequences. The vector itself contained Gaussia luciferase downstream of the promoter of interest, followed by Secreted Alkaline Phosphotase (SeAP) downstream of a CMV promoter to act as an internal control. The test promoters were syntaxin 1A (brain) (STX1A), 978 bp in length; potassium inwardly-rectifying channel, subfamily J, member 11 (KCNJ11), 1417 bp in length; synaptosomal-associated protein 25 kDa (Snap25), 1287 bp in length; or a negative control clone which was a pEZX-PG04 vector with no test promoter.

2.12 RNA Isolation

Cells were plated into 6-well plates and treated with drug or no drug for 48 hours. Afterward, the media was aspirated and then the cells were washed once with 1X PBS. A RNeasy Mini kit from Qiagen was used for the RNA isolation (Qiagen Inc., Mississauga ON). 350 µl of Buffer RLT containing 1% v/v β-mercaptoethanol was added to each well and the cell lysate was collected using a rubber scraper. The cell lysate was then transferred to an Eppendorf tube and vortexed for 10 seconds to mix. 350 µ of 70% ethanol was then added to each tube and was mixed by pipetting. The entire contents of each tube (700 µl) was then transferred into an RNeasy mini spin column and centrifuged at 10,000 rpm for 15 seconds. 700 µl of Buffer RW1 was then pipetted into the RNeasy column and centrifuged again for 15

seconds at 10,000 rpm to wash. 500 µl of Buffer RPE was added, and again centrifuged for 15 seconds at 10,000 rpm, followed by the addition of another 500 µl of Buffer RPE for a second wash. The RNeasy spin column was then placed on top of a new eppendorf tube. 40 µ of RNase-free water was added and then collected by centrifuging again at 10,000 rpm for 1 minute. The concentration was measured afterward using a NanoDrop, ensuring that the A_{260} : A_{230} ratio was greater than 1.7, the A_{260} : A_{280} ratio was between 1.8-2.0, and the concentration determined by the A_{260} was greater than 40 µg/ml.

2.13 cDNA Synthesis

Using isolated RNA from the protocol described above in **2.12**, cDNA was synthesized using the Qiagen RT^2 First Strand Kit (Qiagen). Briefly, 0.8 µg total RNA was added to 2 µl buffer GE and brought to a total volume of 10 µl using high grade RNase-free water. This mixture was then incubated at 42 °C for 5 minutes then placed immediately on ice for 1 minute. This eliminated genomic DNA. 10 µl of reverse-transcription mix was then added to each tube of the genomic DNA elimination mixture and incubated at 42 °C for 15 minutes, followed by a 5 minute incubation at 95 °C to stop the reaction. 90 µl of high grade RNase-free water was then added to each tube containing cDNA. The samples were stored at -20 °C or used immediately.

2.14 RT-qPCR Array

Using the cDNA made via the protocol described above in **2.13**, a PCR component mix was made by adding high-grade RNase free water and RT^2 SYBR Green Mastermix (Qiagen) roughly in a 4:46:50

ratio respectively, as suggested by the manufacturer. A customized PCR array 100-well disc was purchased from SABiosciences and used for all PCR-Array runs. The genes of interest for this custom array included Slc2a2 (Glut-2 transporter), Kcnb1 (K_v2.1 channel), Abcc8 (SUR sub-unit of the K_{ATP} channel), Cacna1c (Ca_v1.2 α1C subunit), Cacna1d (Ca_v1.2 α1D subunit), Kcnj11 (K_{ATP} channel), Ins1 (insulin-1), Ins2 (insulin-2), Hmgcr (HMG-CoA reductase), Dhcr7 (7-dehydrocholesterol reductase), Fdft1 (squalene synthase), Stx1a (syntaxin-1a), Stx4a (syntaxin-4a), Snap25, Snap23, Vamp1 (synaptobrevin-1), Vamp2 (synaptobrevin-2), Abca1 (ATP Binding Cassette A1), Ldlr (low density lipoprotein receptor), and GAPDH (glyceraldehyde-3-phosphate dehydrogenase) to serve as the reference gene. A positive control (Qiagen's Positive PCR Control – PPC) and a negative control (Qiagen's Reverse Transcriptase Control – RTC), were also included in each sample to ensure the polymerase chain reaction occurred succesfully. 25 µl of the complete PCR components mixtures of each treatment group were then added to individual wells containing all the aforementioned gene primer templates. The custom array disc was then sealed using a Qiagen heat sealer, and loaded into a Rotogene-Q thermocycler for reading (Qiagen). The disc was first centrifuged at room temperature at 1000 g to ensure all bubbles in the wells were removed. Afterward, the cycling conditions were designated prior to starting the PCR-Array run. The cycles involved were one 10 minute cycle at 95 °C to activate the HotStart DNA *Taq* polymerase then afterward, forty repetitions of 15 s at 95 °C followed by 1 minute at 60 °C, cycles. Fluorescence was measured during the forty cycles of amplification.

Interpretation of the acquired data was done using the web-based RT² Profiler™ PCR Array Data Analysis program (http://www.sabiosciences.com/pcrarraydataanalysis.php). GAPDH was chosen as the reference gene used as an internal control, while either FBS or LDPS groups with no drugs, were designated as the control group.

2.15 Patch-Clamp

MIN6 cells were treated and incubated for 48 hours with a drug concentration of 10 µM in 1 ml FBS or LPS in 35 mm plates. Following the 48 hour treatment period, the serum was removed and replaced with 1 ml of external bath solution (140 mM NaCl, 4 mM KCl, 1 mM $CaCl_2$, 1 mM $MgCl_2$, 10 mM glucose and 5 mM HEPES) used for patch clamp. Micropipettes were pulled from 4 inch glass filaments manufactured by World Precision Instruments (Sarasota FL, USA) with an inner diameter of 1.12 µm using a Sutter Instruments Co. Model P-97 micropipette puller (Novato CA, USA). The micropipettes were then heat polished at 90°C using a World Precision Instruments MF-200 microforge to remove contaminants and to smooth the edges of the tip. All micropipettes were used the same day that they were made in order to reduce the risk of dust and debris clogging the tip. Micropipettes were filled with approximately 200-300 µl of 0.2 µm filtered internal pipette solution (140 mM KCl, 1 mM $MgCl_2$, 5 mM EGTA, 10 mM HEPES and 5 mM MgATP) using a 1 ml syringe. Micropipettes were then inserted into a HEKA pipette holder connected to a HEKA EPC 10 patch clamp amplifier. Using a syringe connected to the pipette holder via tubing, positive pressure was applied to the micropipette before entering the bath solution to ensure any debris on the surface of the bath solution did not penetrate into the pipette tip. Individual cells were observed through a Nikon Eclipse TE2000-S microscope at 40x and, using a Burleigh PCS-5000 micromanipulator, the pipette was positioned to be directly over the cell membrane until a slight reduction in current pulses became noticeable, which indicated that the pipette tip was touching the membrane causing the seal resistance to increase. At this point, negative pressure was applied via the syringe in combination with hyperpolarizing the pipette to -80 mV in order to form a gigaseal (1 giga-ohm seal). Using the digital controls in the PulseFIT software package, the fast capacitance (C-fast) was adjusted for. The patch membrane was then broken by applying brief and gentle bursts of negative pressure. This provided access to the interior of the cell and caused an increase in capacitance to be

observed. Compensation for cell capacitance was achieved by adjusting the slow capacitance (C-slow) and R-series controls in PulseFIT. Current was then measured in response to voltage changes from -80 mV to 80 mV in increments of 10 mV. Currents were normalized to cell size using the slow capacitance values and a current-voltage relationship was plotted for each treatment group.

2.16 Statistical Analysis

Data was analyzed using Microsoft Excel (Microsoft; Redmond, WA, USA) and GraphPad Prism 5 (GraphPad Software, Inc.; La Jolla, CA, USA) software. Data were analyzed using one-way analysis of variance (ANOVA) followed by the Student-Newman-Keuls test. A p value of less than 0.05 was interpreted to be an indicator of statistical significance. Data are expressed as mean ± standard error of the mean (SEM) unless otherwise indicated.

3.0 Results

3.1 Manipulation of Cellular Cholesterol

The purpose of my thesis was to assess the effects of modifying cholesterol within a β-cell. Thus being able to verify and quantitatively assess the degree of cholesterol reduction under varying treatments was of the utmost importance. It not only laid the groundwork for my analysis and interpretation of all future experiments, but it also provided the option of viewing data with the intention of establishing a potential correlational relationship with cholesterol content. Finally, the cholesterol assays also let me confirm the efficacy of the treatment groups (and drugs) used in my experiments.

Cholesterol availability was manipulated by limiting the two ways through which the β-cell could obtain cholesterol. The first method of cellular cholesterol acquisition was through endogenous means, namely the cholesterol biosynthetic pathway. This pathway was inhibited using one of three different drugs in each treatment group. Two of the treatment groups involved use of statins. Statins selectively inhibit the rate limiting enzyme, 3-hydroxy-3-methyl-glutaryl-CoA reductase (HMGCR) (refer to **fig. 4**). The two statins I used in my thesis are atorvastatin, which is used clinically for intensive lipid lowering therapy, and pravastatin, which is typically used for patients that need to achieve only a moderate decrease in lipid content (Doggrell, 2004). Structurally, atorvastatin is more hydrophobic and pravastatin is more water soluble. The third drug (AY 9944) was used to selectively inhibit the last enzyme in cholesterol biosynthesis pathway, 7-dehydroxycholesterol reductase or DHCR7 (refer to **fig. 4**). AY 9944 is not used clinically, but is regularly employed for research on DHCR7-related pathologies, such as Smith-Lemli-Opitz Syndrome (Herman, 2003; Honda *et al.*, 1998; Kolf-Clauw, 1996; Xu *et al.*, 2012).

The second method by which I limited cellular cholesterol availability was through the use of lipid-free serum (LPS) in cell media. This eliminated the exogenous source of cholesterol by removing all lipids in the extracellular space. Additionally, for assays looking at both exogenous and endogenous manipulation of cholesterol availability, the aforementioned drugs were administered while cells were incubated in LPS media.

As seen in **figure 6**, all treatment groups, when compared to the control group of MIN6 cells grown in FBS media, displayed a significant ($p < 0.05$) reduction in total cholesterol content. Additionally, the treatment groups involving both drug administration and restrictive LPS enriched media usage displayed a further reduction in total cholesterol content than any other treatment groups, and did not significantly differ between the three drugs (atorvastatin, pravastatin, AY 9944). When comparing the efficacy of drug usage in FBS supplemented media, the reduction was uniform across all three drugs used as well, and more interestingly, did not reduce total cholesterol any lower than the cells with no drug but only LPS media.

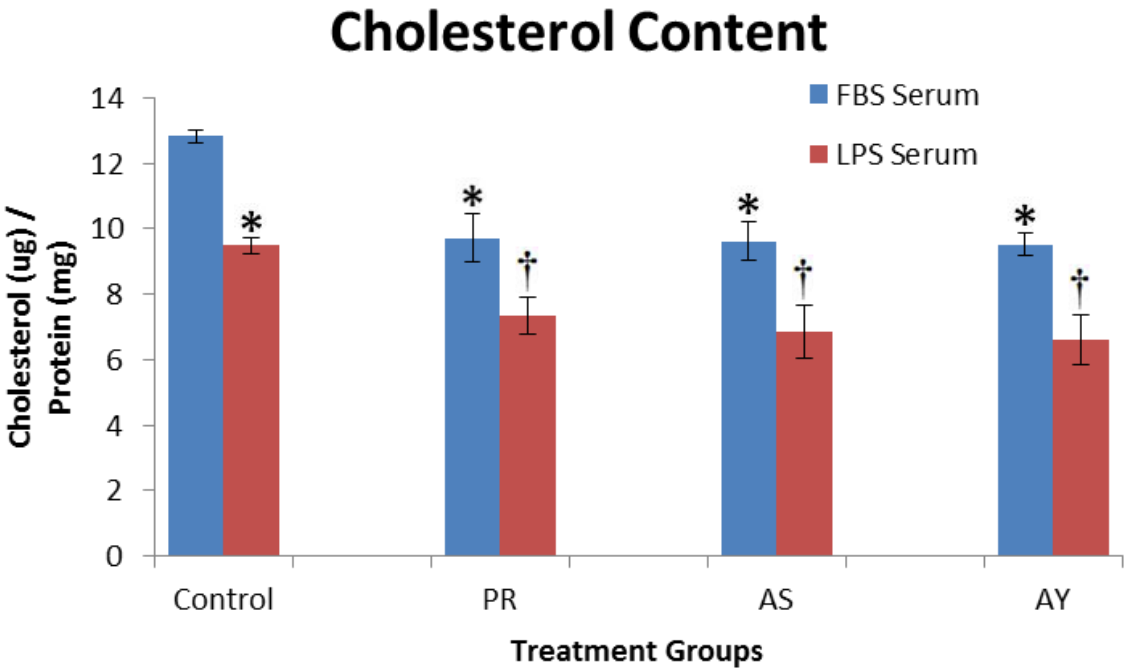

Figure 6. Cholesterol Content in treated MIN6 cells. Control groups were cells cultured in media with either FBS or LPS (Lipid Depleted Serum). LPS control (9.5±0.2 μg cholesterol/mg protein, $p < 0.05$, n=3), pravastatin in FBS (9.7±0.8 μg cholesterol/mg protein , $p < 0.05$, n=3), atorvastatin in FBS (9.6±0.6 μg cholesterol/mg protein, $p < 0.05$, n=3), and AY9944 in FBS (9.5±0.3 μg cholesterol/mg protein, $p < 0.05$, n=3) were all equally reduced when compared to the FBS control group (12.8±0.2 μg cholesterol/mg protein, n=3). A further reduction in cholesterol was seen in treatment groups containing drug and LPS serum. This reduction was significantly lower than FBS serum control, but only AY-LPS was significantly lower than both AY-FBS and LPS alone ($p < 0.05$). Pravastatin in LPS was reduced to 7.4±0.6 μg cholesterol/mg protein ($p < 0.01$, n=3), atorvastatin in LPS was 6.8±0.8 μg cholesterol/mg protein ($p < 0.01$, n=3), and AY9944 6.6±0.8 μg cholesterol/mg protein ($p < 0.01$, n=3) when compared to FBS serum control.

3.2 Cell Viability Assays

After establishing the degree of cholesterol reduction under the varying treatment groups, I conducted a series of experiments to ensure that the changes seen in cholesterol content did not induce any cell toxicity or increased cell death. The trypan blue exclusion test uses a very simple approach to visualizing overall cell health in a particular culture. The principle with which it works off of is that live cells possess intact membranes capable of excluding dyes (such as trypan blue, eosin etc.), whereas dead cells possess compromised membranes and are unable to keep dyes out (Strober, 1997). 6-well plates were incubated with a diluted trypan blue mixture, but washed prior in an attempt to minimize serum staining (which was not always achievable as seen in **Figures 8a-e**). However, it was still quite easy to distinguish cell staining from serum staining when trypan blue stock was diluted with 1X PBS, so this posed as a small issue. Several fields of vision were used to obtain mean cell viability, as seen in **figure 7**. The only significant reduction in cell viability was witnessed in the AY 9944 drug group, roughly a 10% reduction in cell viability (from 85.4 ± 3.1% for control MIN6 cells in FBS, to 75.0 ± 5.2% in AY 9944 treated cells). Cells treated with either pravastatin or atorvastatin were not significantly affected by their respective drug administration, however, AY 9944 results had to be viewed a bit more critically. As such I could still remain confident that cell death had little to no influence on the collected data.

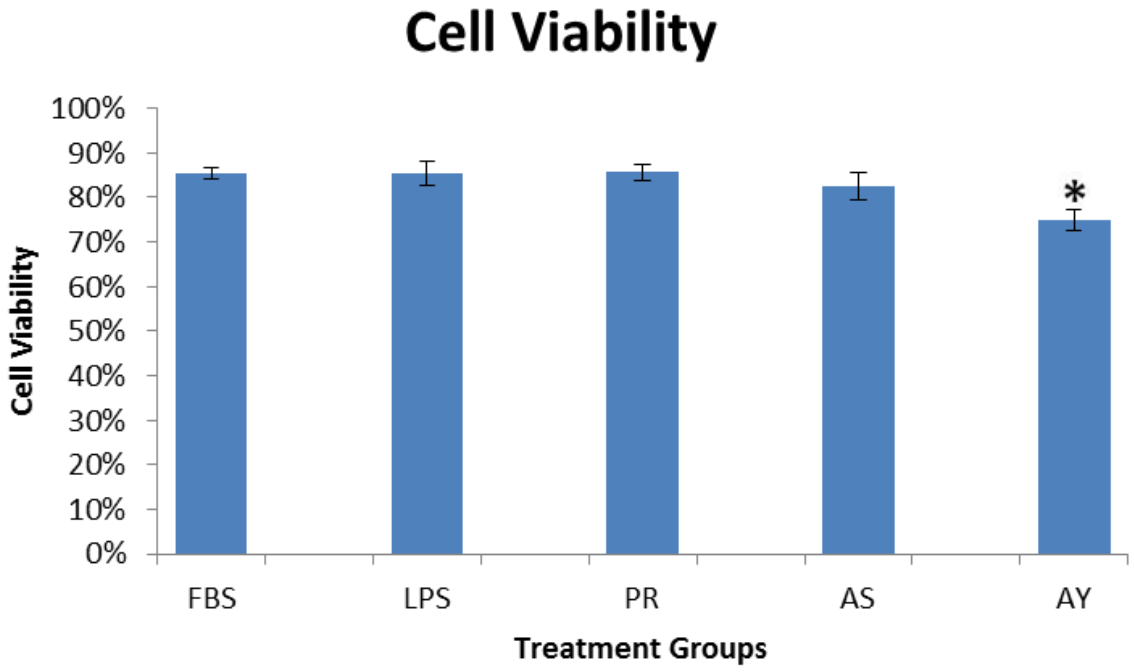

Figure 7. Cell Viability in treated MIN6 cells. Trypan blue exclusion test results did not significantly differ between treatment groups and the FBS control group (85.4±1.4% viability, n=5) except for cells treated with AY9944 (75.0±2.3%, $p < 0.05$, n=5) which differed from all other groups significantly, except for atorvastatin ($p = 0.182$).

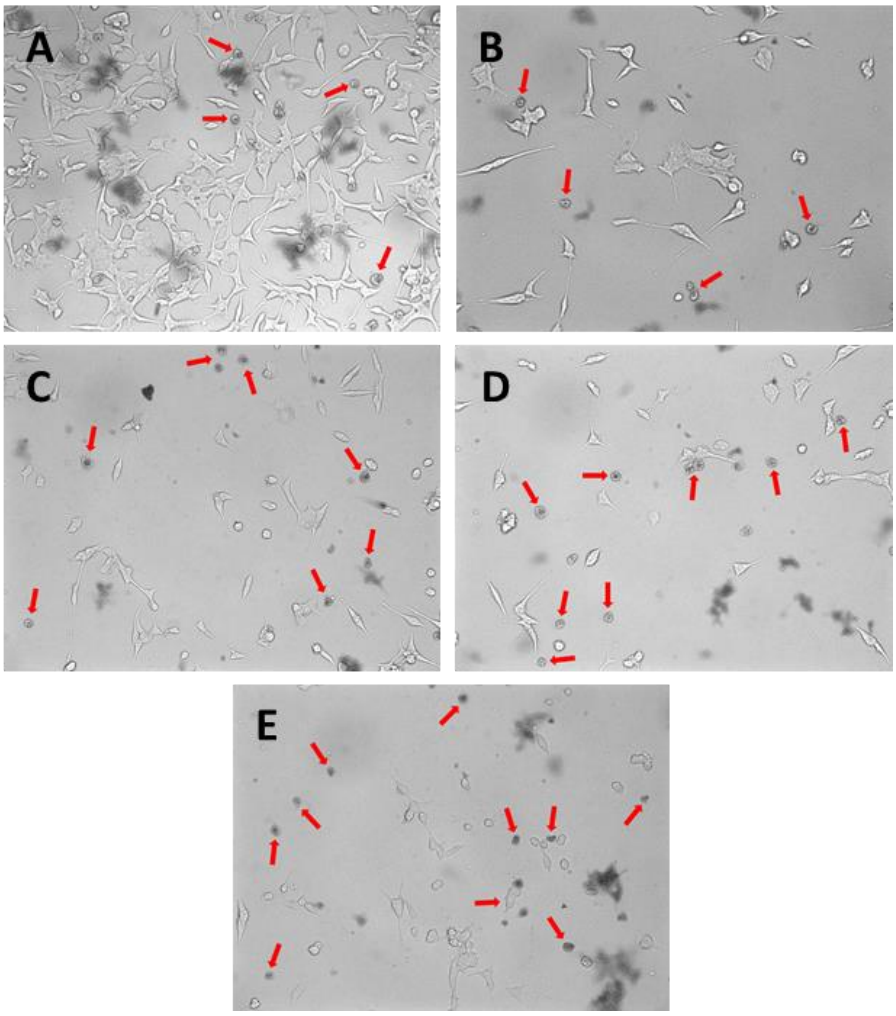

Figures 8a-e. Light microscopy images of trypan blue exclusion test. Light microscopy images of a field of view count for each treatment group (A: FBS, B: LPS, C: 10 µM pravastatin, D: 10 µM atorvastatin, E: 10 µM AY9944). Serum staining is seen as dark blue in the background. Dead cells are circular and filled with the trypan blue dye. Healthy MIN6 cells have excluded the dye and possess a dark, solid blue outline along their membrane.

3.3 Glucose-Stimulated Insulin Secretion and Insulin Content

In order to assess the effects that limiting cholesterol availability had on β-cell function, glucose-stimulated insulin secretion (GSIS) assays were conducted. The data obtained from GSIS assays and insulin content assays provided tremendous insight on the differential effects of my treatment groups, and to what degree the β-cell's ability to mount a response to glucose challenges were reduced. Data was obtained for both basal insulin secretion (1 mM glucose KRB buffer) and glucose stimulation (16.7 mM glucose KRB buffer) conditions. Since 5 mM glucose is typically seen as the threshold for healthy cells to mount a response to glucose (Ashcroft, 2004), the 16.7 mM glucose KRB buffer solution should have elicited a very strong reaction in the cells. As seen in **figure 9**, every treatment group aside from LPS enriched media alone without drug, had a significantly reduced glucose stimulation secretion response, whereas only the AY 9944 in FBS group displayed a signifcant change in basal insulin secretion. Additionally, all drugs in LPS media saw a further reduction in high glucose secretion when compared to their FBS enriched counterpart. This implied that limiting both exogenous and endogenous sources of cholesterol may have had a compounded effect on the ability of a β-cell to mount a response to glucose challeneges, despite LPS enriched media not displaying any significant reductions in GSIS when compared to the FBS control. The only exception to this was AY 9944 treated cells, where both AY 9944 in delipidated (LPS) and regular FBS enriched media were not significanty different.

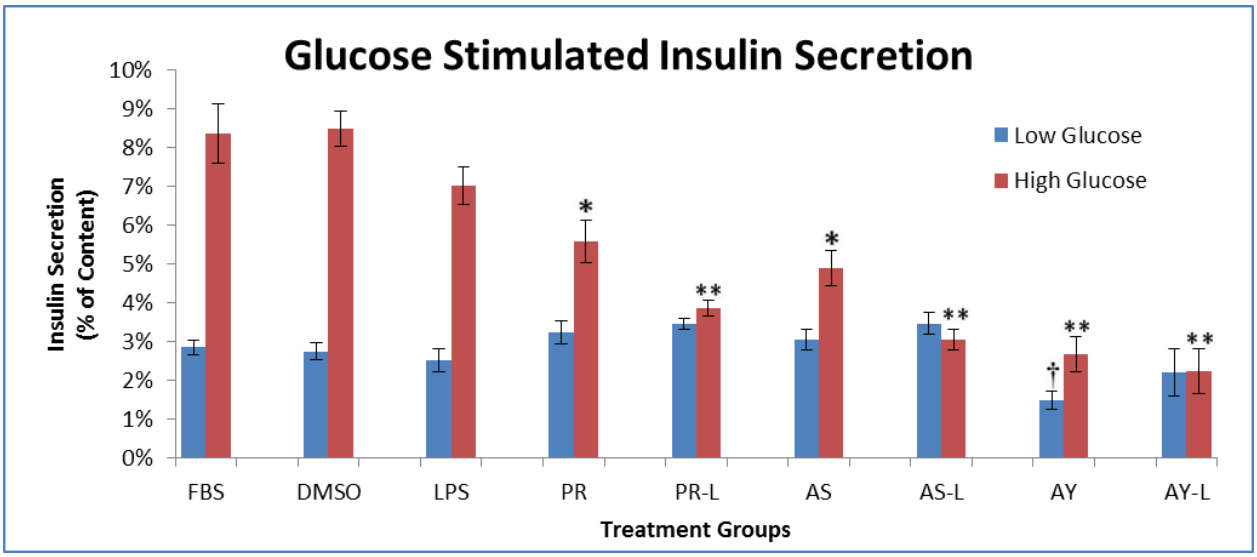

Figure 9. Glucose stimulated insulin secretion profiles of all treatment groups. Secretion was measured as a percent of total insulin content. Basal (1 mM glucose in KRB buffer) secretion is displayed as the blue columns, and high glucose stimulation (16.7 mM glucose in KRB buffer) secretion is displayed as the red columns. The only change in basal secretion occurred in the AY 9944 in FBS supplemented media treatment group (1.48 ± 0.23 % of total content). Changes in glucose stimulated secretion (16.7 mM glucose) was seen in all drug treatment groups, PR (5.58 ± 0.55 %) and AS (4.90 ± 0.46 %), with a further reduction in the LPS enriched groups, PR-L (3.86 ± 0.19 %), AS-L (3.05 ± 0.26 %), AY-L (2.23 ± 0.58 %), as well as AY 9944 in FBS (2.67 ± 0.45 %); $p < 0.05$, $n = 3\text{-}9$. * $p<0.0.5$ ** $p<0.01$ from FBS high glucose treated group.

Because of the differences seen in the secretion profiles of the treatment groups, the insulin content was measured to see if the changes were due to a decrease in overall content. As seen in **figure 10**, insulin content was normalized to overall protein content. Only four of the groups were found to have significantly reduced insulin content when compared to cells cultured normally in FBS enriched media (2.03 ± .06 μg insulin/mg protein). Pravastatin in LPS media (PR-L) was 1.26 ± 0.02 μg insulin/mg protein, atorvastatin in LPS media (AS-L) was 1.29 ± 0.07 μg insulin/mg protein, AY9944 in FBS media (AY) was 1.58 ± 0.12 μg insulin/mg protein, and AY9944 in LPS media (AY-L) was 1.170 ± 0.12 μg insulin/mg protein. The data suggests that the treatment groups with the most significant reduction in glucose stimulated secretion also had the only significantly different insulin content from the control group. However, the pravastatin and atorvastatin in FBS media could not be explained in this way, which had also seen a more modest, but significant, reduction in glucose stimulated secretion.

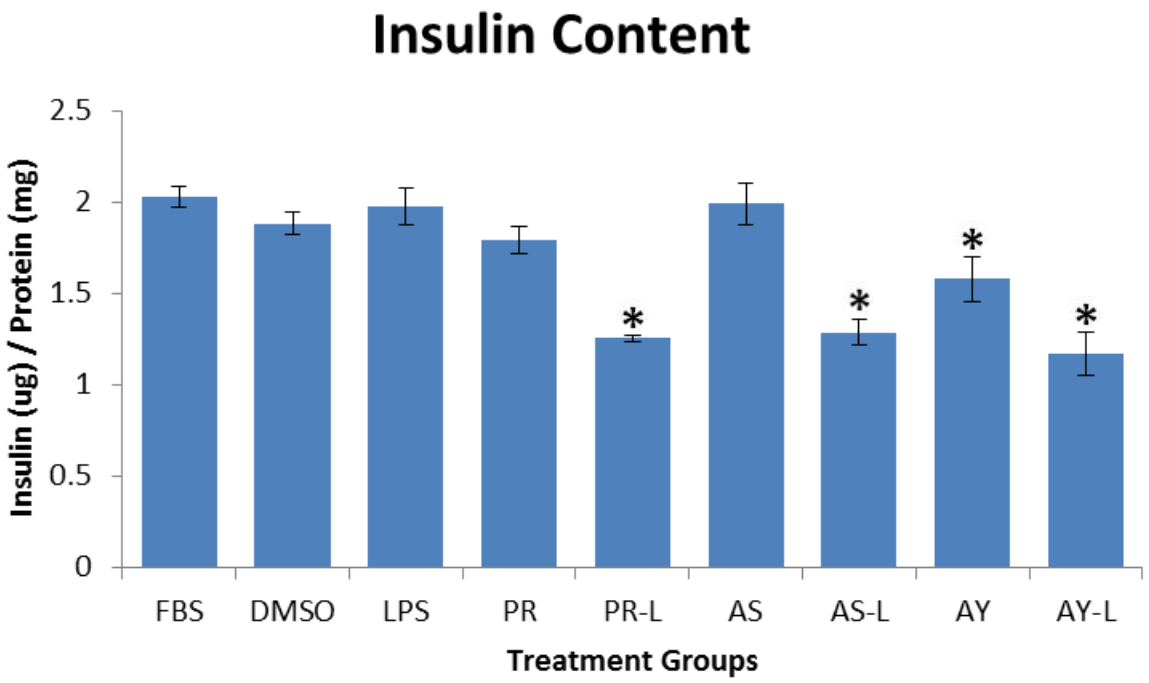

Figure 10. Insulin Content in treated MIN6 cells. Insulin content of each treatment group was normalized to protein content of each sample collected. Significant reductions in insulin content were seen in AY 9944 treated MIN6 cells (1.58 ± 0.12 µg insulin/mg protein), and in the cells grown in the presence of either statin or AY 9944 and delipidated serum (LPS) (PR-L, 1.26 ± 0.02 µg insulin/mg protein; AS-L, 1.29 ± 0.07 µg insulin/mg protein; AY-L, 1.17 ± 0.12 µg insulin/mg protein). * $p < 0.05$, n = 3-6.

3.4 Luciferase Assays

After establishing that a change in GSIS profiles resulted in select treatment groups, it became of great interest to determine at what point within the secretion process this could be attributed to. I first examined whether manipulating cellular cholesterol in MIN6 cells affected the transcription of a number of proteins important for regulating insulin secretion. Promoter assays were carried out to search for any aberrant promoter activity of genes important both in the transduction of the electrical signal ($Ca_V1.2$, $K_V1.2$, Kir6.2 (KCNJ11) and synthesis of insulin required for secretion. Additionally, genes (STX1A, SNAP25) involved in the exocytotic fusion events became of great interest, as cholesterol is an important component of fusion pores.

Looking at the promoter activity of the insulin gene was the logical first step, as a trend did appear to exist between specific treatment groups' reduced secretion and decreased insulin content (see **figures 9** and **10**). The reduction in insulin promoter activity was also reflected in the insulin content assays. However, the remarkable reduction in promoter activity found in the AY 9944 group (38.6% the activity of the control group) was not reflected in the insulin content results.

The promoter activity of the $Ca_v1.2$ gene did not change significantly (Figure 12), except with a reduction in the AY 9944 group (~22%). However that is not to say that any changes in actual cellular content of this calcium channel or the localization of it, did not occur as a result of drug treatment with either statin or AY 9944. The $K_v2.1$ promoter activity assays however, displayed a great deal of changes due to drug treatment or LPS-enriched media alone. This subunit is part of the voltage-gated potassium channel responsible for stopping secretion.

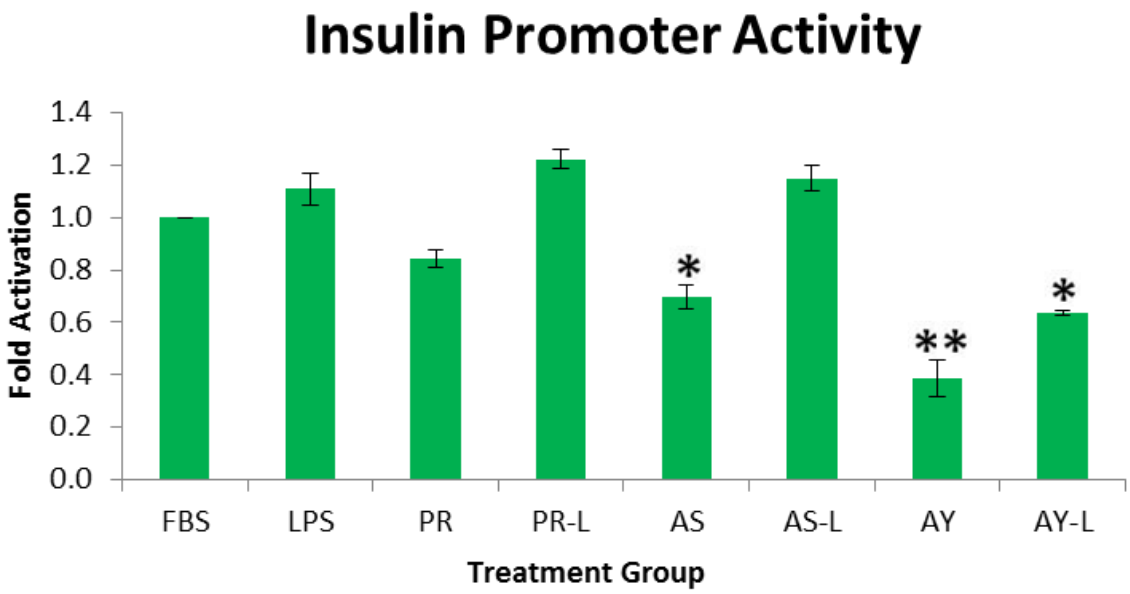

Figure 11. Insulin Promoter Activity. Gene promoter activity was measured as fold activation relative to the target gene's promoter activity under control conditions (MIN6 cells grown in FBS media). Three groups displayed reduced insulin-1 gene promoter activity, atorvastatin (AS; 0.69 ± 0.05, $p < 0.01$, $n = 6$), AY 9944 (AY; 0.39 ± 0.09, $p < 0.01$, $n = 3$), and AY 9444 in LPS media (AY-L; 0.63 ± 0.01, $p < 0$ .01, $n = 3$). * $p < 0.05$ and ** $p<0.01$ compared to FBS group.

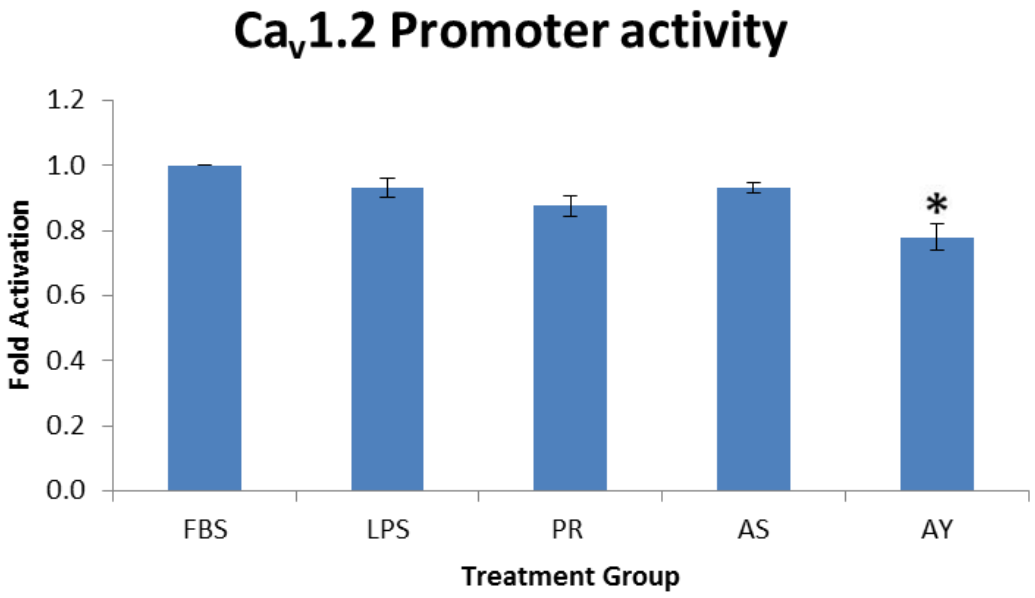

Figure 12. Voltage-Gated Calcium Channel Promoter Activity. The gene promoter activity for the α1C subunit of the L-type voltage-gated Ca^{2+} channel, $Ca_V1.2$, was measured as fold activation relative to the target gene's promoter activity under control conditions. The gene promoter activity was significantly reduced only in the AY 9944-treated group (AY; 0.78 ± 0.04, * $p < 0.01$, $n = 3$).

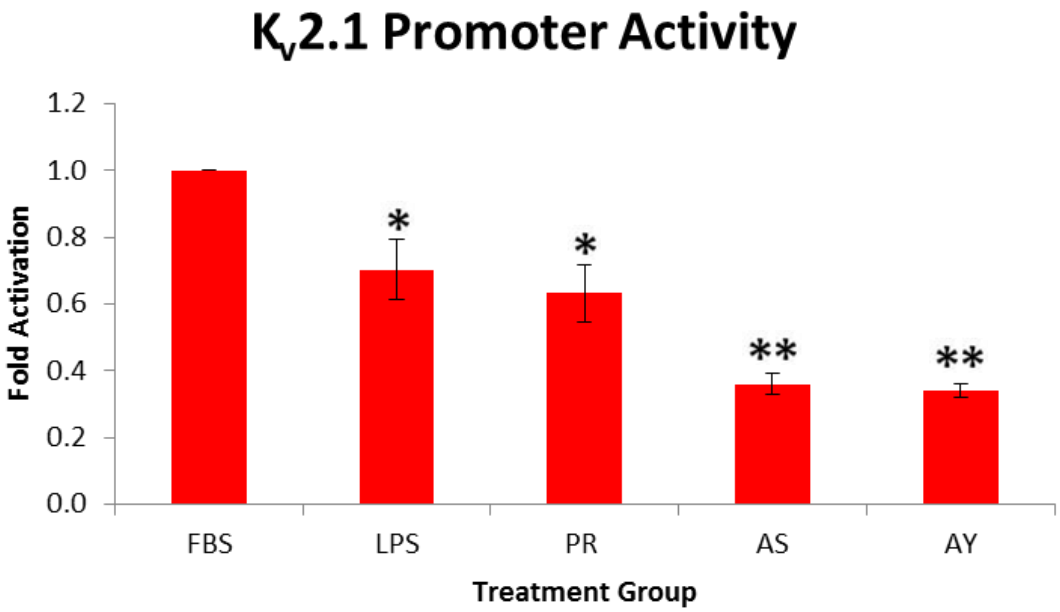

Figure 13. Voltage-gated Potassium Channel Promoter Activity. Promoter activity was measured as fold activation relative to the target gene's promoter activity under control conditions (FBS-enriched, no drug). Both LPS (0.703 ± .09, $p < 0.05$, $n = 3$) and PR (0.632 ± .087, $p < 0.01$, $n = 3$) were reduced by approximately 1/3 of normal activity, whereas AS (0.36 ± .031, $p < 0.01$, $n = 3$) and AY (0.342 ± .022, $p < 0.01$, $n = 3$), were reduced by more than half the fold activation of control. * $p < 0.05$ and ** $p < 0.01$ from FBS group.

Dual Luciferase

Dual luciferase assays were used to determine promoter activity of the remaining genes of interest. This new system employed the use of secreted alkaline phosphatase to normalize Gaussia luciferase signal across all samples collected. This method was used because of the availability of multiple reporters of interest from Genecopoeia®. The *KCNJ11* is the corresponding gene for the channel subunit, Kir6.2, of the ATP-sensitive potassium channel. This channel is essentially responsible for the initiation of the secretion response. As seen in **figure 14**, reporter activity for this gene was unaffected by drug treatment with the exception of MIN6 cells treated with atorvastatin. Surprisingly, there was approximately a 1.5-2 times enhancement of KCNJ11 promoter activity. Neither pravastatin nor AY9944 had any effect of KCNJ11 promoter activity.

The remaining reporter assays then looked specifically at SNARE proteins involved in the actual fusion of insulin-containing secretory granules. The reporter assays for the two SNARE proteins (STX-1A and SNAP25) involved in insulin granule fusion did not show any changes in reporter activity under any treatment group. The significance of this finding will be further discussed later on.

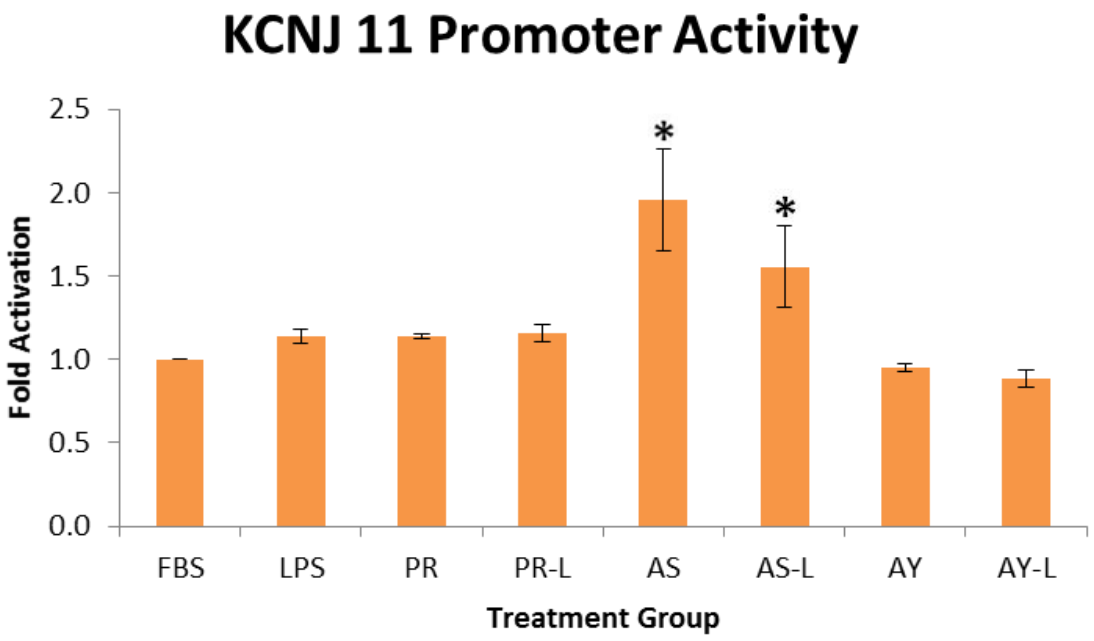

Figure 14. ATP-Sensitive Potassium Channel Promoter Activity. Promoter activity was measured as fold activation relative to the target gene's promoter activity under control conditions (FBS-enriched, no drug). Inwardly-rectifying potassium channel, subfamily J, member 11 (KCNJ11) promoter activity displayed little changes from the control group except when treated with atorvastatin (AS) in either FBS or LPS enriched media. AS (1.96 ± .306, $p < 0.05$, $n = 3$) and AS-L (1.56 ± .239, $p < 0.05$, $n = 3$) showed a significant increase in promoter activity, when compared control conditions. * $p < 0.05$ from FBS group

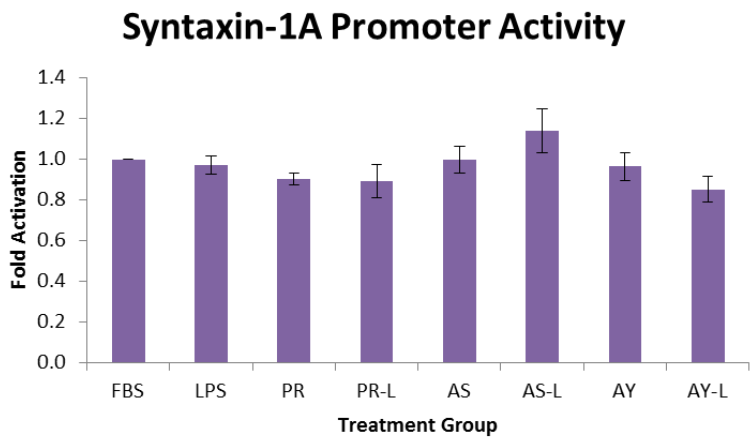

Figure 15. Syntaxin-1A Promoter Activity. Promoter activity was measured as fold activation relative to the target gene's promoter activity under control conditions (FBS-enriched, no drug). All treatment groups were performed 3-4 times. Syntaxin-1A promoter activity was not affected by any treatment group.

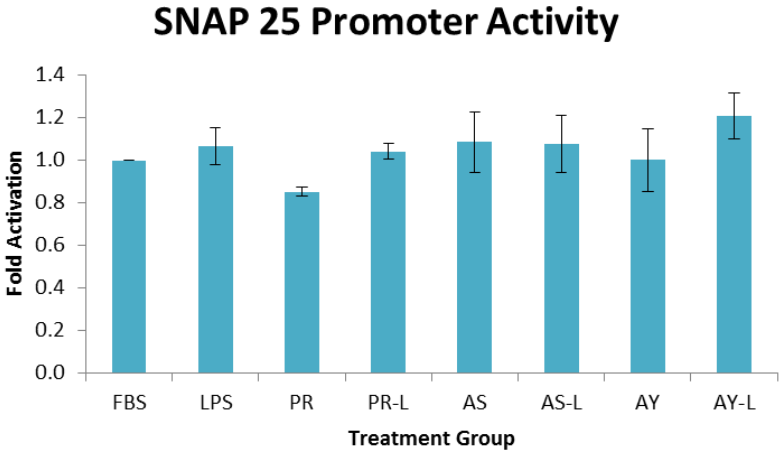

Figure 16. SNAP25 Promoter Activity. Promoter activity was measured as fold activation relative to the target gene's promoter activity under control conditions (FBS-enriched, no drug). All treatment groups were repeated with an n = 3-4. No significant changes in the activity of the promoter regulating SNAP25 were seen in any groups.

3.5 RT-qPCR Array Fold Regulation Analysis

To further explore the results obtained from the numerous gene reporter studies conducted to better understand potential expression changes in important proteins involved in insulin secretion, a large RT-qPCR Array experiment was designed. The analysis of mRNA content in cells treated with the different drugs, or drugs in LPS enriched media, could provide more insight on how much influence the changes at the transcriptional level had on the resulting GSIS profiles seen in **figure. 9**. The following series of fold regulation scatter plots were set to detect a minimum 2-fold change in mRNA content of the specific genes of interest (gene list available in appendix **A.13.**). **Figures 17a-f** show mRNA content change in treatment groups when the control group is normally cultured cells in FBS enriched DMEM cell media. **Figures 18a-c** show mRNA content changes in LPS enriched media treatment groups, when compared to normally cultured cells in LPS enriched DMEM cell media. **Table 1 and 2** summarize the total fold changes (numerically) of the mRNA content of the different treatment groups.

Atorvastatin had the most profound affect on the message level. Significant increases were measured for the mRNA levels of the voltage-gated calcium channel, α1D (Cacna1d), SNARE protein syntaxin1A (Stx1a), and the message for the enzymes in the cholesterol biosynthesis pathway, Hmgcr (HMG-CoA reductase), Dhcr7 (7-dehydrocholesterol reductase) and Fdft1 (farnesyl-diphosphate farnesyltransferase 1; also known as squalene synthase) when compared to MIN6 cells grown in control media. Reductions in the relative mRNA content for cholesterol efflux transporter, Abca1, was also seen (**figure 17b**). In contrast, no changes were observed with any of the mRNA levels in the pravastain group (**figure 17a**), and only Abca1 message content was decreased in MIN6 cells treated with AY9944 (**figure 17c**).

I hypothesized that treatment of MIN6 cells with the statins or AY9944 in delipidated serum-containing media would lead to greater changes in mRNA levels when compared to cells grown in delipidated media alone because of the previous results displaying a compounded effect of drug use and lipid restriction in the media. As seen in **figures 18a-c** and **Table 2**, pravastain, atorvastatin and AY9944 induced significant reductions (3- to 16.5-fold) in Abca1, as well as Kcnj11 and Vamp2 (AY9944). Surprisingly, only atorvastatin elicited a significant increase in the mRNA content of Hmgcr, Dhcr7, Fdft1 and Ldlr (low-density lipoprotein receptor).

Lastly, I did not observe any change in the mRNA levels of Kcnb1 ($K_V2.1$), Cancna1c ($Ca_V1.2$), Ins1 (insulin-1 gene) or Ins2 (insulin-2 gene) as seen with the promoter assays when referring to any of the aforementioned results.

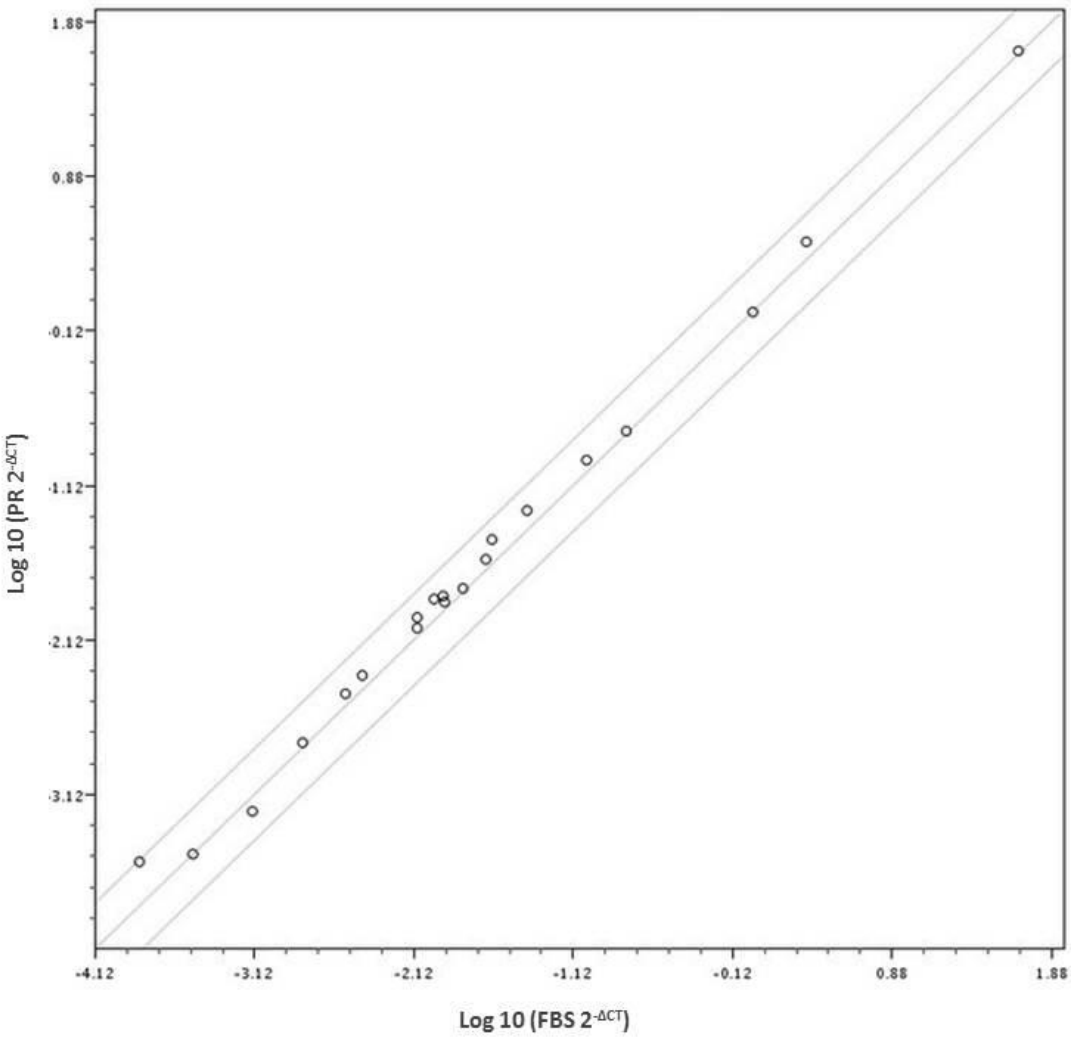

Figure 17a. Fold changes in mRNA content in MIN6 cells treated with pravastatin in FBS media (y-axis) relative to cells grown control FBS medium (x-axis). The outside lines denote a 2-fold up- or down-regulation of mRNA levels.

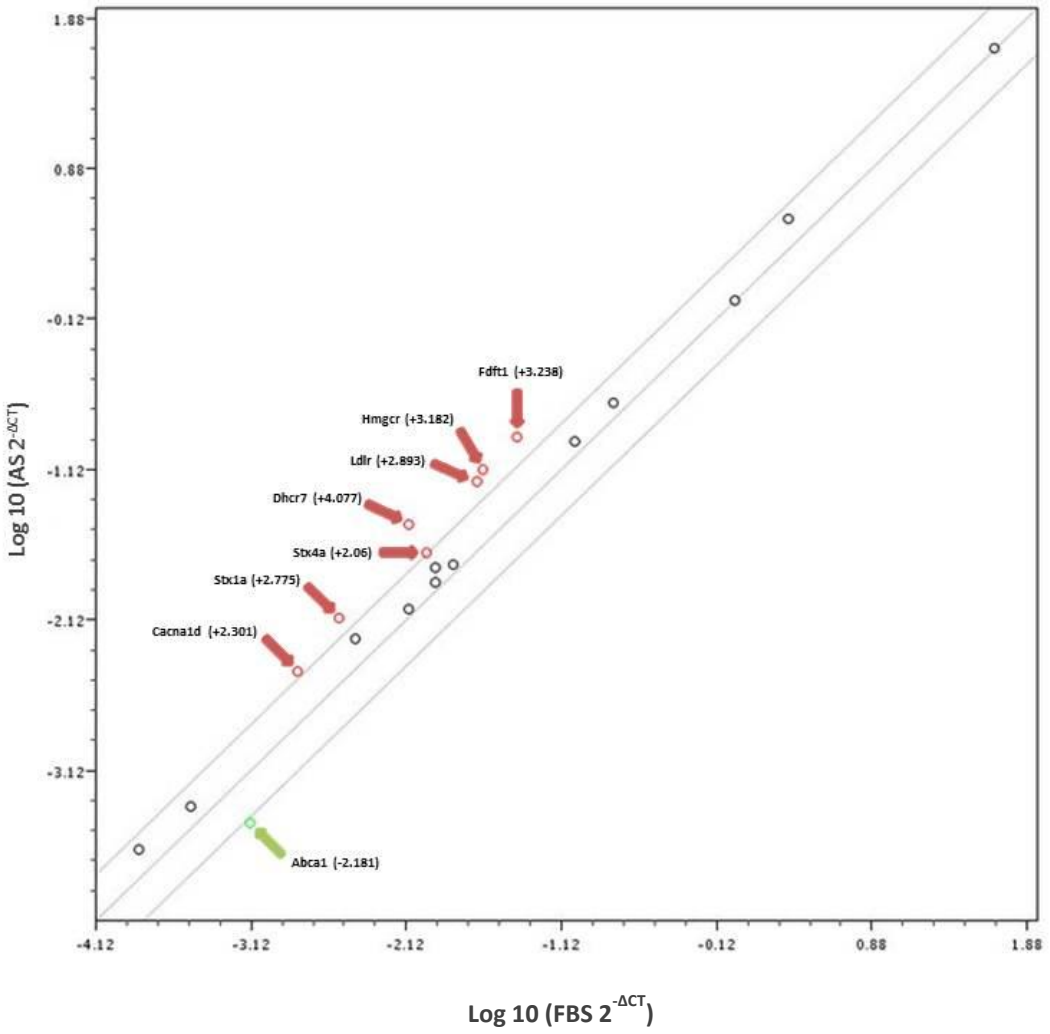

Figure 17b. Fold changes in mRNA content in MIN6 cells treated with atorvastatin in FBS media (y-axis) relative to cells grown control FBS media (x-axis). The outside lines denote a 2-fold up- or down-regulation of mRNA levels. Specific fold changes are identified by the red arrows (upregulated) or green arrow (downregulated).

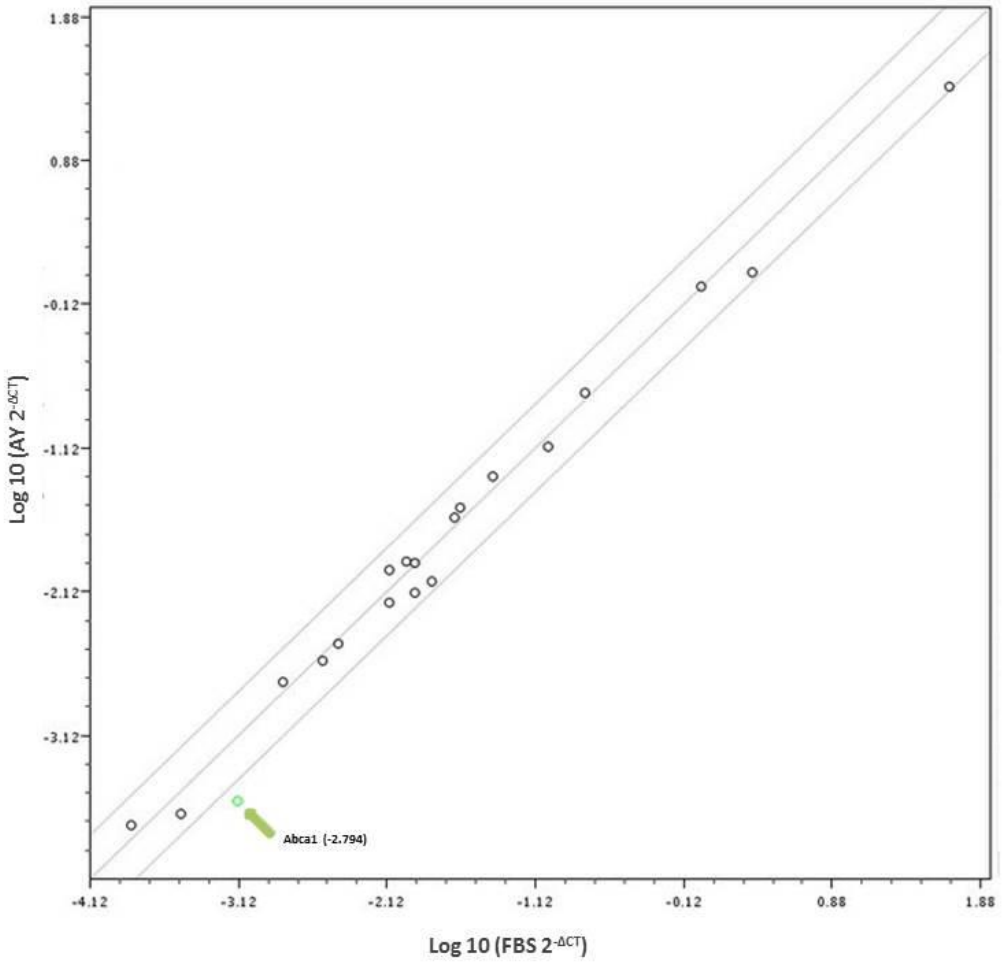

Figure 17c. Fold changes in mRNA content in MIN6 cells treated with AY9944 in FBS media (y-axis) relative to cells grown control FBS media (x-axis). The outside lines denote a 2-fold up- or down-regulation of mRNA levels. Specific fold changes are identified by the red arrows (upregulated) green arrow (downregulated).

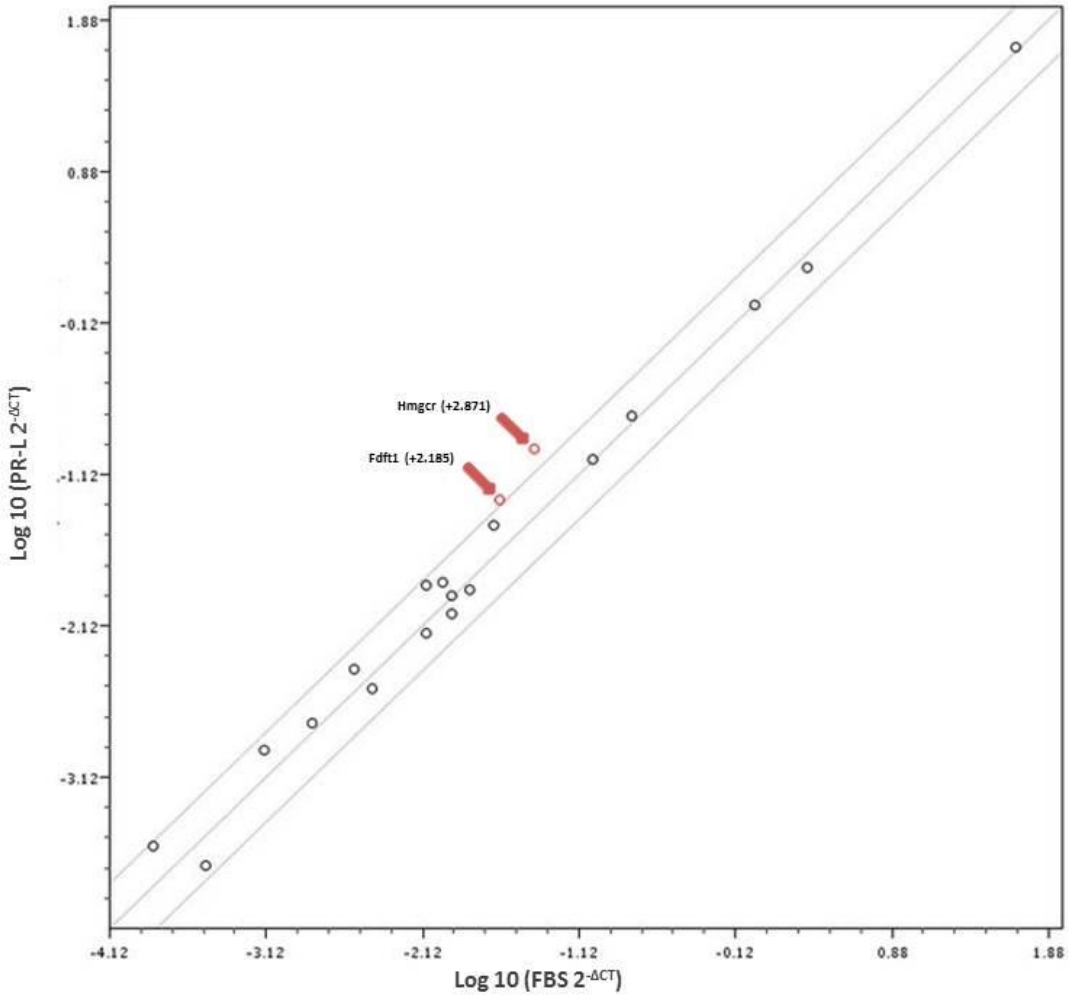

Figure 17d. Fold changes in mRNA content in MIN6 cells treated with pravastatin in LPS media (y-axis) relative to cells grown control FBS media (x-axis). The outside lines denote a 2-fold up- or down-regulation of mRNA levels. Specific fold changes are identified by the red arrows (upregulated).

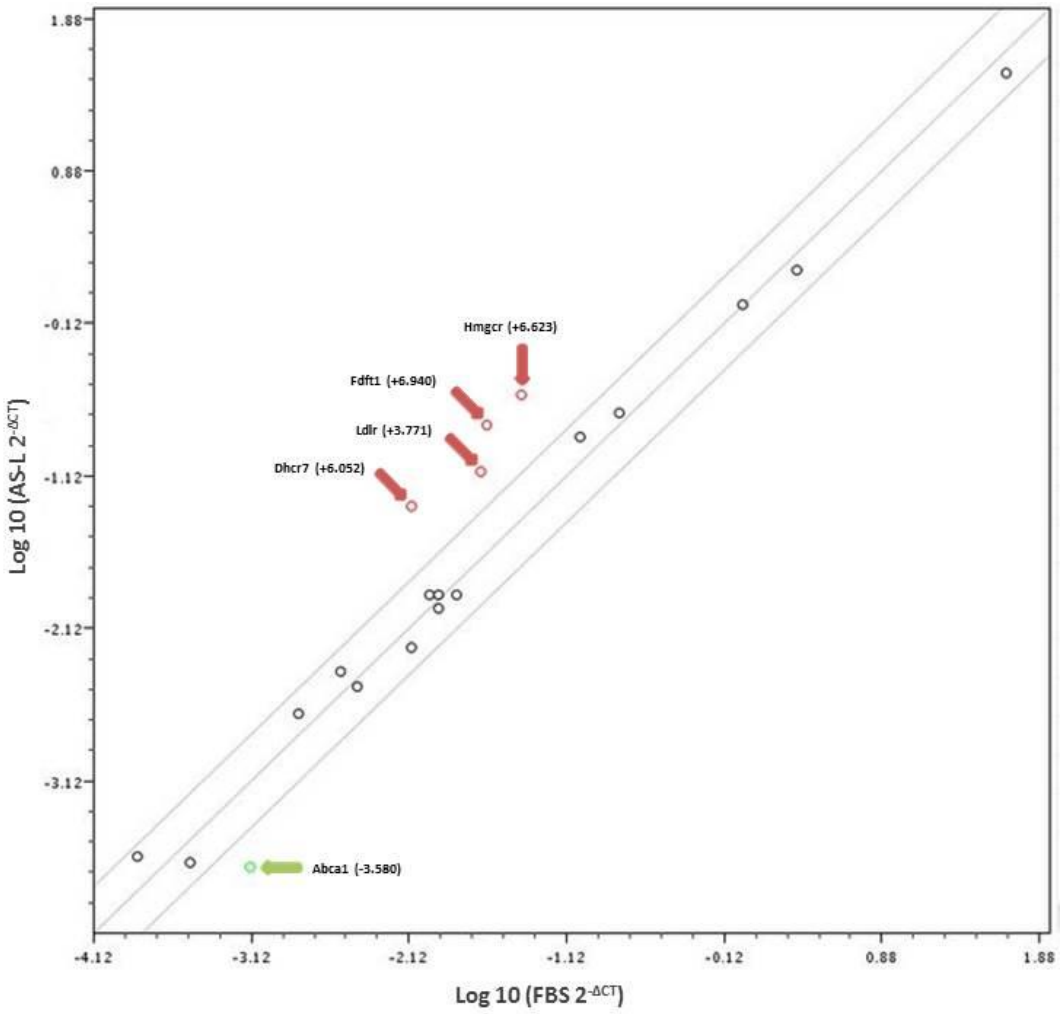

Figure 17e. Fold changes in mRNA content in MIN6 cells treated with atorvastatin in LPS media (y-axis) relative to cells grown control FBS media (x-axis). The outside lines denote a 2-fold up- or down-regulation of mRNA levels. Specific fold changes are identified by the red arrows (upregulated) or green arrow (downregulated).

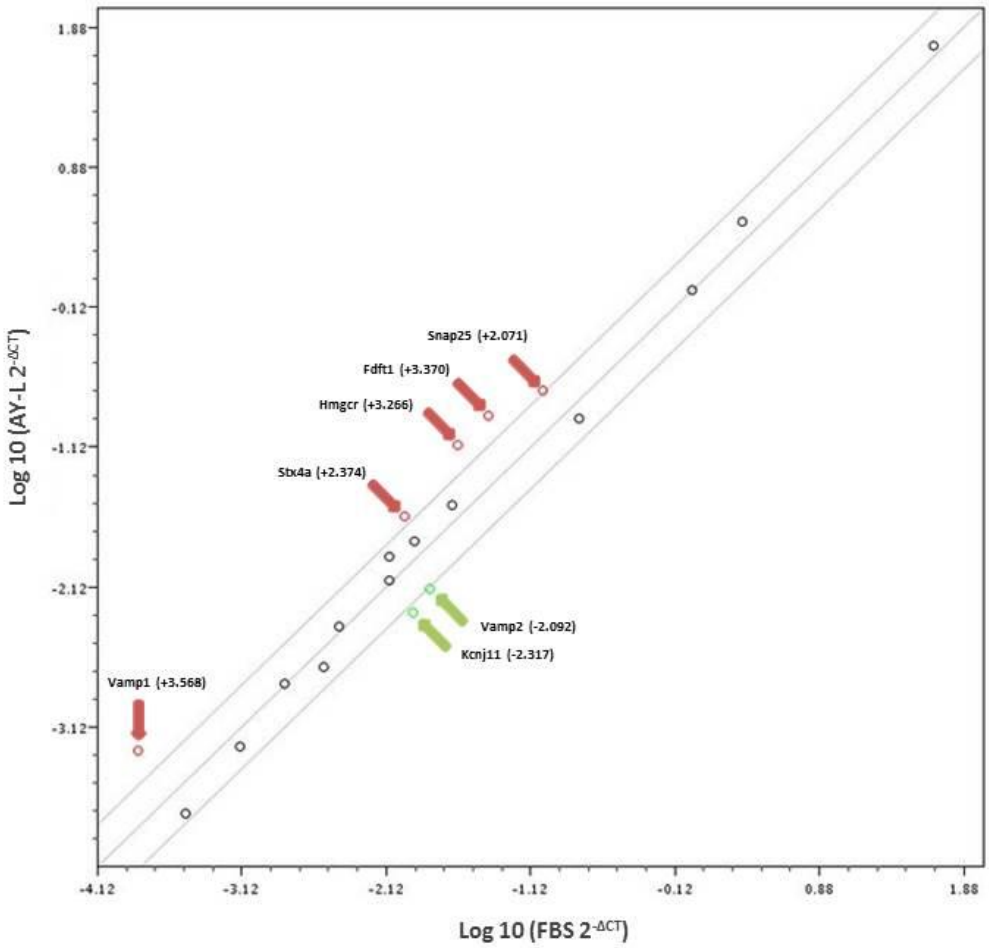

Figure 17f. Fold changes in mRNA content in MIN6 cells treated with AY9944 in LPS media (y-axis) relative to cells grown control FBS media (x-axis). The outside lines denote a 2-fold up- or down-regulation of mRNA levels. Specific fold changes are identified by the red arrows (upregulated) green arrow (downregulated).

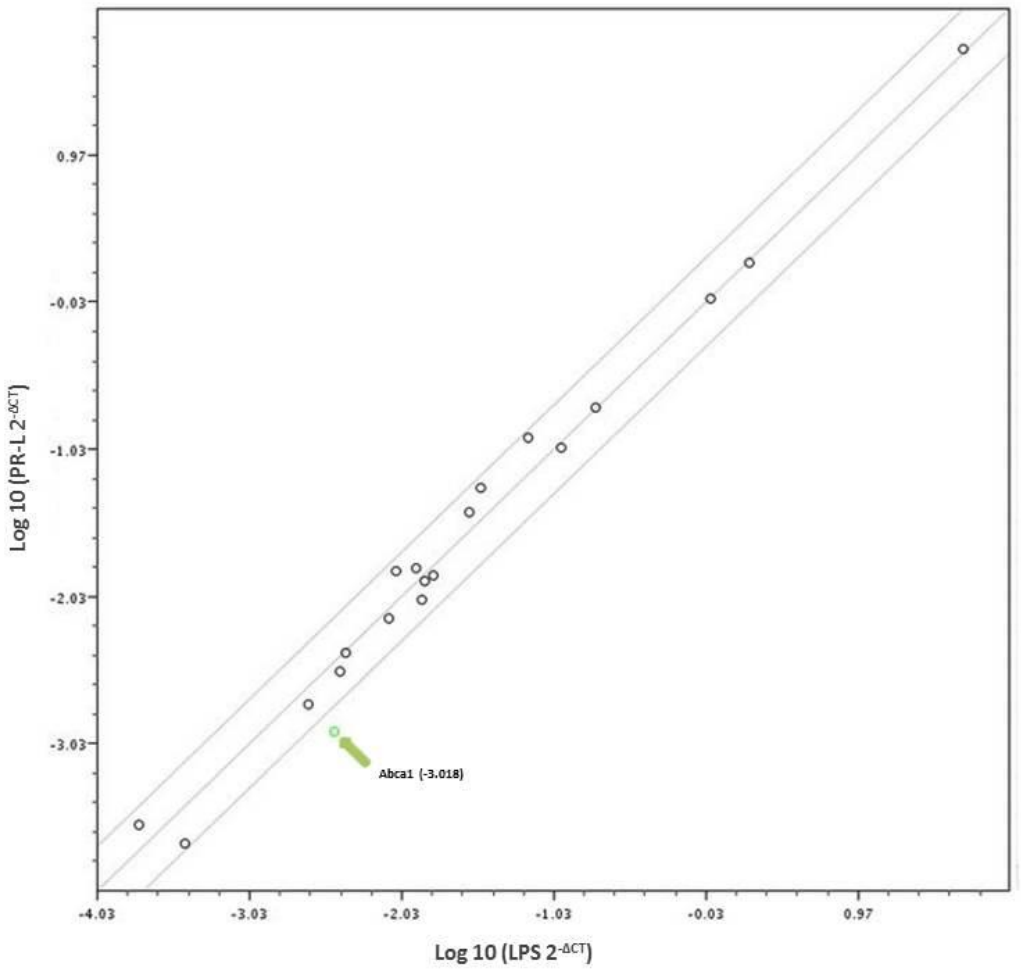

Figure 18a. Fold changes in mRNA content in MIN6 cells treated with pravastatin in LPS media (y-axis) relative to cells grown LPS media (x-axis). The outside lines denote a 2-fold up- or down-regulation of mRNA levels. Specific fold changes are identified by the green arrow (downregulated).

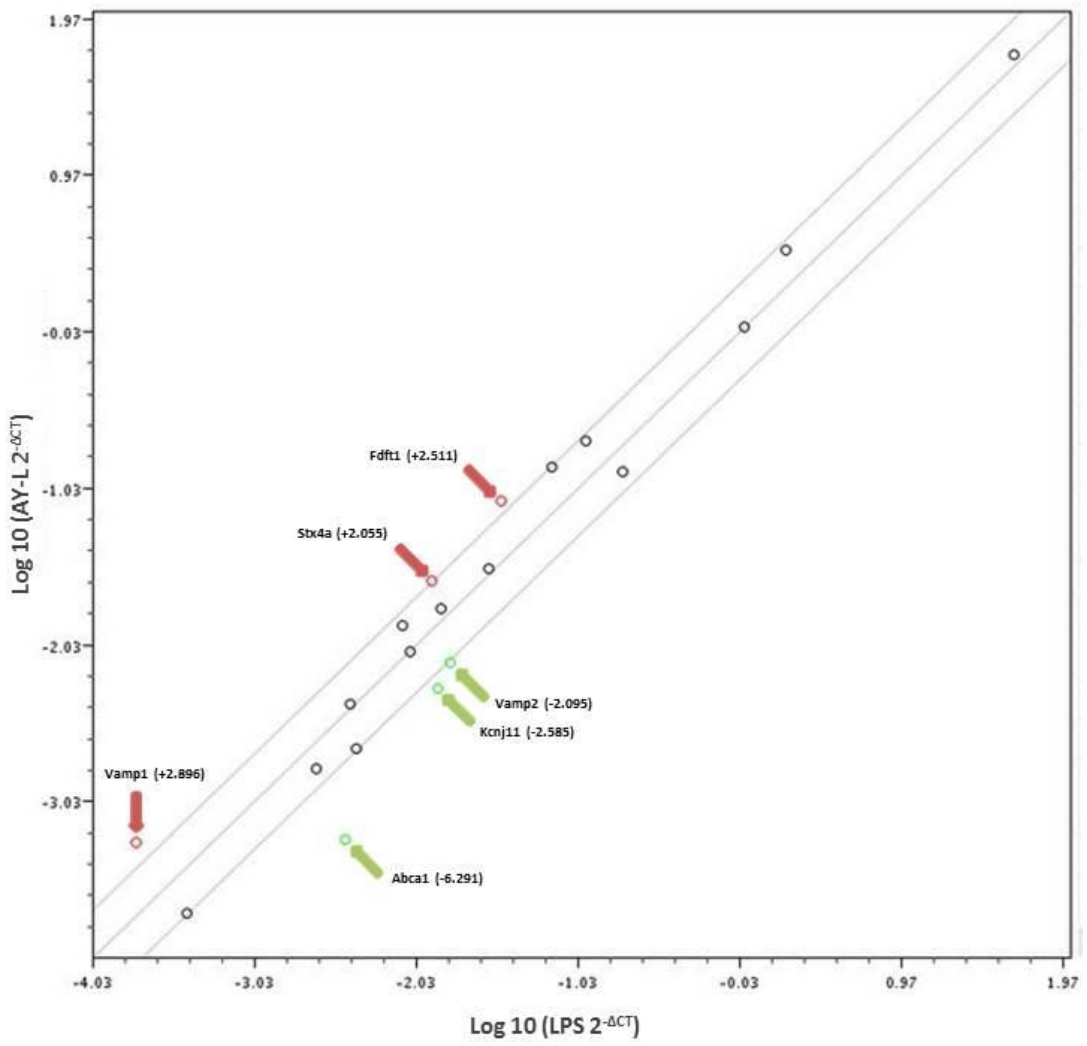

Figure 18b. Fold changes in mRNA content in MIN6 cells treated with atorvastatin in LPS media (y-axis) relative to cells grown control LPS media (x-axis). The outside lines denote a 2-fold up- or down-regulation of mRNA levels. Specific fold changes are identified by the red arrows (upregulated) or green arrow (downregulated).

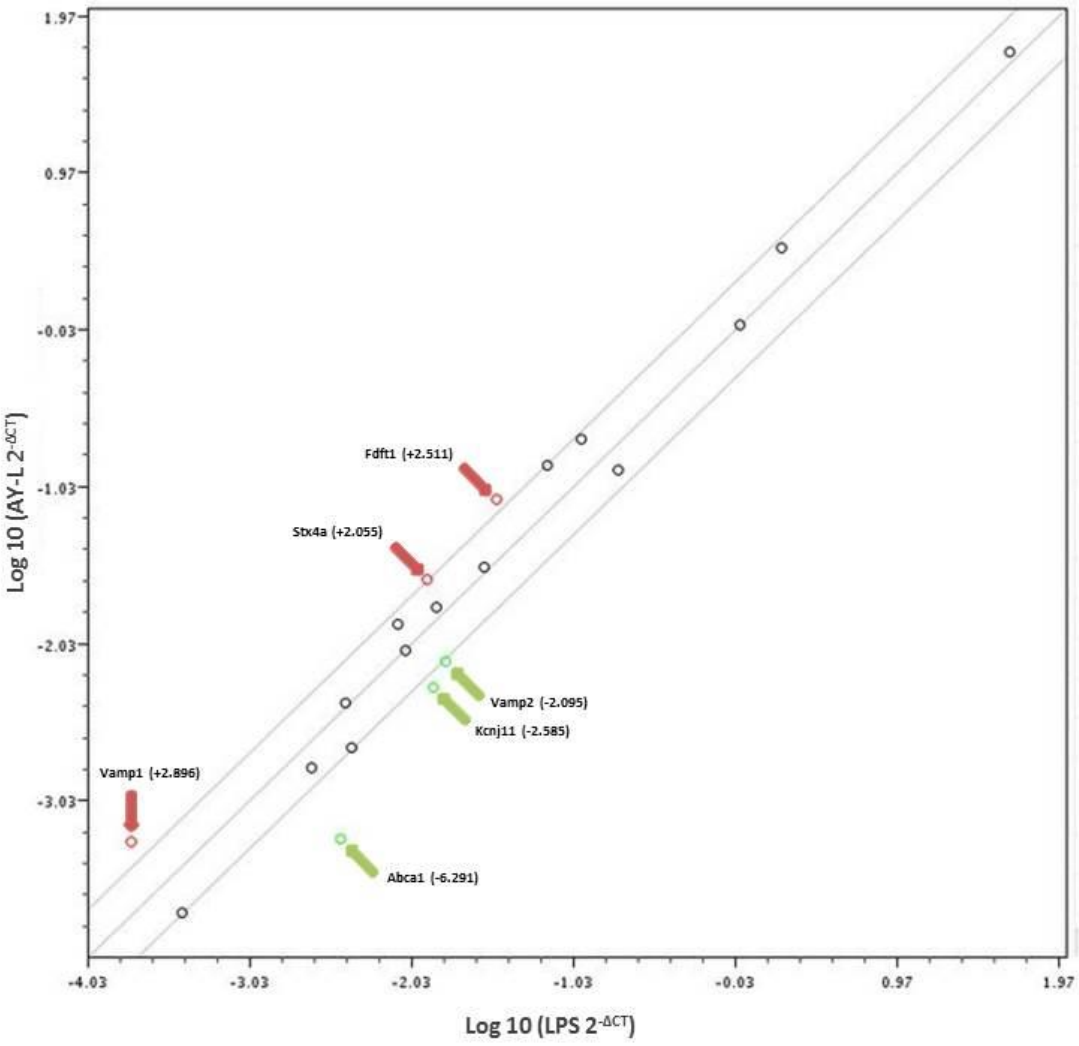

Figure 18c. Fold changes in mRNA content in MIN6 cells treated with AY9944 in LPS media (y-axis) relative to cells grown control LPS media (x-axis). The outside lines denote a 2-fold up- or down-regulation of mRNA levels. Specific fold changes are identified by the red arrows (upregulated) green arrow (downregulated).

Table 1. Summary of Fold Regulation Changes – Normalized to FBS Control

Test Group: LPS

Genes Over-Expressed in

Gene Symbol	Fold Regulation	P-value
Abca1	4.6214	0.000129

Test Group: PR

NO CHANGES ABOVE 2 FOLD

Test Group: PR-L

Genes Over-Expressed in

Gene Symbol	Fold Regulation	P-value
Hmgcr	2.8712	0.001398
Fdft1	2.1848	0.005538

Test Group: AS

Genes Over-Expressed in

Gene Symbol	Fold Regulation	P-value
Cacna1d	2.3014	0.016876
Hmgcr	3.1821	0.000026
Dhcr7	4.077	0.000014
Fdft1	3.2378	0.00002
Stx1a	2.775	0.162995
Stx4a	2.0598	0.005872
Ldlr	2.8929	0.000184

Genes Under-Expressed in

Gene Symbol	Fold Regulation	P-value
Abca1	-2.181	0.000169

Table 1, continued

Test Group: AS-L

Genes Over-Expressed in

Gene Symbol	Fold Regulation	P-value
Hmgcr	6.6231	0.000034
Dhcr7	6.0524	0.000088
Fdft1	6.9403	0.000261
Ldlr	3.7711	0.000254

Test Group: AY

Genes Over-Expressed in

Gene Symbol	Fold Regulation	P-value

Genes Under-Expressed in

Gene Symbol	Fold Regulation	P-value
Abca1	-2.7943	0.000111

Test Group: AY-L

Genes Over-Expressed in

Gene Symbol	Fold Regulation	P-value
Hmgcr	3.2659	0.024798
Fdft1	3.3694	0.025561
Stx4a	2.3743	0.186175
Snap25	2.0705	0.145231
Vamp1	3.5677	0.047309

Genes Under-Expressed in

Gene Symbol	Fold Regulation	P-value
Kcnj11	-2.3174	0.009977
Vamp2	-2.0922	0.014558

Table 2. Summary of Fold Regulation Changes – Normalized to LPS Control

Test Group: PR-L

Genes Over-Expressed in

Gene Symbol	Fold Regulation	P-value

Genes Under-Expressed in

Gene Symbol	Fold Regulation	P-value
Abca1	-3.0175	0.001856

Test Group: AS-L

Genes Over-Expressed in

Gene Symbol	Fold Regulation	P-value
Hmgcr	4.0255	0.000838
Dhcr7	5.55	0.001577
Fdft1	5.1724	0.000227
Ldlr	3.1113	0.000176

Genes Under-Expressed in

Gene Symbol	Fold Regulation	P-value
Abca1	-16.5451	0.000439

Test Group: AY-L

Genes Over-Expressed in

Gene Symbol	Fold Regulation	P-value
Fdft1	2.5111	0.079098
Stx4a	2.055	0.28946
Vamp1	2.8962	0.125864

Genes Under-Expressed in

Gene Symbol	Fold Regulation	P-value
Kcnj11	-2.5847	0.000289
Vamp2	-2.0946	0.001112
Abca1	-6.2912	0.000165

3.6 Immunoblotting

Western blotting was conducted on two ion channels important in regulating GSIS in pancreatic β-cells; the voltage-gated calcium channel ($Ca_V1.2$) and voltage-gated potassium channel, $K_V2.1$. A sample blot of 3 different trials is shown. Densitometry was then conducted on the resultant blots using ImageJ (NIH, United States), which could calculate the differences in the density of a blot's protein signal versus background. **Figure 21-22.** show the mean fold densitometry of each channel when compared to FBS control. The results depicted below show that although the $K_v2.1$ western blots did not have any statistically significant changes in protein content of the voltage-gated potassium channel, the $Ca_v1.2$ western blots did find some changes. Both LPS and AY treatment groups displayed significant increases in $Ca_v1.2$ protein content (3.01 ± 0.238 fold densitometry ratio, $n = 4$, $p < 0.01$; and 2.78 ± 0.266 fold densitometry ratio, $n = 3$, $p < 0.01$, respectively), however the other treatment groups lacked such a response.

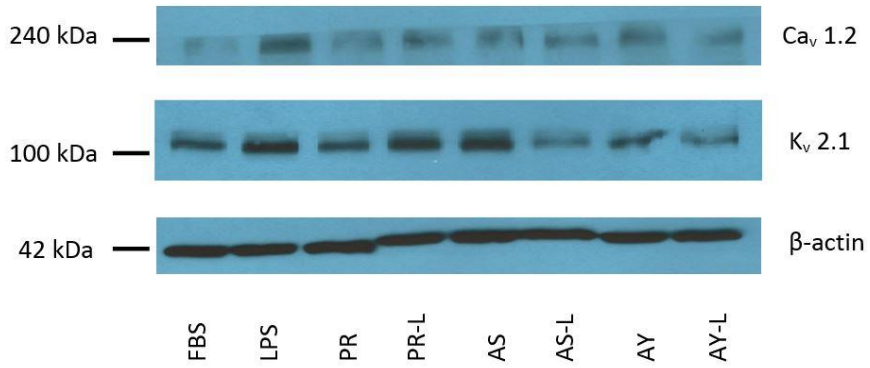

Figure 20. Western blot depicting Ca_v1.2 subunit and K_v2.1 subunit protein content. Voltage-gated calcium channels were measured using the Ca_v1.2 subunit, depicted as the top row at a size of 240 kDa. The voltage-gated potassium channels were measured using the K_v2.1 subunit, depicted as the center row at 100 kDa. The last row was the loading control for each well, β-actin, at 42 kDa. Densitometry measurements were taken to quantitatively access the differences in protein content for each channel as well as loading control. Western blots were repeated three times for each treatment group. Both LPS and AY treatment groups displayed significant increases in Ca_v1.2 protein content (3.01 ± 0.238 fold densitometry ratio, $n = 4$, $p < 0.01$; and 2.78 ± 0.266 fold densitometry ratio, $n = 3$, $p < 0.01$, respectively).

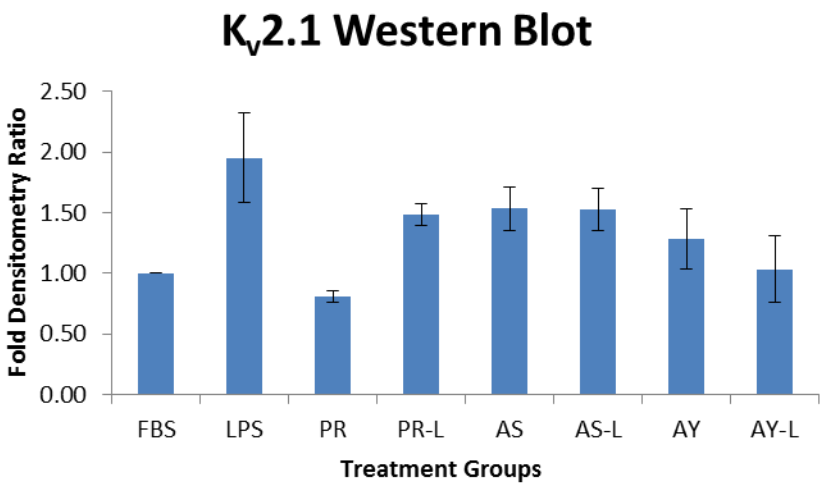

Figure 21. Densitometry results for K_v2.1 subunit protein content. Fold densitometry ratios were calculated by taking the background density of the blot and determining the density of the protein signal. All treatment groups' fold densitometry ratios were calculated against their corresponding loading control, then normalized to the FBS control. After determining densitometry ratios over a sample size of three, none of the treatment groups displayed any significant changes in protein content (refer to **Figure A.12.**)

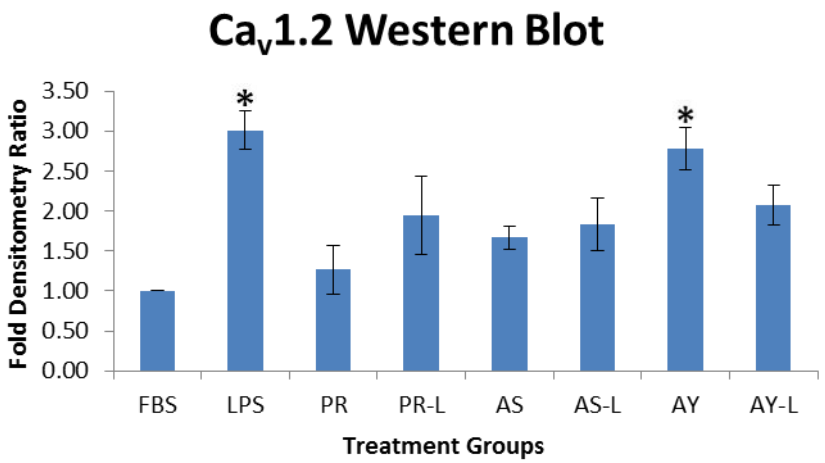

Figure 22. Densitometry results for $Ca_v1.2$ subunit protein content. Fold densitometry ratios were calculated by taking the background density of the blot and determining the density of the protein signal. All treatment groups' fold densitometry ratios were calculated against their corresponding loading control, then normalized to the FBS control. After determining densitometry ratios over a sample size of three, the LPS (delipidated serum media only) group was found to increase voltage-gated calcium content by 3.01 ± 0.238 fold densitometry ratio ($n = 4$, $p < 0.01$), and the AY 9944 in normal FBS serum group increased by 2.78 ± 0.266 fold densitometry ratio ($n = 3$, $p < 0.01$).

3.7 Patch-Clamp Analysis

Patch-clamp experiments were conducted looking at whole-cell voltage clamped current on treated MIN6 cells. Below is a current-voltage relationship graph of voltage-gated potassium channel currents under different drug treatments for 48 hours. Potassium channels were activated by stepping to different voltages. It is important to note that patch-clamp analysis measures only functional ion channels at the surface membrane. In MIN6 cells, the primary voltage-gated potassium channel is $K_V2.1$ (Ashcroft, 2005). From **figure 23**, the results clearly indicate reduced voltage-gated potassium channel function in MIN6 cells treated with any of the drug groups (statins or AY 9944). The least affected were cells grown LPS media, having almost the same current-voltage curve as the control FBS group. At 80 mV, the drug groups have half or significantly less than half the current than control MIN6 cells.

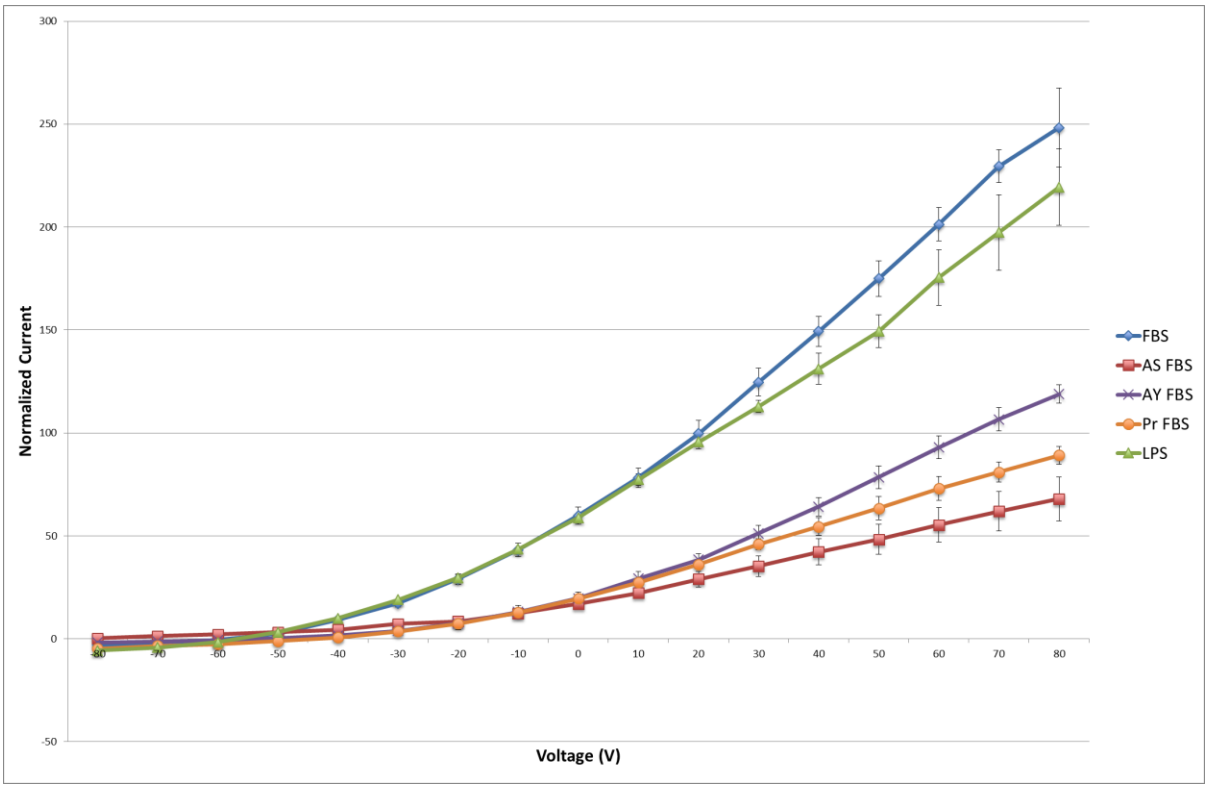

Figure 23. Current-voltage relationship graph of Kv2.1 channels under different treatment groups in FBS. Currents were measured using the whole-cell patch clamp technique while keeping voltage clamped. MIN6 cells treated with either 10 µM statin (atorvastatin or pravastatin) or AY 9944 exhibited significantly reduced K_v2.1 activity compared to control FBS and LPS cells. Sample size was between n = 4-5, and treatment was for 48 hours.

4.0 Discussion

4.1 Experimental Rationale

In this thesis, a large variety of experiments were carried out in order to obtain a better understanding of the effects that limiting both endogenous and exogenous sources of cholesterol had on β-cell function. In light of this, I feel that it is both important and beneficial to explore the rationale behind each of the conducted experiments, and to discuss the significance of the findings of each individually before consolidating the information into a final conclusion.

4.1.1 Cell Viability Assays

The trypan blue exclusion test (refer to section **2.3**) was conducted mainly for two reasons. The first was to confirm that cell death did not play any significant role in the observed changes in either the genetic regulation/expression of proteins of interest, or in the cholesterol content and resultant changes in GSIS profiles in the various treatment groups. The second reason was to confirm the findings of Tsuchiya *et al.* (2010), who claimed that 48 hour treatment of MIN6 cells with LPS enriched media exceeded 30% cell necrosis, and that treatment with statin led to over 50% cell necrosis (cf Tsuchiya *et al.*, 2010, supplemental figure 2). However, the results seen in **figure 7** of my experiments suggest that cell viability does not significantly change from normally cultured cells in FBS enriched media in any of my treatment groups, except for AY 9944, which elicited only a modest reduction in viability.

4.1.2 Cholesterol Assays

The second set of experiments conducted was aimed at establishing the degree of cholesterol reduction that occurred in response to statin or AY 9944 treatment. These assays were integral in establishing any potential correlational relationships that could exist between cholesterol content and aberrant insulin secretion. It was also able to measure the degree of reduction when only exogenous sources of cholesterol (LPS enriched media) was limited, along with compounded effects of limiting both exogenous and endogenous sources (LPS and drug). As seen in **figure 6**, cholesterol reduction was uniform among the different drugs, as well as the compounded reduction seen when drugs were administered in lipid free media. Thus, it was established that a reduction in cholesterol was seen throughout my treatment groups, all of which also saw a change in GSIS secretion profiles.

4.1.3 GSIS Assays

The glucose-stimulated insulin secretions assays were an extremely important aspect of my thesis research as these assays directly measured the functional capacity of the β-cells after treatment with drugs or lipid free serum, or both. The values obtained from the GSIS assays were able to communicate any changes in basal insulin secretion as well as the cell's ability to respond to glucose challenges. However, given the nature of the experimental design, one of the limiting factors was that I was unable to tease apart the amount of insulin released in first phase versus second phase of biphasic insulin secretion. The experiment called for an incubation time on treated MIN6 cells of approximately 1 hour, however, first phase secretion lasts for approximately 8 minutes, and second phase persists beyond the 35 minute mark (Straub and Sharp, 2002). Despite that, total insulin secretion was still measured as a percentage of total insulin content. This still conveyed a great deal of information when

also taking into account any differences in total content among the treatment groups. As seen in **figure 9**, all treatment groups (except for LPS enriched media only), displayed a significant reduction in glucose stimulated insulin secretion when compared to normally cultured MIN6 cells in FBS enriched media. However, contrary to the findings in my cholesterol assays, the reduction in GSIS profiles was not uniform across all groups. There clearly exists other factors that contribute to β-cell dysfunction beyond the degree of cholesterol reduction seen within the cell.

4.1.4 Luciferase Assays

After having had established that treatment groups experiencing a cholesterol reduction also saw decreases in ability to secrete insulin in response to glucose, it became of great interest to determine where the basis of this dysfunction existed. A paper published by Amemia-Kudo *et al*. (2005) discovered that the insulin promoter was a novel target for SREBP-1c nuclear proteins, which are important in cholesterol regulation. Promoter activity could provide insight into whether or not my treatment groups had similar effects on other gene targets involved in the GSIS response. As seen in **figures 11 – 16**, promoter activity did in fact change in certain treatment groups. The promoters that were assayed for were either involved with insulin synthesis (*Ins-1*), ion channels important in signal transduction ($Ca_V1.2$, $K_V2.1$, K_{ATP}), or SNARE proteins that helped mediate insulin granule fusion and secretion (STX-1A, SNAP 25). The obtained results provided a great deal of insight on changes in promoter activity; however, as we all know, changes in gene promoters do not necessarily translate to changes in mRNA expression.

4.1.5 RT-PCR Arrays

RT-PCR array plates were then designed and ordered that could measure mRNA levels of various important genes involved in the multiple stages of the GSIS response. This not only allowed me to cross-reference promoter activity results with mRNA content, but also allowed me to look at a variety of other genes of interest (such as *Vamp1/2*, *DHCR7*, *Fdft1*, *HMGCR*, and *ABCA1*). The nature of RT-PCR arrays made high throughput data collection possible, and really provided that extra bit of information to infer how much of an effect a change in promoter activity had on the expression of some proteins' mRNA. As previously mentioned, the threshold for recognizing a change in mRNA expression was set at 2-fold as per the minimum suggested threshold by the manufacturer. As seen in **figures 17-19**, a large amount of mRNA content changes did in fact occur in many of the treatment groups. The significance of these changes will be discussed, along with the significance of other experiments, in section 4.2.

4.1.6 Immunoblotting Experiments

Western blotting was performed for $K_V2.1$ and $Ca_V1.2$ protein subunits. The intention was to determine whether the changes (if any) seen within the promoter assays or the RT-PCR arrays translated to changes in cellular channel protein content. These immunoblotting experiments could potentially help conclude the information gathered from previous experiments, or infer that changes to the secretion or current occur post-translationally. Given the time-constraints, Western blots were not created for ATP-dependant potassium channel subunits, Kir6.2 or SUR1.

4.1.7 Patch-Clamp Experiments

Patch-clamp experiments were then conducted to determine if any of the treatment groups caused functional or surface expression changes of the specific channel protein. It should be noted however, that given the stimulating conditions used to assess channel function, results could not infer if changes in signal-coupling between different ion channels (e.g. voltage-dependent calcium channel activity is required for voltage-dependent potassium currents) were disrupted. The patch-clamp method could only determine if statin treatment or AY 9944 treatment had any direct effects on channel function, independent of the glucose stimulated insulin secretion signal transduction pathway that occurs from ATP-sensitive potassium channels, opening voltage-dependent calcium channels which would finally open voltage-gated potassium channels.

4.2 Results Analysis

In this section, the significance of the changes seen in each experiment will be taken into perspective in reference to other findings, both from my experiments as well as current research from other groups.

4.2.1 Cholesterol Reduction and GSIS Profiles

As seen in **Figure 6**, the reduction of cholesterol in all groups treated with drug in FBS enriched media, was comparable to the reduction in the LPS control (no drug, only LPS enriched media). These results imply that pharmacological means of inhibiting cellular cholesterol could potentially result in a

similar reduction as limiting exogenous sources of cholesterol for 48 hours. When cells were treated with both drug and LPS enriched media, the statins atorvastatin (AS) and pravastatin (PR), did not see a statistically significant further reduction when compared to either LPS control or with their drug in FBS counterparts ($p > .05$). However, the effect was almost doubled for AY-L. Sample size was the limiting factor for the drug in LPS groups, with a repetition of n=3. Further experiments should include more repetitions to verify whether or not these groups do in fact see a statistically significant increased reduction than drug in FBS alone (like the AY-L group did). The consistently lower cholesterol content seen in **figure 6** does however imply the possibility of this relationship existing.

When viewing cholesterol reduction with reference to altered GSIS profiles, several relationships can be teased apart from the comparison. For example, the reduction in cholesterol between all drug groups in FBS serum are statistically different from FBS control, but the same when comparing them with each other. However, when viewing **Figure 9**, a difference in severity of impaired GSIS exists between some of the drug groups. Cells treated with AY 9944 in FBS media show a significantly reduced ability to secrete insulin in response to 16.7 mM glucose when compared to pravastatin, but not atorvastatin. However, no significant differences between the two statins themselves are apparent. Additionally, the LPS-serum only group does not appear to significantly differ from FBS control cells, despite cholesterol being similarly reduced in LPS as it is with drug in FBS groups. Thus, it is fair to conclude that a reduction in cholesterol via pharmacological means is in fact associated with a reduction in a β-cell's ability to secret insulin in response to glucose. The only group that also displayed a potential reduction in basal insulin secretion is AY in FBS serum. It should also be noted that the degree of reduction in cholesterol content may not be the only factor contributing to the reduced secretion, as LPS serum only had a similar loss of cellular cholesterol as drug in FBS, but did not see the same aberrant secretion profile. Lastly, AY 9944 appeared to have the most drastic changes in secretion, but displayed the same degree in cholesterol reduction as the two statin groups.

4.2.2 GSIS Profiles and Genetic Expression Changes

The promoter and RT-qPCR array experiments were conducted in hopes of better understanding the factors involved in the reduced GSIS capacity of my treated cells. The first promoter of interest was the *Ins-1* insulin gene promoter, which would allow me to see if treatment conditions had any effect on insulin transcriptional regulation. When comparing **figure 10** to **figure 11**, changes in promoter activity generally agree well with observed changes in insulin content. Barring the AS and AS-L treatment groups, statistically significant reductions in promoter activity when compared to the FBS control group resulted in reductions of total cellular insulin. However, when taking into account the data from RT-PCR arrays, no changes greater than 2-fold occurred in ins-1 mRNA product. This could possibly be explained by the fact that *Ins-1* promoter activity fold activation was only reduced by 0.5 or more in one treatment group, AY ($0.386 \pm .086$, $p < 0.01$, $n = 3$). Regardless, it appears that whatever causes the changes in total insulin occurs post-translationally, as promoter activity reduction does not appear to affect the mRNA load of insulin, and mRNA load does not correspond to insulin content of certain treatment groups. One possible explanation to this is that insulin degradation enzyme (IDE) may increase its activity within the β-cell when secretion is reduced due to statin or AY 9944 treatment. As it has been well established, IDE not only targets insulin but is also largely responsible for the breaking down of amyloid structures in pancreatic islets, helping to also regulate amylin turnover (Bennett *et al.*, 2000; Yfanti *et al.*, 2008). Insulin can be degraded within any cell that has the ability to respond to it, including the pancreatic β-cell (Harada *et al.*, 1993). Islet amyloid deposits have been found in over 90% of T2DM patients upon autopsy and have been implicated in the progressive β-cell failure commonly seen in these patients (Marzban and Verchere, 2004). Because IDE can target both insulin as well as amyloid structures, the addition of insulin to amyloid being exposed to IDE has an inhibitory effect on amyloid degradation (Yfanti *et al.*, 2008). The reduction of insulin within the cells that have undergone statin or AY 9944

treatment has broader implications than my current research can explain, and is something I would strongly recommend for future research.

Another focus of my research was to assess the changes that may have occurred to SNARE protein expression within treated MIN6 mouse insulinoma cells. Syntaxin-1A and SNAP 25 are the two commonly found plasma membrane SNARE proteins involved in GSIS (Daniel *et al.*, 1999; Ohara-Imaizumi *et al.*, 2004), so preliminary promoter assays on SNARE proteins focused exclusively on those two. It should also be noted that the extent of my research investment into SNARE protein changes in statin or AY 9944 treated cells extended only as far as promoter and RT-PCR array experiments, and immunoblotting experiments could go a long way into confirming those results. When viewing **figure 15** and **figure 16**, no significant changes were apparent in STX-1A and SNAP 25 promoter activity in any of the treatment groups. However, when looking at the RT-PCR array data, some changes in SNARE mRNA content can be seen in AY 9944 and atorvastatin treatment groups (refer to **figure 19a-b**). For atorvastatin treated cells, STX-4A was increased by 2.06 fold ($p < 0.01$), and in AY 9944 in LPS media, the changes were limited to vesicle associated proteins, VAMP 1 and VAMP 2 (3.57 fold increase, $p < 0.05$; 2.09 fold decrease, $p < 0.05$, respectively). I speculated that this might have occurred because although VAMP2 is normally the vesicle associated protein employed in insulin producing cells, it was reduced as a result of treatment and the less commonly used VAMP protein was upregulatd (VAMP2).

The approximate 2-fold increase in STX-4A mRNA was interesting since that particular syntaxin isoform has been implicated in serving as important a role as STX-1A in β HC-9, a hyperplastic mouse insulin secreting cell line (Saito *et al.*, 2003). The increased mRNA load of STX-4A in MIN6 (also a mouse insulin secreting cell line) may be indicative of a compensating mechanism to increase secretion capacity. However it is still curious as to why this was not seen in any other treatment group including atorvastatin in delipidated media, begging the question that if more trials were done ($n > 4$) if this 2-fold

increase would no longer be significant. The changes seen in AY 9944 in delipidated media was also very intriguing as VAMP-2, which is well known to facilitate fusion pore formation in pancreatic β-cells, is reduced but VAMP-1, which has not been known to play an important part in GSIS, was increased (Regazzi *et al.*, 1995). Regardless, much more research should be invested into exploring the changes in SNARE protein content and expression in statin and AY 9944 treated insulin-secreting cells.

4.2.3 Ion Channels and Electrophysiology Changes

Three ion channels were looked at extensively given the time constraints. They were the voltage-gated calcium channels, voltage-gated potassium channels, and the ATP-dependent potassium channels. For the voltage-gated calcium channel, the L type α1C subunit was looked at specifically for promoter activity, mRNA content, and protein content (with the addition of the α1D $Ca_V1.3$ subunit for RT-PCR arrays). For the voltage-gated potassium channel, the voltage gated channel, Shab-related subfamily, member 1 protein was looked at for promoter activity, mRNA content, protein content, and electrical activity. The ATP-dependent potassium channel was the last channel of interest but only mRNA content and promoter activity was assayed for the Kir6.2 subunit (protein content for this subunit was not determined).

The promoter assays for the $Ca_V1.2$ subunit displayed little to no change in activity, with the AY group displaying a marginal decrease in promoter activity (0.78 ± 0.04 fold activation of the promoter, $p < 0.01$, $n = 3$). This lack of large significant changes in promoter activity was mirrored in the RT-PCR array data, where no changes in the α1C subunit mRNA was seen. Interestingly, in the AS treatment group, an approximate increase of 2.3 fold in mRNA content ($p < 0.05$, $n = 3$) occurred in the α1D subunit. Western blot results, however, noted that there were significant increases in the total cellular protein content in

both the LPS and AY groups for the α1C subunit, by 3.01 ± 0.24 fold densitometry ratio ($n = 4$, $p < 0.01$), and 2.78 ± 0.27 fold densitometry ratio ($n = 3$, $p < 0.01$), respectively. Even when viewing the graph showing relative change in protein content, despite the other groups not being significant, there appears to be an upward trend in protein content of the voltage-gated calcium channel (refer to **figure 22**). The only probable exception to this trend is pravastatin, which may potentially be because pravastatin is by far one of the mildest statins currently on the market. Unfortunately, this channel was not tested for any electrical activity changes. The impact that these changes have on the reduced GSIS efficiency found in some of my treatment groups, could be much easier assessed once patch-clamp data could be obtained for this channel.

The voltage-gated potassium channel results, however, were a bit more puzzling. When viewing the changes in promoter activity (refer to **figure 13**), there is a very significant and noticeable decrease in $K_V2.1$ promoter activity across all treatment groups. The mildest changes occurred in the LPS and PR groups (0.70 ± 0.09, $p < 0.05$, $n = 3$; and 0.63 ± .09, $p < 0.01$, $n = 3$, respectively), with more drastic reductions in fold activation found in the AS and AY groups (0.36 ± 0.03, $p < 0.01$, $n = 3$; and 0.34 ± 0.02, $p < 0.01$, $n = 3$, respectively). The RT-qPCR data however, showed no significant changes in mRNA content across all treatment groups, not reflecting the drastic reductions in promoter activity. Even when referring to the western blot data, there were no significant changes in protein content of this channel subunit. It should be noted that, similar to the calcium α1C subunit, a trend appeared to exist of increasing protein content in the densitometry data, with the exception of the PR group (refer to **figure 21.**). Unlike the other two channels, extensive path-clamp experiments were also conducted to assess channel currents of voltage-dependent potassium channels after treatment with either statin or AY 9944. When viewing **figure 23**, it is apparent that a reduction in whole-cell potassium currents occur in the drug treatments. It is important to note however, that these experiments were only able to assess the functionality of $K_v2.1$ channels and not assess the electrical activity of it during a GSIS response.

Thus, one of the most intriguing results arise from this, as protein content does not seem to be influenced by promoter activity, and yet a reduction in channel function is seen despite having the same channel protein content as the FBS control group. This could be attributed to various different reasons, but I suspect that either localization of channel microdomains or channel regulation should be the more likely explanations for this perceived result.

Finally, the ATP-sensitive potassium channels presented with increases in promoter activity in atorvastatin groups. Both AS and AS-L displayed increased activity (1.96 ± .31, $p < 0.05$, $n = 3$; and 1.56 ± 0.24, $p < 0.05$, $n = 3$, respectively) despite no increases in mRNA content. In fact, the only significant change found in the mRNA content of the Kir6.2 subunit of the K_{ATP} channel was a 2.32 fold decrease ($p < 0.01$) in the AY-L treatment group. Unfortunately, neither immunoblot experiments to determine channel protein content, nor patch-clamp experiments to determine functional changes in cell currents, were carried out for this channel. Carrying out both would greatly benefit the understanding of the effects of statin or AY 9944 drug administration in β-cell function.

4.2.4 K_V2.1 Results Discussion

Given that the voltage-dependent potassium channel subunit, K_V2.1, underwent the most comprehensive study (from promoter activity to whole-cell current and channel function experiments), I believe the reasons behind the perceived results merited further discussion. As previously eluded to, post-translational causes seemed to have the most significant effect on the perceived changes in protein content and whole-cell current generated by this K_V channel. I believe that these post-translational causes are in fact due to a disruption in channel localization and surface expression. It is already well established that localization of ion channels with secretory granules, SNARE proteins, and with each

other, is required for normal β-cell function (Barg *et al*., 2001; Bickel, 2002; Xia *et al*., 2004; Xia *et al*., 2008). To further reinforce this idea, K_v2.1 specifically has been found to target SNARE proteins such as Syntaxin-1 when being inserted into the membrane of insulin secreting β-cells (Leung *et al.*, 2003; Singer-Lahat *et al.*, 2008). It has also been recently demonstrated that even in neurons, K_v2.1 trafficking can be very site-specific and directed, with a multitude of signal peptides, anchor protein interactions, and lipid interactions helping to polarize channel distribution as well as retain membrane configuration (Jensen *et al.*, 2011). Thus, it is within reason to propose the idea that the recycling of this channel, along with other important ion channels in the β-cell, is site specific and directed. With the loss of lipid raft integrity, presumably due to a reduction in cellular cholesterol, many anchor proteins and lipid-lipid interactions may dissipate along with it. The ion channel proteins expressed in the β-cell have been known to have a general half-life from 90 seconds to upwards of 20 minutes (Jindal *et al.*, 2008; Thion *et al.*, 1996; Yan *et al.*, 2005). If loss of site-directed insertion also led to loss of directed recycling, increased retention of ion channels far beyond their functional life-span could ensue, potentially explaining the reduced electrical activity seen in the treated MIN6 cell K_V2.1 whole cell currents. Additionally, prolonged retention could also explain the seemingly normal channel protein content, even despite the reduced promoter activities for some of the treated cells. Experiments directed at determining the validity of these hypotheses could very well help in expanding the current understanding of the effects of reducing cholesterol in pancreatic β-cells.

4.3 Conclusions

The treatment of MIN6 pancreatic β-cells with either statin (atorvastatin or pravastatin) or AY 9944 has clear detrimental effects on glucose stimulated insulin secretion. The severity of these effects are most evident in cells treated with AY 9944, with milder reductions with atorvastatin treatment, and least of all pravastatin treatment. Changes in insulin, as well as ion channel proteins important to insulin secretion, are most likely due to post-translational modifications. Disruption in localization, directed surface expression of channel proteins, as well as channel protein recycling have been proposed to play the biggest parts in the reduced functionality of the MIN6 β-cell after cholesterol biosynthesis inhibition. These would all arise from the fact that the microdomains housing the channel complexes have been disrupted due to a reduction in cellular cholesterol. Additionally, IDE activity increasing within the β-cell due to reduced insulin secretion could also play a part in exacerbating the perceived effects. Additionally, this could also potentially explain the increased amyloid formation typical of T2DM patients. A wide array of future experiments will be proposed to help verify these theories and will also hopefully lead to an increase in the present knowledge of statin effects on T2DM development.

4.4 Future Experiments

4.4.1 Assays to Determine Changes in IDE Activity

One of the first observations made when viewing my results was the change in insulin content without any detectable changes in insulin mRNA. This observation led me to believe that insulin degradation enzyme (IDE) had increased activity within the pancreatic β-cell when the cells were treated with either statin or AY 9944. Additionally, as previously mentioned in section *4.2.2*, amylin turnover is highly dependent upon IDE activity. Thus, increased IDE activity within the β-cell could potentially be one of the factors involved in increased amyloid formation characteristically seen in T2DM diseased islets. A variety of experiments could be designed and conducted to detect changes in IDE activity within the pancreatic islet. However, I would strongly recommend the use of mice for these experiments, as being able to run these experiments on cultured islets could provide a much more accurate picture of the physiological effects of statin or AY 9944 treatment.

Co-immunoprecipitation can be done on different fractions of collected islets, involving either precipitating both IDE with insulin in the fraction containing the β-cell, versus precipitating both IDE with amylin in the extracellular fraction. Changes in relative amounts between the two, in addition to measuring amyloid formation, could provide compelling evidence that changes in IDE activity exist, and that amyloid formation ensues as a result of this change.

Another way to view changes in IDE expression would be to carry out RT-qPCR on IDE mRNA, or promoter assays on the gene reporter responsible for IDE transcription. Changes in reporter activity or changes in IDE mRNA could also indicate a change in insulin degradation rate in statin or AY 9944 treated cells.

4.4.2 Pulse-Chase Assays to Determine Ion Channel half-life

The pulse-chase assay could provide a tremendous amount of insight into the half-life of all ion channels that have been proposed to exist within the lipid-raft microdomains responsible for GSIS. One of my speculations into the contributing factors of the reduced GSIS capacity of statin and AY 9944 treated cells, is the reduction in directed site-specific surface expression of important proteins and channels. Thus if insertion into the membrane is directed, such as using anchor proteins ankyrin-G and βIV spectrin for Na_V channels in neurons (Jensen *et al.*, 2011), disruption of differential surface expression could also lead to aberrant recycling of these proteins. To determine any changes in the half-life of the proteins of interest, I would propose an experiment similar to the one conducted by Hitesh *et al*. (2008) where a pulse-chase assay was carried out on the $K_V1.5$ channel. After a pulse with radioactive labeled amino acid, and subsequent chase with an abundance of non-labeled amino acid, the channel of interest can be collected using anti-channel antibody. In 5-15 minute intervals, cells can be collected after the chase, and a scintillation counter can be used to measure the amount of radioactive label. After normalizing to protein content, the reduction in amount of radioactive label can tell us if channel proteins were recycled at a much later time than the control treatments' channels. Alternatively, immunocytochemistry could be used to assay for the same thing.

4.4.3 TIRFm to Determine Changes in Surface Expression of Channels and Secretion

Total internal reflection fluorescence microscopy (TIRFm) provides a multitude of benefits when wishing to assess events that occur exclusively along the cell's plasma membrane. Because the membrane is the plane of focus when using this method of microscopy, background noise is greatly diminished as signals from fluorophores are apparent only once they reach the membrane or are very close to it. This provides a great deal of information on structural localization, dynamics, and organization of proteins of interest, and excludes the background fluorescence that occurs within the cell cytoplasm away from the membrane. This is made possible because TIRF primarily illuminates only fluorophores very close (i.e. within 100 nm) to the cover-slip sample interface (i.e. the membrane surface). Any fluorophores away from the cover-slip-sample interface has its signal decay exponentially the further it is from the *z* plane, and thus greatly increases the signal-to-noise ratio.

Additionally, because of the nature of TIRF microscopy, fixation of dead cells is not necessarily a requirement for good imaging. This allows the assessment of protein dynamics and localization while the cell is still alive, and will give a better picture of membrane structural organization without the use of detergents and other invasive reagents. TIRF microscopy would be an excellent method to make use of in order to study not only the localization and structural organization of important ion channels involved in glucose-stimulated insulin secretion, but also to assess the impact of certain treatments on the separate phases of insulin secretion and to quantitatively assess the changes in number of fusion events over specific time points after a cell is stimulated by glucose or other ions.

However, we are not limited to conducting the study of spatial organization of ion channels and assessment of changes in fusion profiles in the different phases of insulin secretion as separate experiments. They can also be done in tandem to assess the relative location of these ion channel

organizations to that of the actual site of insulin secretion and to assess the changes in secretion profiles due to any detectable changes in protein organization. This can provide additional insight on the cellular dynamics behind insulin secretion and how different treatments may potentially cause these secretory 'complexes' to act as a result of changes in cholesterol homeostasis.

4.4.4 Completion of Current Experiments on Remaining Channels

Lastly, I strongly recommend the completion of my previously conducted experiments for the two remaining channels. K_{ATP} channels would greatly benefit from protein content analysis (western blot) as well as both Ca_V and K_{ATP} channels undergoing patch-clamp technique to analyze functional changes. Being able to analyze those two channels the same way that K_V channels were could go a long way in determining if similar trends existed with those two ion channels as well. And if this was the case, it could be eluded to that the effects of the statin or AY 9944 treatment extended to all the channels involved in the lipid raft microdomains proposed to be responsible for the GSIS response.

References

Clinical Guidelines Task Force, International Diabetes Federation (2005). "Glucose control: oral therapy". In: Global Guideline for Type 2 Diabetes. Brussels: International Diabetes Federation, 35–8.

Abbas A, Milles J, Ramachandran S. 2012. Rosuvastatin and Atorvastatin: Comparative Effects on Glucose Metabolism in Non-Diabetic Patients with Dyslipidaemia. Clinical Medicine Insights: Endocrinology and Diabetes, 5: 13-29.

Anderson C, van Gaal L, Caterson ID, Weeke P, James WPT, Couthino W, Finer N, Sharma AM, Maggioni AP, Torp-Pedersen C. 2012. Relationship between HbA1c levels and risk of cardiovascular adverse outcomes and all-cause mortality in overweight and obese cardiovascular high-risk women and men with type 2 diabetes. Diabetologia, 0(0):0-4.

Anderson JW, Kendall CWC, Jenkins DJA. 2003. Importance of Weight Management in Type 2 Diabetes: Review with Meta-analysis of Clinical Studies. Journal of the American College of Nutrition, 22(5): 331-339.

Ashcroft FM. 2005. ATP-Sensitive potassium channelopathies: focus on insulin secretion. The Journal of Clinical Investigation, 115(8): 2047-2058.

Ashcroft FM, Rorsman P. 2004. Molecular Defects in Insulin Secretion in Type-2 Diabetes. Reviews in Endocrine & Metabolic Disorders, 5: 135-142.

Atlas, D. 2001. Functional and physical coupling of voltage-sensitive calcium channels with exocytotic proteins: ramifications for the secretion mechanism. Journal of Neurochemistry, 77: 972-985.

Barg S, Rorsman P. 2004. Insulin Secretion: A High-affinity Ca2+ Sensor After All? The Journal of General Physiology, 124: 623-625.

Bennett RG, Duckworth WC, Hamel FG. 2000. Protein Synthesis Post-Translation Modification and Degradation: Degradation of Amylin by Insulin-degrading Enzyme. Journal of Biological Chemistry, 275: 36621-36625.

Bickel PE. 2002. Lipid rafts and insulin signaling. American Journal of Physiological Endocrinology and Metabolism, 282: E1-E10.

Bogan JS, Xu Y, Hao M. 2012. Cholesterol Accumulation Increases Insulin Granule Size and Impairs Membrane Trafficking. Traffic, 13: 1466-1480.

Brunham LR, Kruit JK, Hayden MR, Verchere CB. 2010. Cholesterol in β-Cell Dysfunction: The Emerging Connection Between HDL Cholesterol and Type 2 Diabetes. Current Diabetes Reports, 10: 55-60.

Butler AE, Janson J, Bonner-Weir S, Ritzel R, Rizza RA, Butler PC. 2003. β-Cell Deficit and Increased β-Cell Apoptosis in Humans With Type 2 Diabetes. Diabetes, 52: 102-110.

Buchwald H, Estok R, Fahrbach K, Banel D, Jensen MD, Pories WJ, Bantle JP, Sledge I. 2009. Weight and Type 2 Diabetes after Bariatric Surgery: Systematic Review and Meta-analysis. The American Journal of Medicine, 122: 248-256.

Capozza F, Combs TP, Cohen AW, Cho YR, Park SY, Schubert W, Williams TM, Brasaemle DL, Jelicks LA, Scherer PE, Kim JK, Lisanti MP. 2005. Caveolin-3 knockout mice show increased adiposity and whole body insulin resistance, with ligand-induced insulin receptor instability in skeletal muscle. American Journal of Physiology and Cell Physiology, 288: C1317-C1331.

Castillo JJ, Mull N, Reagan JL, Nemr S, Mitri J. 2012. Increased incidence of non-Hodgkin lymphoma, leukemia, and myeloma in patients with diabetes mellitus type 2: a meta-analysis of observational studies. Blood, 119(21): 4845-4850.

Cerasi, E. 1992. Aetiology of type II diabetes. Insulin-Molecular Biology to Pathology, edited by F.M. Ashcroft and S. J. H. Ashcroft. Oxford, UK: IRL p. 352 – 392.

Chen L, Magiliano DJ, Zimmet PZ. 2012. The worldwide epidemiology of type 2 diabetes mellitus-present and future perspectives. Nature Reviews in Endocrinology, 8: 228-236.

Chen YA, Scheller RH. 2001. SNARE-Mediated Membrane Fusion. Nature Reviews, 2: 98-106.

Clark R, Proks P. 2010. ATP-Sensitive Potassium Channels in Health and Disease. Advances in Experimental Medicine and Biology, 654: 165-192.

Colbert JD, Stone JA. 2012. Statin Use and the Risk of Incident Diabetes Mellitus: A Review of the Literature. Canadian Journal of Cardiology, 28: 581-589.

Davis SN and Granner DK. 2001. Insulin, oral hypoglycemic agents, and the pharmacology of the endocrine pancreas. Goodman and Gilman's The Pharmacological Basis of Therapeutics. 10th Edition.

DeFronzo RA, Abdul-Ghani MA. 2011. Preservation of β-Cell Function: The Key to Diabetes Prevention. Journal of Clinical Endocrinology & Metabolism, 96: 2354-2366.

Del Guerra S, Lupi R, Marselli L, Masini M, Bugliani M, Sbrana S, Torri S, Pollera M, Boggi U, Mosca F, Del Prato S, Marchetti P. 2005. Functional and Molecular Defects of Pancreatic Islets in Human Type 2 Diabetes. Diabetes, 54: 727-735.

Drews G, Krippeit-Drews P, Dufer M. 2010. Electrophysiology of islet cells. Advances in Experimental Medicine and Biology. 654: 115-163.

Duckworth WC, Bennett RG, Hamel FG. 1998. Insulin Degradation: Progress and Potential. Endocrine Reviews, 19(5): 608-624.

Eliasson L, Abdulkader F, Braun M, Galvanoskis J, Hoppa MB, Rorsman P. 2008. Novel aspects of the molecular mechanisms controlling insulin secretion. Journal of Physiology, 586(14): 3313-3324.

Flegal KM, Carol MD, Kuczmarski RJ, Johnson CL. 1998. Overweight and obesity in the United States: prevalence and trends, 1960-1994. International Journal of Obesity, 22(1): 39-47.

Gastaldelli A. 2011. Role of beta-cell dysfunction, ectopic fat accumulation and insulin resistance in the pathogenesis of type 2 diabetes mellitus. Diabetes Research and Clinical Practice, 93S: S60-S65.

Gedam R, Shah I, Ali U, Ohri A. 2012. Smith-Lemli-Opitz-syndrome: A case study. Indian Journal of Human Genetics. 18(2): 235-237.

Goedeke L, Fernandez-Hernando C. 2012. Regulation of cholesterol homeostasis. Cellular and Molecular Life Sciences, 69: 915-930.

Goldfine AB. 2012. Statins: Is it Really Time to Reassess Benefits and Risks? The New England Journal of Medicine, 366: 1752-1755.

George J, Schroepfer Jr. 2000. Oxysterols: Modulators of Cholesterol Metabolism and Other Processes. Physiological Reviews, 80 (1): 361-554

Guillausseau PJ, Meas T, Virally M, Laloi-Michelin M, Medeau V, Kevorkian JP. 2008. Abnormalities in insulin secretion in type 2 diabetes mellitus. Diabetes & Metabolism, 34: S43-S48.

Gustavsson N, Wei SH, Hoang DN, Lao Y, Zhang Q, Radda GK, Rorsman P, Südhof TC, Han W. 2009. Synaptotagmin-7 is a principal Ca^{2+} sensor for Ca^{2+}-induced glucagon exocytosis in pancreas. The Journal of Physiology, 587(6): 1169-1178.

Harada S, Smith RM, Smith JA, Jarett L. 1993. Inhibition of insulin-degrading enzyme increases translocation of insulin to the nucleus in H35 rat hepatoma cells: evidence of a cytosolic pathway. Endocrinology, 132(6): 2293-2298.

Harashima SI, Horiuchi T, Wang Y, Notkins AL, Seino Y, Inagaki N. 2012. Sorting nexin 19 regulates the number of dense core vesicles in pancreatic β-Cells. Journal of Diabetes Investigation, 3(1): 52-60.

Harder T, Rodekamp E, Schellong K, Dudenhausen JW, Plagemann A. 2007. Birth Weight and Subsequent Risk of Type 2 Diabetes: A Meta-Analysis. American Journal of Epidemiology, 165(8): 849-857.

Helsm JB, Zurzolo C. 2004. Lipids as Targeting Signals: Lipid Rafts and Intracellular Trafficking. Traffic, 5: 247-254.

Henquin, JC. 2000. Triggering and amplifying pathways of regulation of insulin secretion by glucose. Diabetes, 49: 1751-1760.

Herman GE. 2003. Disorders of cholesterol biosynthesis: prototypic metabolic malformation syndromes. Human Molecular Genetics, 12(1): R75-R88.

Herrington J, Sanchez M, Wunderler D, Yan L, Bugianesi RM, Dick IE, Clark SA, Brochu RM, Priest BT, Kohler MG, McManus OB. 2005. Biophysical and pharmacological properties of the voltage-gated potassium current of human pancreatic β-cells. Journal of Physiology, 567(1): 159-175.

Horwitz MS, Bradley LM, Barbertson J, Krahl T, Lee J, Sarvetnick N. 1998. Diabetes induced by Coxsackie virus: Initiation by bystander damage and not molecular mimicry. Nature Medicine, 4(7): 781-785.

Ikonen, E. 2008. Cellular Cholesterol Trafficking and Compartmentalization. Nature Reviews. 9: 125-138.

Ikonen, E. 2006. Mechanisms for cellular cholesterol transport: defects and human disease. Physiology Reviews. 86: 1237-1261.

Ismail-Beigi F. 2012. Pathogenesis and Glycemic Management of Type 2 Diabetes Mellitus: A Physiological Approach. Archives of Iranian Medicine, 15(4): 239-246.

Jacobson DA, Kuznetsov A, Lopez JP, Kash S, Ammala CE, Philipson LH. 2007. Kv2.1 Ablation Alters Glucose Induced Islet Electrical Activity, Enhancing Insulin Secretion. Cell Metabolism, 6(3): 229-235.

Jahn R, Fasshauer D. 2012. Molecular machines governing exocytosis of synaptic vesicles. Nature, 490: 201-207.

Jensen CS, Rasmussen HB, Misonou H. 2011. Neuronal trafficking of voltage-gated potassium channels. Molecular and Cellular Neuroscience, 48: 288-297.

Jeon TI, Osborne TF. 2012. SREBPs: metabolic integrators in physiology and metabolism. Cell, 23(2): 65-72.

Jeremic A, Kelly M, Cho J A, Cho SJ, Horber JK, Jena BP. 2004. Calcium drives fusion of SNARE-apposed bilayers. Cell Biology International. 28: 19-31.

Jewell JL, Oh E, Thurmond DC. 2010. Exocytosis mechanisms underlying insulin release and glucose uptake: conserved roles for Munc18c and syntaxin 4. American Journal of Physiology – Regulatory, Integrative, 298: R517-R531.

Jindal HK, Folco EJ, Liu GX, Koren G. 2008. Posttranslational modification of voltage-dependant potassium channel Kv1.5: COOH-terminal palmitoylation modulates its biological properties. American Journal of Physiology – Heart and Circulatory, 294: H2012-H2021.

Kang Y, Zhang Y, Liang T, Leung YK, Ng B, Xie H, Chang N, Chan J, Shyng SL, Tsushima RG, Gaisano HY. 2011. ATP Modulates Interaction of Syntaxin-1A with Sulfonylurea Receptor 1 to Regulate Pancreatic β-Cell K_{ATP} Channels. Journal of Biological Chemsitry, 286(7): 5876-5883.

Karlsson M, Thorn H, Parpal S, Stralfors P, Gustavsson J. 2002. Insulin induces translocation of glucose transporter GLUT4 to plasma membrane caveolae in adipocytes. FASEB J. 16: 249-251.

Kasuga M. 2006. Insulin resistance and pancreatic β cell failure. The Journal of Clinical Investigation, 116: 1756-1760.

Kieffer TJ, Habener JF. 1999. The Glucagon-Like Peptides. Endocrine Reviews, 20(6): 876-913.

Kim SJ, Choi WS, Han JSM, Wanock G, Fedida D, McIntosh CHS. 2005. A Novel Mechanism for the Suppression of a Voltage-gated Potassium Channel by Glucose-dependent Insulinotropic Polypeptide. The Journal of Biological Chemistry, 280(31): 28692-28700.

Kirpichnikov D, McFarlane SI, Sowers, JR. 2002. Metformin: An Update. Annual Internal Medicine, 137(1): 25-33.

Kruit JK, Wijesekara N, Westwell-Roper C, Vanmierlo T, de Haan W, Bhattacharjee A, Tang R, Wellington CL, LutJohann D, Johnson JD, Brunham LR, Verchere CB, Hayden MR. 2012. Loss of Both ABCA1 and ABCG1 Results in Increased Disturbances in Islet Sterol Homeostasis, Inflammation, and Impaired β-Cell Function. Diabetes, 61: 1-6.

Lakschevitz F, Aboodi G, Tenenbaum H, Glogauer M. 2012. Diabetes and Periodontal Diseases: Interplay and Links. Current Diabetes Reviews, 6(7): 433-439.

Lang T. 2007. SNARE proteins and 'membrane rafts'. Journal of Physiology, 585(3): 693-698.

Leech CA, Dzhura I, Chepurny OG, Kang G, Schwede F, Genieser HG, Holz GC. 2011. Molecular Physiology of glucagon-like peptide-1 insulin secretagogue action in pancreatic β-Cells. Progress in Biophysics and Molecular Biology, 107: 236-247.

Leung YM, Kang Y, Gao X, Xia F, Xie H, Sheu L, Tsuk S, Lotan I, Tsushima RG, Gaisano HY, 2003. Syntaxin 1A binds to the cytoplasmic C terminus of Kv2.1 to regulate channel gating and trafficking. Journal or Biological Chemsitry, 278: 17532–17538.

MacDonald PE, Eliasson L, Rorsman P. 2005. Calcium increases endocytotic vesicle size and accelerates membrane fission in insulin-secreting INS-1 cells. Journal of Cell Science, 118: 5911-5920.

Marzban L, Verchere CB. 2004. The Role of Islet Amyloid Polypeptide in Type 2 Diabetes. Canadian Journal of Diabetes, 28(4) 39-47.

Menge BA, Tannapfel A, Belyaev O, Drescher R, Muller C, Uhl W, Schmidt WE, Meier JJ. 2008. Partial Pancreatectomy in Adult Does Not Provoke β-Cell Regeneration. Diabetes, 57: 142-149.

Narne P, Ponnaluri KC, Sing S, Siraj M, Ishaq M. 2012. Relationship between angiotensin converting enzyme gene insertion/deletion polymorphism, angiographically defined coronary artery disease and myocardial infarction in patients with type 2 diabetes mellitus. Journal of Renin-Angiotensin-Aldosteron System. Epub ahead of print. 0(0) 0-9.

Oldfield S, J. Hancock, Mason A, Hobson SA, Wynick D, Kelly E, Randall AD, Marrion NV. 2009. Receptor-Mediated Suppression of Potassium Currents Requires Colocalization within Lipid Rafts. Molecular Pharmacology, 76(6): 1279-1289.

Olofsson CS, Gopel SO, Barg S, Galvanovskis J, Ma X, Salehi A, Rorsman P, Eliasson L. 2002. Fast insulin secretin reflects exocytosis of docked granules in mouse pancreatic β-cells. European Journal of Physiology, 444: 43-51.

Ooi EMM, Ng TWK, Chan DC, Watts GF. 2009. Plasma markers of cholesterol homeostasis in metabolic syndrome subjects with or without type-2 diabetes. Diabetes Research and Clinical Practice, 85: 310-316.

Portha B, Chavey A, Movassat J. 2011. Early-Life Origins of Type 2 Diabetes: Fetal Programming of the Beta-Cell Mass. Experimental Diabetes Research, Article ID 105076, 16 pages, 2011. doi:10.1155/2011/105076

Preiss D, Seshasai SRK, Welsh P, Murphy SA, Ho JE, Waters DD, DeMicco DA, Barter P, Cannon CP, Sabatine MS, Braunwald E *et al*. 2012. American Medical Association, 305(24): 2556-2564.

Preiss D, Sattar N. 2011. Statins and the risk of new-onset diabetes: a review of the recent evidence. Current Opinions in Lipidology, 22:460-466.

Prentki M, Madiraju SRM. 2011. Glycerol/free fatty acid cycle and islet β-Cell function in health, obesity and diabetes. Molecular and Cellular Endicronology, 13 pages, doi:10.1016/j.mce.2011.11.004.

Prentki M, Nolan CJ. 2006. Islet β-cell failure in type 2 diabetes. The Journal of Clinical Investigation, 116(7): 1802-1812.

Ramakrishnan NA, Drescher MJ, Drescher DG. 2012. The SNARE complex in neuronal and sensory cells. Molecular and Cellular Neuroscience, 50: 58-69.

Razani B, Woodman SE, Lisanti MP. 2002. Caveolae: From Cell Biology to Animal Physiology. Pharmacological Reviews, 54(3): 431–467.

Regazzi R, Wollheim CB, Lang J, Theler JM, Rossetto O, Montecucco C, Sadoul K, Weller U, Palmer M, Thorens B. 1995. The EMBO Journal, 14(12): 2723-2730.

Reverter M, Rentero C, de Muga SV, Alvarez-Guaita A, Mulay V, Cairns R, Wood P, Monastyrskaya K, Pol A, Tebar F, Blasi J, Grewal T, Enrich C. 2011. Cholesterol transport from late endosomes to the Golgi regulates t-SNARE trafficking, assembly, and function. Molecular Biology of the Cell, 22: 4108-4123.

Rhodes CJ. 2005. Type 2 Diabetes – a Matter of β-Cell Life and Death? Science, 307: 380-384.

Risselada GJ, Grubmuller H. 2012. How SNARE molecules mediate membrane fusion: Recent insights from molecular simulations. Current Opinion in Structural Biology, 22:187-196.

Rituper B, Flasker A, Gucek A, Chowdhury HH, Zorec R. 2012. Cholesterol and regulated exocytosis: A requirement of unitary exocytotic events. Cell Calcium, 52: 250-258.

Rorsman P, Braun M, Zhang Q. 2012. Regulation of calcium in pancreatic α- and β-cells in health and disease. Cell Calcium, 51: 300-308.

Rorsman P, Eliasson L, Kanno T, Zhang Q, Gopel S. 2011. Electrophysiology of pancreatic β-cells in intact mouse islets of Langerhans. Progress in Biophysics and Molecular Biology, 107: 224-235.

Rorsman P, Salehi SA, Abdulkader F, Braun M, MacDonald PE. 2008. K_{ATP}-channels and glucose-regulated glucagon secretion. Trends in Endocrinology and Metabolism, 19(8): 277-284.

Rorsman P. 2005. Insulin secretion: function and therapy of pancreatic beta-cells in diabetes. The British Journal of Diabetes and Vascular Disease, 5(4): 187-191.

Rorsman P, Eliasson L, Renstrom E, Gromada J, Barg S, Gopel S. 2000. The Cell Physiology of Biphasic Insulin Secretion. News Physiol. Sci., 15: 72-77.

Sattar N, Preiss D, Murray HM, Welsh P, Buckley BM, de Craen AJM, Seshasai SRK, McMurray JJ, Freeman DJ, Jukema JW, MacFarlane PW, Packard CJ *et al.* 2010. Statins and risk of incident diabetes: a collaborative meta-analysis of randomised statin trials. Lancet, 375: 735-742.

Schafer SA, Machicao F, Fritsche A, Haring HU, Kantartzis K. 2011. New type 2 diabetes risk genes provide new insights in insulin secretion mechanisms. Diabetes Research and Clinical Practice, 93S: S9-S24.

Schulla V, Renstrom E, Feil R, Feil S, Franklin I, Gjinovci A, Jing XJ, Laux D, Lundquist I, Magnuson MA, Obermuller S, Olofsson CS, Salehi A *et al*. 2003. Impaired insulin secretion and glucose tolerance in β cell-selective $Ca_V1.2$ Ca^{2+} channel null mice. The EMBO Journal, 22(15): 3844-3854.

Seino S, Shibasaki T, Minami K. 2011. Dynamics of Insulin secretion and the clinical implications for obesity and diabetes. Journal of Clinical Investigation, 121(6): 2118-21.

Shimizu H, Timratana P, Schauer PR, Rogula T. 2012. Review of Metabolic Surgery for Type 2 Diabetes in Patients with a BMI <35 kg/m2. Journal of Obesity, 2012: 1-9.

Singer-Lahat, D., Chikvashvili, D., Lotan, I., 2008. Direct interaction of endogenous kv channels with syntaxin enhances exocytosis by neuroendocrine cells. PLoS ONE 3, e1381.

Staiger H, Machicao F, Stefan N, Tschritter O, Thamer C, Kantartzis K, Schafer SA, Kirchhoff K, Fritsche A, Haring HU. 2007. Polymorphisms within Novel Risk Loci for Type 2 Diabetes Determine β-cell Function. PLOS One, 9: e832.

Straub SG, Sharp GWG. 2002. Glucose-stimulated signaling pathways in biphasic insulin secretion. Diabetes/Metabolism Research and Reviews, 18: 451-463.

Stumvoll M, Goldstein BJ, van Haeften TW. 2005. Type 2 diabetes: principles of pathogenesis and therapy. Lancet, 365: 1333-1346.

Sturek JM, Castle JD, Trace AP, Page LC, Castle AM, Evans-Molina C, Parks JS, Mirmira RG, Hedrick CC. An intracellular role for ABCG1-mediated cholesterol transport in the regulated secretory pathway of mouse pancreatic beta cells. Journal of Clinical Investigation, 120: 2575–2589.

Thion L, Mazars C, Thuleau P, Graziana A, Rossingnol M, Moreau M, Ranjeva R. 1996. Activation of plasma membrane voltage-dependant calcium-permeable channels by disruption of microtubules in carrot cells. FEBS Letters, 393: 13-18.

Tsuchiya M, Hosaka M, Moriguchi T, Zhang S, Suda M, Yokota-Hashimoto H, Shinozuka K, Takeuchi T. 2010. Cholesterol Biosynthesis Pathway Intermediates and Inhibitors Regulate Glucose-Stimulated Insulin Secretion and Secretory Granule Formation in Pancreatic β-Cells. Endocrinology, 151(10): 4705-4716.

Wang CCL, Reusch JEB. 2012. Diabetes and Cardiovascular Disease: Changing the Focus from Glycemic Control to Improving Long-Term Survival. The American Journal of Cardiology, 110: 58B-68B.

Wiser O, Trus M, Hernandez A, Renstrom E, Barg S, Rorsman P, Atlas D. 1999. The voltage sensitive Lc-type Ca2+ channel is functionally coupled to the exocytotic machinery. Proceedings of the National Academy of Science USA, 96: 248-253.

Wiser O, Tobi D, Trus M, Atlas D. 1997. Synaptotagmin restores kinetic properties of a syntaxin-associated N-type voltage sensitive calcium channel. FEBS Lett. 404: 203-207.

Xia F, Xie L, Mihic A, Gao X, Chen Y, Gaisano HY, Tsushima RG. 2008. Inhibition of Cholesterol Biosynthesis Impairs Insulin Secretion and Voltage-Gated Calcium Channel Function in Pancreatic β-Cells. Endocrinology, 149(10): 5136-5145.

Yamakawa T, Saith S, Li Y, Gao X, Gaisano HY, Tsushima RG. 2007. Interaction of Syntaxin 1A with the N-Terminus of Kv4.2 Modulates Channel Surface Expression and Gating. Biochemistry, 46: 10942-10949.

Yamamoto M, Toya Y, Schwencke C, Lisanti MP, Myers MG, Ishikawa Y. 1998. Caveolin is an activator of insulin receptor signaling. Journal of Biological Chemistry, 273: 26962-26968.

Yan FF, Lin CW, Cartier EA, Shyng SL. 2005. Role of ubiquitin-proteasome degradation pathway in biogenesis efficiency of β-Cell ATP-sensitive potassium channels. American Journal of Physiology – Cell Physiology, 289: C1351-C1359.

Yan L, Figueroa DJ, Austin CP, Liu Y, Bugianesi RM, Slaughter RS, Kaczorowski GJ, Kohler MG. 2004. Expression of Voltage-Gated Potassium Channels in Human and Rhesus Pancreatic Islets. Diabetes, 53: 597-607.

Yang SN, Berggren PO. 2006. The role of voltage-gated calcium channels in pancreatic beta-cell physiology and pathophysiology. Endocrinology Reviews, 27: 621-676.

Yang SN, Berggren PO. 2005. B-Cell Cav channel regulation in physiology and pathophysiology. American Journal of Physiology and Endocrinology Metabolism, 288: E16-E28.

Appendix

A.1. Statistical Analysis – Cholesterol Content

Multiple Comparisons – Cholesterol Content						
(I) Groups	(J) Groups	Mean Difference (I-J)	Std. Error	Sig.	95% Confidence Interval	
					Lower Bound	Upper Bound
FBS	LPS	3.349501*	.814145	.014	.53081	6.16819
	PR	3.106117*	.814145	.026	.28743	5.92481
	PR-L	5.472525*	.814145	.000	2.65383	8.29122
	AS	3.207836*	.814145	.020	.38914	6.02653
	AS-L	5.979707*	.814145	.000	3.16102	8.79840
	AY	3.302296*	.814145	.016	.48360	6.12099
	AY-L	6.237608*	.814145	.000	3.41892	9.05630
PR	FBS	-3.349501*	.814145	.014	-6.16819	-.53081
	LPS	.243384	.814145	1.000	-2.57531	3.06208
	PR-L	2.366408	.814145	.136	-.45228	5.18510
	AS	.101718	.814145	1.000	-2.71697	2.92041
	AS-L	2.873590*	.814145	.044	.05490	5.69228
	AY	.196179	.814145	1.000	-2.62251	3.01487
	AY-L	3.131491*	.814145	.024	.31280	5.95018
PR-L	FBS	-5.472525*	.814145	.000	-8.29122	-2.65383
	LPS	-2.123024	.814145	.222	-4.94172	.69567
	PR	-2.366408	.814145	.136	-5.18510	.45228
	AS	-2.264689	.814145	.168	-5.08338	.55400
	AS-L	.507182	.814145	.998	-2.31151	3.32587
	AY	-2.170229	.814145	.203	-4.98892	.64846
	AY-L	.765083	.814145	.977	-2.05361	3.58377
AS	FBS	-3.207836*	.814145	.020	-6.02653	-.38914
	LPS	.141666	.814145	1.000	-2.67703	2.96036
	PR	-.101718	.814145	1.000	-2.92041	2.71697
	PR-L	2.264689	.814145	.168	-.55400	5.08338
	AS-L	2.771872	.814145	.056	-.04682	5.59056
	AY	.094460	.814145	1.000	-2.72423	2.91315
	AY-L	3.029772*	.814145	.031	.21108	5.84846

AS-L	FBS	-5.979707*	.814145	.000	-8.79840	-3.16102
	LPS	-2.630206	.814145	.077	-5.44890	.18849
	PR	-2.873590*	.814145	.044	-5.69228	-.05490
	PR-L	-.507182	.814145	.998	-3.32587	2.31151
	AS	-2.771872	.814145	.056	-5.59056	.04682
	AY	-2.677411	.814145	.069	-5.49610	.14128
	AY-L	.257901	.814145	1.000	-2.56079	3.07659
AY	FBS	-3.302296*	.814145	.016	-6.12099	-.48360
	LPS	.047205	.814145	1.000	-2.77149	2.86590
	PR	-.196179	.814145	1.000	-3.01487	2.62251
	PR-L	2.170229	.814145	.203	-.64846	4.98892
	AS	-.094460	.814145	1.000	-2.91315	2.72423
	AS-L	2.677411	.814145	.069	-.14128	5.49610
	AY-L	2.935312*	.814145	.038	.11662	5.75400
AY-L	FBS	-6.237608*	.814145	.000	-9.05630	-3.41892
	LPS	-2.888106*	.814145	.043	-5.70680	-.06941
	PR	-3.131491*	.814145	.024	-5.95018	-.31280
	PR-L	-.765083	.814145	.977	-3.58377	2.05361
	AS	-3.029772*	.814145	.031	-5.84846	-.21108
	AS-L	-.257901	.814145	1.000	-3.07659	2.56079
	AY	-2.935312*	.814145	.038	-5.75400	-.11662
LPS	FBS	-3.349501*	.814145	.014	-6.16819	-.53081
	PR	-.243384	.814145	1.000	-3.06208	2.57531
	PR-L	2.123024	.814145	.222	-.69567	4.94172
	AS	-.141666	.814145	1.000	-2.96036	2.67703
	AS-L	2.630206	.814145	.077	-.18849	5.44890
	AY	-.047205	.814145	1.000	-2.86590	2.77149
	AY-L	2.888106*	.814145	.043	.06941	5.70680

*. The mean difference is significant at the 0.05 level.

Cholesterol Content - Descriptives								
	N	Mean	Std. Deviation	Std. Error	95% Confidence Interval for Mean		Minimum	Maximum
					Lower Bound	Upper Bound		
FBS	3	12.83004	.335356	.193618	11.99697	13.66311	12.446	13.065
LPS	3	9.48054	.423161	.244312	8.42935	10.53173	9.001	9.800
PR	3	9.72393	1.309063	.755788	6.47203	12.97582	8.285	10.845
PR-L	3	7.35752	.986036	.569288	4.90807	9.80697	6.340	8.308
AS	3	9.62221	1.036767	.598577	7.04674	12.19768	8.439	10.370
AS-L	3	6.85034	1.372685	.792520	3.44040	10.26027	5.905	8.425
AY	3	9.52775	.565089	.326254	8.12399	10.93151	8.964	10.094
AY-L	3	6.59244	1.303098	.752344	3.35536	9.82951	5.106	7.540
Total	24	8.99810	2.121556	.433061	8.10224	9.89395	5.106	13.065

A.2. Statistical Analysis – Cell Viability

(I) Groups	(J) Groups	Mean Difference (I-J)	Std. Error	Sig.	95% Confidence Interval	
					Lower Bound	Upper Bound
FBS	LPS	-.001000	.032444	1.000	-.09809	.09609
	PR	-.002200	.032444	1.000	-.09929	.09489
	AS	.028800	.032444	.898	-.06829	.12589
	AY	.103800*	.032444	.033	.00671	.20089
LPS	FBS	.001000	.032444	1.000	-.09609	.09809
	PR	-.001200	.032444	1.000	-.09829	.09589
	AS	.029800	.032444	.886	-.06729	.12689
	AY	.104800*	.032444	.030	.00771	.20189
PR	FBS	.002200	.032444	1.000	-.09489	.09929
	LPS	.001200	.032444	1.000	-.09589	.09829
	AS	.031000	.032444	.871	-.06609	.12809
	AY	.106000*	.032444	.028	.00891	.20309
AS	FBS	-.028800	.032444	.898	-.12589	.06829
	LPS	-.029800	.032444	.886	-.12689	.06729
	PR	-.031000	.032444	.871	-.12809	.06609
	AY	.075000	.032444	.182	-.02209	.17209
AY	FBS	-.103800*	.032444	.033	-.20089	-.00671

	LPS	-.104800*	.032444	.030	-.20189	-.00771
	PR	-.106000*	.032444	.028	-.20309	-.00891
	AS	-.075000	.032444	.182	-.17209	.02209
*. The mean difference is significant at the 0.05 level.						

Cell Viability - Descriptives								
	N	Mean	Std. Deviation	Std. Error	95% Confidence Interval for Mean		Minimum	Maximum
					Lower Bound	Upper Bound		
FBS	5	.85380	.030866	.013804	.81547	.89213	.812	.895
LPS	5	.85480	.060899	.027235	.77918	.93042	.769	.918
PR	5	.85600	.037041	.016565	.81001	.90199	.795	.885
AS	5	.82500	.066705	.029831	.74218	.90782	.782	.943
AY	5	.75000	.051720	.023130	.68578	.81422	.695	.810
Total	25	.82792	.062562	.012512	.80210	.85374	.695	.943

A.3. Statistical Analysis – Glucose Stimulated Insulin Secretion

Low Glucose

(I) Groups	(J) Groups	Mean Difference (I-J)	Std. Error	Sig.	95% Confidence Interval	
					Lower Bound	Upper Bound
FBS	LPS	.0032500	.0036835	.992	-.008962	.015462
	PR	-.0039000	.0036835	.976	-.016112	.008312
	PR-L	-.0059667	.0045113	.917	-.020924	.008990
	AS	-.0019500	.0036835	1.000	-.014162	.010262
	AS-L	-.0061333	.0045113	.905	-.021090	.008824
	AY	.0136833*	.0036835	.019	.001471	.025896
	AY-L	.0064333	.0045113	.880	-.008524	.021390
	DMSO	.0010000	.0045113	1.000	-.013957	.015957
LPS	FBS	-.0032500	.0036835	.992	-.015462	.008962
	PR	-.0071500	.0036835	.592	-.019362	.005062
	PR-L	-.0092167	.0045113	.526	-.024174	.005740
	AS	-.0052000	.0036835	.885	-.017412	.007012

	AS-L	-.0093833	.0045113	.503	-.024340	.005574
	AY	.0104333	.0036835	.144	-.001779	.022646
	AY-L	.0031833	.0045113	.998	-.011774	.018140
	DMSO	-.0022500	.0045113	1.000	-.017207	.012707
PR	FBS	.0039000	.0036835	.976	-.008312	.016112
	LPS	.0071500	.0036835	.592	-.005062	.019362
	PR-L	-.0020667	.0045113	1.000	-.017024	.012890
	AS	.0019500	.0036835	1.000	-.010262	.014162
	AS-L	-.0022333	.0045113	1.000	-.017190	.012724
	AY	.0175833*	.0036835	.001	.005371	.029796
	AY-L	.0103333	.0045113	.376	-.004624	.025290
	DMSO	.0049000	.0045113	.972	-.010057	.019857
PR-L	FBS	.0059667	.0045113	.917	-.008990	.020924
	LPS	.0092167	.0045113	.526	-.005740	.024174
	PR	.0020667	.0045113	1.000	-.012890	.017024
	AS	.0040167	.0045113	.992	-.010940	.018974
	AS-L	-.0001667	.0052092	1.000	-.017437	.017104
	AY	.0196500*	.0045113	.003	.004693	.034607
	AY-L	.0124000	.0052092	.327	-.004871	.029671
	DMSO	.0069667	.0052092	.912	-.010304	.024237
AS	FBS	.0019500	.0036835	1.000	-.010262	.014162
	LPS	.0052000	.0036835	.885	-.007012	.017412
	PR	-.0019500	.0036835	1.000	-.014162	.010262
	PR-L	-.0040167	.0045113	.992	-.018974	.010940
	AS-L	-.0041833	.0045113	.990	-.019140	.010774
	AY	.0156333*	.0036835	.005	.003421	.027846
	AY-L	.0083833	.0045113	.645	-.006574	.023340
	DMSO	.0029500	.0045113	.999	-.012007	.017907
AS-L	FBS	.0061333	.0045113	.905	-.008824	.021090
	LPS	.0093833	.0045113	.503	-.005574	.024340
	PR	.0022333	.0045113	1.000	-.012724	.017190
	PR-L	.0001667	.0052092	1.000	-.017104	.017437
	AS	.0041833	.0045113	.990	-.010774	.019140
	AY	.0198167*	.0045113	.003	.004860	.034774
	AY-L	.0125667	.0052092	.311	-.004704	.029837
	DMSO	.0071333	.0052092	.901	-.010137	.024404
AY	FBS	-.0136833*	.0036835	.019	-.025896	-.001471
	LPS	-.0104333	.0036835	.144	-.022646	.001779
	PR	-.0175833*	.0036835	.001	-.029796	-.005371

	PR-L	-.0196500*	.0045113	.003	-.034607	-.004693
	AS	-.0156333*	.0036835	.005	-.027846	-.003421
	AS-L	-.0198167*	.0045113	.003	-.034774	-.004860
	AY-L	-.0072500	.0045113	.794	-.022207	.007707
	DMSO	-.0126833	.0045113	.150	-.027640	.002274
8	FBS	-.0064333	.0045113	.880	-.021390	.008524
	LPS	-.0031833	.0045113	.998	-.018140	.011774
	PR	-.0103333	.0045113	.376	-.025290	.004624
	PR-L	-.0124000	.0052092	.327	-.029671	.004871
	AS	-.0083833	.0045113	.645	-.023340	.006574
	AS-L	-.0125667	.0052092	.311	-.029837	.004704
	AY	.0072500	.0045113	.794	-.007707	.022207
	DMSO	-.0054333	.0052092	.978	-.022704	.011837
DMSO	FBS	-.0010000	.0045113	1.000	-.015957	.013957
	LPS	.0022500	.0045113	1.000	-.012707	.017207
	PR	-.0049000	.0045113	.972	-.019857	.010057
	PR-L	-.0069667	.0052092	.912	-.024237	.010304
	AS	-.0029500	.0045113	.999	-.017907	.012007
	AS-L	-.0071333	.0052092	.901	-.024404	.010137
	AY	.0126833	.0045113	.150	-.002274	.027640
	AY-L	.0054333	.0052092	.978	-.011837	.022704

High Glucose

(I) Groups	(J) Groups	Mean Difference (I-J)	Std. Error	Sig.	95% Confidence Interval Lower Bound	Upper Bound
FBS	LPS	.0113792	.0071242	.799	-0.01224	0.034999
	PR	.0258088*	.0071242	.024	.002189	.049428
	PR-L	.0429973*	.0087253	.001	.014069	.071925
	AS	.0326748*	.0071242	.002	.009055	.056294
	AS-L	.0511430*	.0087253	.000	.022215	.080071
	AY	.0549073*	.0071242	.000	.031288	.078527
	AY-L	.0593477*	.0087253	.000	.030420	.088276
	DMSO	-.0031980	.0087253	1.000	-.032126	.025730
LPS	FBS	-.0113792	.0071242	.799	-.034999	.012240
	PR	.0144297	.0071242	.538	-.009190	.038049

	PR-L	.0316182*	.0087253	.024	.002690	.060546
	AS	.0212957	.0071242	.104	-.002324	.044915
	AS-L	.0397638*	.0087253	.002	.010836	.068692
	AY	.0435282*	.0071242	.000	.019909	.067148
	AY-L	.0479685*	.0087253	.000	.019041	.076896
	DMSO	-.0145772	.0087253	.759	-.043505	.014351
PR	FBS	-.0258088*	.0071242	.024	-.049428	-.002189
	LPS	-.0144297	.0071242	.538	-.038049	.009190
	PR-L	.0171885	.0087253	.573	-.011739	.046116
	AS	.0068660	.0071	.987	-.016754	.030486
	AS-L	.0253342	.0087	.125	-.003594	.054262
	AY	.0290985*	.0071242	.007	.005479	.052718
	AY-L	.0335388*	.0087253	.013	.004611	.062467
	DMSO	-.0290068*	.0087253	.049	-.057935	-.000079
PR-L	FBS	-.0429973*	.0087253	.001	-.071925	-.014069
	LPS	-.0316182*	.0087253	.024	-.060546	-.002690
	PR	-.0171885	.0087253	.573	-.046116	.011739
	AS	-.0103225	.0087253	.955	-.039250	.018605
	AS-L	.0081457	.0100751	.996	-.025257	.041549
	AY	.0119100	.0087253	.903	-.017018	.040838
	AY-L	.0163503	.0100751	.786	-.017053	.049753
	DMSO	-.0461953*	.0100751	.002	-.079598	-.012792
AS	FBS	-.0326748*	.0071242	.002	-.056294	-.009055
	LPS	-.0212957	.0071242	.104	-.044915	.002324
	PR	-.0068660	.0071242	.987	-.030486	.016754
	PR-L	.0103225	.0087253	.955	-.018605	.039250
	AS-L	.0184682	.0087253	.480	-.010460	.047396
	AY	.0222325	.0071242	.078	-.001387	.045852
	AY-L	.0266728	.0087253	.090	-.002255	.055601
	DMSO	-.0358728*	.0087253	.007	-.064801	-.006945
AS-L	FBS	-.0511430*	.0087	.000	-.080071	-.022215
	LPS	-.0397638*	.0087253	.002	-.068692	-.010836
	PR	-.0253342	.0087253	.125	-.054262	.003594
	PR-L	-.0081457	.0100751	.996	-.041549	.025257
	AS	-.0184682	.0087253	.480	-.047396	.010460
	AY	.0037643	.0087253	1.000	-.025164	.032692
	AY-L	.0082047	.0100751	.996	-.025198	.041608
	DMSO	-.0543410*	.0100751	.000	-.087744	-.020938
AY	FBS	-.0549073*	.0071242	.000	-.078527	-.031288

	LPS	-.0435282*	.0071242	.000	-.067148	-.019909
	PR	-.0290985*	.0071242	.007	-.052718	-.005479
	PR-L	-.0119100	.0087253	.903	-.040838	.017018
	AS	-.0222325	.0071242	.078	-.045852	.001387
	AS-L	-.0037643	.0087253	1.000	-.032692	.025164
	AY-L	.0044403	.0087253	1.000	-.024488	.033368
	DMSO	-.0581053*	.0087253	.000	-.087033	-.029177
AY-L	FBS	-.0593477*	.0087253	.000	-.088276	-.030420
	LPS	-.0479685*	.0087253	.000	-.076896	-.019041
	PR	-.0335388*	.0087253	.013	-.062467	-.004611
	PR-L	-.0163503	.0100751	.786	-.049753	.017053
	AS	-.0266728	.0087	.090	-.055601	.002255
	AS-L	-.0082047	.0100751	.996	-.041608	.025198
	AY	-.0044403	.0087253	1.000	-.033368	.024488
	DMSO	-.0625457*	.0100751	.000	-.095949	-.029143
DMSO	FBS	.0031980	.0087253	1.000	-.025730	.032126
	LPS	.0145772	.0087253	.759	-.014351	.043505
	PR	.0290068*	.0087253	.049	.000079	.057935
	PR-L	.0461953*	.0100751	.002	.012792	.079598
	AS	.0358728*	.0087253	.007	.006945	.064801
	AS-L	.0543410*	.0100751	.000	.020938	.087744
	AY	.0581053*	.0087253	.000	.029177	.087033
	AY-L	.0625457*	.0100751	.000	.029143	.095949

Low Glucose

Glucose Stimulated Insulin Secretion - Descriptives							
	Mean	Std. Deviation	Std. Error	95% Confidence Interval for Mean		Minimum	Maximum
				Lower Bound	Upper Bound		
FBS	.028500	.0047887	.0019550	.023475	.033525	.0210	.0344
LPS	.025250	.0074693	.0030493	.017411	.033089	.0150	.0325
DMSO	.027500	.0037041	.0021385	.018299	.036701	.0247	.0317
PR	.032400	.0071764	.0029297	.024869	.039931	.0211	.0402
PR-L	.034467	.0023459	.0013544	.028639	.040294	.0326	.0371
AS	.030450	.0065650	.0026801	.023560	.037340	.0201	.0366
AS-L	.034633	.0049339	.0028486	.022377	.046890	.0308	.0402
AY	.014817	.0056796	.0023187	.008856	.020777	.0076	.0222
AY-L	.022067	.0106819	.0061672	-.004469	.048602	.0127	.0337

High Glucose

FBS	.081600	.0187824	.0076679	.061889	.101311	.0564	.1036
LPS	.070233	.0119676	.0048857	.057674	.082793	.0563	.0856
DMSO	.084800	.0077505	.0044747	.065547	.104053	.0770	.0925
PR	.055800	.0134398	.0054868	.041696	.069904	.0374	.0716
PR-L	.038633	.0033501	.0019342	.030311	.046956	.0353	.0420
AS	.048950	.0113257	.0046237	.037064	.060836	.0354	.0687
AS-L	.030500	.0044978	.0025968	.019327	.041673	.0254	.0339
AY	.026717	.0111094	.0045354	.015058	.038375	.0135	.0402
AY-L	.022267	.0099962	.0057713	-.002565	.047099	.0134	.0331
Total	.053057	.0241992	.0037340	.045516	.060598	.0134	.1036

A.4. Statistical Analysis – Insulin Content

(I) Treatment	(J) Treatment	Mean Difference (I-J)	Std. Error	Sig.	95% Confidence Interval	
					Lower Bound	Upper Bound
FBS	LPS	.0515184	.1251703	1.000	-.363471	.466508
	DMSO	.1430946	.1533017	.989	-.365162	.651351
	PR	.2339352	.1251703	.638	-.181055	.648925
	PR-L	.7736126*	.1533017	.000	.265356	1.281869
	AS	.0352541	.1251703	1.000	-.379736	.450244
	AS-L	.7391245*	.1533017	.001	.230868	1.247381
	AY	.4461257*	.1251703	.027	.031136	.861116
	AY-L	.8603438*	.1533017	.000	.352087	1.368601
LPS	FBS	-.0515184	.1251703	1.000	-.466508	.363471
	DMSO	.0915762	.1533017	1.000	-.416681	.599833
	PR	.1824167	.1251703	.867	-.232573	.597407
	PR-L	.7220941*	.1533017	.001	.213837	1.230351
	AS	-.0162643	.1251703	1.000	-.431254	.398726
	AS-L	.6876061*	.1533017	.002	.179349	1.195863
	AY	.3946072	.1251703	.073	-.020383	.809597
	AY-L	.8088253*	.1533017	.000	.300569	1.317082
DMSO	FBS	-.1430946	.1533017	.989	-.651351	.365162
	LPS	-.0915762	.1533017	1.000	-.599833	.416681
	PR	.0908405	.1533017	1.000	-.417416	.599097

	PR-L	.6305179*	.1770176	.028	.043634	1.217402
	AS	-.1078405	.1533017	.998	-.616097	.400416
	AS-L	.5960299*	.1770176	.044	.009146	1.182914
	AY	.3030310	.1533017	.569	-.205226	.811288
	AY-L	.7172492*	.1770176	.008	.130365	1.304134
PR	FBS	-.2339352	.1251703	.638	-.648925	.181055
	LPS	-.1824167	.1251703	.867	-.597407	.232573
	DMSO	-.0908405	.1533017	1.000	-.599097	.417416
	PR-L	.5396774*	.1533017	.031	.031421	1.047934
	AS	-.1986810	.1251703	.805	-.613671	.216309
	AS-L	.5051894	.1533017	.052	-.003067	1.013446
	AY	.2121905	.1251703	.745	-.202799	.627180
	AY-L	.6264086*	.1533017	.007	.118152	1.134665
PR-L	FBS	-.7736126*	.1533017	.000	-1.281869	-.265356
	LPS	-.7220941*	.1533017	.001	-1.230351	-.213837
	DMSO	-.6305179*	.1770176	.028	-1.217402	-.043634
	PR	-.5396774*	.1533017	.031	-1.047934	-.031421
	AS	-.7383584*	.1533017	.001	-1.246615	-.230102
	AS-L	-.0344880	.1770176	1.000	-.621372	.552396
	AY	-.3274869	.1533017	.468	-.835744	.180770
	AY-L	.0867312	.1770176	1.000	-.500153	.673616
AS	FBS	-.0352541	.1251703	1.000	-.450244	.379736
	LPS	.0162643	.1251703	1.000	-.398726	.431254
	DMSO	.1078405	.1533017	.998	-.400416	.616097
	PR	.1986810	.1251703	.805	-.216309	.613671
	PR-L	.7383584*	.1533017	.001	.230102	1.246615
	AS-L	.7038704*	.1533017	.002	.195614	1.212127
	AY	.4108715	.1251703	.054	-.004118	.825861
	AY-L	.8250896*	.1533017	.000	.316833	1.333346
AS-L	FBS	-.7391245*	.1533017	.001	-1.247381	-.230868
	LPS	-.6876061*	.1533017	.002	-1.195863	-.179349
	DMSO	-.5960299*	.1770176	.044	-1.182914	-.009146
	PR	-.5051894	.1533017	.052	-1.013446	.003067
	PR-L	.0344880	.1770176	1.000	-.552396	.621372
	AS	-.7038704*	.1533017	.002	-1.212127	-.195614
	AY	-.2929989	.1533017	.611	-.801256	.215258
	AY-L	.1212193	.1770176	.999	-.465665	.708104
AY	FBS	-.4461257*	.1251703	.027	-.861116	-.031136
	LPS	-.3946072	.1251703	.073	-.809597	.020383

	DMSO	-.3030310	.1533017	.569	-.811288	.205226
	PR	-.2121905	.1251703	.745	-.627180	.202799
	PR-L	.3274869	.1533017	.468	-.180770	.835744
	AS	-.4108715	.1251703	.054	-.825861	.004118
	AS-L	.2929989	.1533017	.611	-.215258	.801256
	AY-L	.4142181	.1533017	.186	-.094039	.922475
AY-L	FBS	-.8603438*	.1533017	.000	-1.368601	-.352087
	LPS	-.8088253*	.1533017	.000	-1.317082	-.300569
	DMSO	-.7172492*	.1770176	.008	-1.304134	-.130365
	PR	-.6264086*	.1533017	.007	-1.134665	-.118152
	PR-L	-.0867312	.1770176	1.000	-.673616	.500153
	AS	-.8250896*	.1533017	.000	-1.333346	-.316833
	AS-L	-.1212193	.1770176	.999	-.708104	.465665
	AY	-.4142181	.1533017	.186	-.922475	.094039
*. The mean difference is significant at the 0.05 level.						

Descriptives – Insulin Content

	Mean	Std. Deviation	Std. Error	95% Confidence Interval for Mean		Minimum	Maximum
				Lower Bound	Upper Bound		
FBS	2.0302	.14042	.05733	1.8828	2.1775	1.82	2.16
LPS	1.9787	.24188	.09875	1.7248	2.2325	1.65	2.30
DMSO	1.8871	.10802	.06236	1.6188	2.1554	1.80	2.01
PR	1.7962	.18982	.07750	1.5970	1.9954	1.59	2.15
PR-L	1.2566	.02902	.01676	1.1845	1.3287	1.24	1.29
AS	1.9949	.28032	.11444	1.7007	2.2891	1.63	2.35
AS-L	1.2911	.12469	.07199	.9813	1.6008	1.15	1.39
AY	1.5841	.29912	.12211	1.2701	1.8980	1.17	1.90
AY-L	1.1698	.20427	.11794	.6624	1.6773	1.02	1.40
Total	1.7409	.35950	.05547	1.6289	1.8529	1.02	2.35

A.5. Statistical Analysis – $Ca_v1.2$ Promoter Activity

(I) Treatment	(J) Treatment	Mean Difference (I-J)	Std. Error	Sig.	95% Confidence Interval	
					Lower Bound	Upper Bound
FBS	LPS	.06833	.03784	.421	-.0562	.1929
	PR	.12300	.03784	.053	-.0015	.2475
	AS	.06633	.03784	.448	-.0582	.1909
	AY	.22033*	.03784	.001	.0958	.3449
LPS	FBS	-.06833	.03784	.421	-.1929	.0562
	PR	.05467	.03784	.616	-.0699	.1792
	AS	-.00200	.03784	1.000	-.1265	.1225
	AY	.15200*	.03784	.016	.0275	.2765
PR	FBS	-.12300	.03784	.053	-.2475	.0015
	LPS	-.05467	.03784	.616	-.1792	.0699
	AS	-.05667	.03784	.586	-.1812	.0679
	AY	.09733	.03784	.150	-.0272	.2219
AS	FBS	-.06633	.03784	.448	-.1909	.0582
	LPS	.00200	.03784	1.000	-.1225	.1265
	PR	.05667	.03784	.586	-.0679	.1812
	AY	.15400*	.03784	.015	.0295	.2785
AY	FBS	-.22033*	.03784	.001	-.3449	-.0958
	LPS	-.15200*	.03784	.016	-.2765	-.0275
	PR	-.09733	.03784	.150	-.2219	.0272
	AS	-.15400*	.03784	.015	-.2785	-.0295

*. The mean difference is significant at the 0.05 level.

Descriptives – $Ca_v1.2$ Promoter Activity

	Mean	Std. Deviation	Std. Error	95% Confidence Interval for Mean		Minimum	Maximum
				Lower Bound	Upper Bound		
FBS	1.0000	.00000	.00000	1.0000	1.0000	1.00	1.00
LPS	.9317	.04786	.02763	.8128	1.0506	.88	.97
PR	.8770	.05367	.03099	.7437	1.0103	.83	.93
AS	.9337	.02669	.01541	.8674	1.0000	.91	.96
AY	.7797	.06969	.04024	.6065	.9528	.71	.84
Total	.9044	.08562	.02211	.8570	.9518	.71	1.00

A.6. Statistical Analysis – Kv2.1 Promoter Activity

(I) Treatment	(J) Treatment	Mean Difference (I-J)	Std. Error	Sig.	95% Confidence Interval	
					Lower Bound	Upper Bound
FBS	LPS	.29733*	.08270	.031	.0252	.5695
	PR	.36767*	.08270	.009	.0955	.6398
	AS	.63967*	.08270	.000	.3675	.9118
	AY	.65767*	.08270	.000	.3855	.9298
LPS	FBS	-.29733*	.08270	.031	-.5695	-.0252
	PR	.07033	.08270	.908	-.2018	.3425
	AS	.34233*	.08270	.014	.0702	.6145
	AY	.36033*	.08270	.010	.0882	.6325
PR	FBS	-.36767*	.08270	.009	-.6398	-.0955
	LPS	-.07033	.08270	.908	-.3425	.2018
	AS	.27200	.08270	.050	-.0002	.5442
	AY	.29000*	.08270	.036	.0178	.5622
AS	FBS	-.63967*	.08270	.000	-.9118	-.3675
	LPS	-.34233*	.08270	.014	-.6145	-.0702
	PR	-.27200	.08270	.050	-.5442	.0002
	AY	.01800	.08270	.999	-.2542	.2902
AY	FBS	-.65767*	.08270	.000	-.9298	-.3855
	LPS	-.36033*	.08270	.010	-.6325	-.0882
	PR	-.29000*	.08270	.036	-.5622	-.0178
	AS	-.01800	.08270	.999	-.2902	.2542

*. The mean difference is significant at the 0.05 level.

Descriptives – K_V2.1 Promoter Activity

	Mean	Std. Deviation	Std. Error	95% Confidence Interval for Mean		Minimum	Maximum
				Lower Bound	Upper Bound		
FBS	1.0000	.00000	.00000	1.0000	1.0000	1.00	1.00
LPS	.7027	.15659	.09041	.3137	1.0917	.59	.88
PR	.6323	.15021	.08673	.2592	1.0055	.53	.80
AS	.3603	.05300	.03060	.2287	.4920	.32	.42
AY	.3423	.03743	.02161	.2493	.4353	.32	.39
Total	.6075	.26565	.06859	.4604	.7546	.32	1.00

A.7. Statistical Analysis – Insulin Promoter Activity

Multiple Comparisons – Ins-1 Promoter Activity						
(I) Treatment	(J) Treatment	Mean Difference (I-J)	Std. Error	Sig.	95% Confidence Interval	
					Lower Bound	Upper Bound
FBS	LPS	-.168333	.052915	.058	-.34011	.00344
	PR	.157667	.074833	.433	-.08526	.40059
	PR-L	-.224333	.074833	.087	-.46726	.01859
	AS	.304833*	.059161	.000	.11278	.49688
	AS-L	-.150333	.074833	.492	-.39326	.09259
	AY	.614000*	.074833	.000	.37107	.85693
	AY-L	.365000*	.074833	.001	.12207	.60793
LPS	FBS	.168333	.052915	.058	-.00344	.34011
	PR	.326000*	.074833	.003	.08307	.56893
	PR-L	-.056000	.074833	.995	-.29893	.18693
	AS	.473167*	.059161	.000	.28112	.66522
	AS-L	.018000	.074833	1.000	-.22493	.26093
	AY	.782333*	.074833	.000	.53941	1.02526
	AY-L	.533333*	.074833	.000	.29041	.77626
PR	FBS	-.157667	.074833	.433	-.40059	.08526
	LPS	-.326000*	.074833	.003	-.56893	-.08307
	PR-L	-.382000*	.091652	.005	-.67952	-.08448
	AS	.147167	.079373	.590	-.11050	.40483
	AS-L	-.308000*	.091652	.038	-.60552	-.01048
	AY	.456333*	.091652	.001	.15881	.75386
	AY-L	.207333	.091652	.345	-.09019	.50486
PR-L	FBS	.224333	.074833	.087	-.01859	.46726
	LPS	.056000	.074833	.995	-.18693	.29893
	PR	.382000*	.091652	.005	.08448	.67952
	AS	.529167*	.079373	.000	.27150	.78683
	AS-L	.074000	.091652	.991	-.22352	.37152
	AY	.838333*	.091652	.000	.54081	1.13586
	AY-L	.589333*	.091652	.000	.29181	.88686
AS	FBS	-.304833*	.059161	.000	-.49688	-.11278
	LPS	-.473167*	.059161	.000	-.66522	-.28112
	PR	-.147167	.079373	.590	-.40483	.11050
	PR-L	-.529167*	.079373	.000	-.78683	-.27150

	AS-L	-.455167*	.079373	.000	-.71283	-.19750
	AY	.309167*	.079373	.010	.05150	.56683
	AY-L	.060167	.079373	.994	-.19750	.31783
AS-L	FBS	.150333	.074833	.492	-.09259	.39326
	LPS	-.018000	.074833	1.000	-.26093	.22493
	PR	.308000*	.091652	.038	.01048	.60552
	PR-L	-.074000	.091652	.991	-.37152	.22352
	AS	.455167*	.079373	.000	.19750	.71283
	AY	.764333*	.091652	.000	.46681	1.06186
	AY-L	.515333*	.091652	.000	.21781	.81286
AY	FBS	-.614000*	.074833	.000	-.85693	-.37107
	LPS	-.782333*	.074833	.000	-1.02526	-.53941
	PR	-.456333*	.091652	.001	-.75386	-.15881
	PR-L	-.838333*	.091652	.000	-1.13586	-.54081
	AS	-.309167*	.079373	.010	-.56683	-.05150
	AS-L	-.764333*	.091652	.000	-1.06186	-.46681
	AY-L	-.249000	.091652	.155	-.54652	.04852
AY-L	FBS	-.365000*	.074833	.001	-.60793	-.12207
	LPS	-.533333*	.074833	.000	-.77626	-.29041
	PR	-.207333	.091652	.345	-.50486	.09019
	PR-L	-.589333*	.091652	.000	-.88686	-.29181
	AS	-.060167	.079373	.994	-.31783	.19750
	AS-L	-.515333*	.091652	.000	-.81286	-.21781
	AY	.249000	.091652	.155	-.04852	.54652

*. The mean difference is significant at the 0.05 level.

Descriptives – Insulin-1 Promoter Activity

	Mean	Std. Deviation	Std. Error	95% Confidence Interval for Mean		Minimum	Maximum
				Lower Bound	Upper Bound		
FBS	1.00000	.000000	.000000	1.00000	1.00000	1.000	1.000
LPS	1.16833	.159129	.053043	1.04602	1.29065	.838	1.358
PR	.84233	.069745	.040267	.66908	1.01559	.763	.894
PR-L	1.22433	.077700	.044860	1.03132	1.41735	1.139	1.291
AS	.69517	.121984	.049800	.56715	.82318	.604	.921
AS-L	1.15033	.152317	.087940	.77196	1.52871	1.004	1.308
AY	.38600	.149790	.086481	.01390	.75810	.278	.557
AY-L	.63500	.016523	.009539	.59396	.67604	.618	.651
Total	.93333	.274046	.043883	.84450	1.02217	.278	1.358

A.8. Statistical Analysis – Syntaxin 1A Promoter Activity (Dual Luciferase)

(I) Treatment	(J) Treatment	Mean Difference (I-J)	Std. Error	Sig.	95% Confidence Interval	
					Lower Bound	Upper Bound
FBS	LPS	.02500	.10021	1.000	-.3096	.3596
	PR	.09750	.10021	.974	-.2371	.4321
	PR-L	.10250	.10021	.966	-.2321	.4371
	AS	.00333	.10824	1.000	-.3581	.3647
	AS-L	-.14000	.10824	.892	-.5014	.2214
	AY	.03750	.10021	1.000	-.2971	.3721
	AY-L	.14750	.10021	.814	-.1871	.4821
LPS	FBS	-.02500	.10021	1.000	-.3596	.3096
	PR	.07250	.10021	.995	-.2621	.4071
	PR-L	.07750	.10021	.993	-.2571	.4121
	AS	-.02167	.10824	1.000	-.3831	.3397
	AS-L	-.16500	.10824	.787	-.5264	.1964
	AY	.01250	.10021	1.000	-.3221	.3471
	AY-L	.12250	.10021	.916	-.2121	.4571
PR	FBS	-.09750	.10021	.974	-.4321	.2371
	LPS	-.07250	.10021	.995	-.4071	.2621
	PR-L	.00500	.10021	1.000	-.3296	.3396
	AS	-.09417	.10824	.986	-.4556	.2672
	AS-L	-.23750	.10824	.392	-.5989	.1239
	AY	-.06000	.10021	.999	-.3946	.2746
	AY-L	.05000	.10021	1.000	-.2846	.3846
PR-L	FBS	-.10250	.10021	.966	-.4371	.2321
	LPS	-.07750	.10021	.993	-.4121	.2571
	PR	-.00500	.10021	1.000	-.3396	.3296
	AS	-.09917	.10824	.981	-.4606	.2622
	AS-L	-.24250	.10824	.367	-.6039	.1189
	AY	-.06500	.10021	.998	-.3996	.2696
	AY-L	.04500	.10021	1.000	-.2896	.3796
AS	FBS	-.00333	.10824	1.000	-.3647	.3581
	LPS	.02167	.10824	1.000	-.3397	.3831
	PR	.09417	.10824	.986	-.2672	.4556
	PR-L	.09917	.10824	.981	-.2622	.4606
	AS-L	-.14333	.11571	.911	-.5297	.2430
	AY	.03417	.10824	1.000	-.3272	.3956

	AY-L	.14417	.10824	.877	-.2172	.5056
AS-L	FBS	.14000	.10824	.892	-.2214	.5014
	LPS	.16500	.10824	.787	-.1964	.5264
	PR	.23750	.10824	.392	-.1239	.5989
	PR-L	.24250	.10824	.367	-.1189	.6039
	AS	.14333	.11571	.911	-.2430	.5297
	AY	.17750	.10824	.723	-.1839	.5389
	AY-L	.28750	.10824	.189	-.0739	.6489
AY	FBS	-.03750	.10021	1.000	-.3721	.2971
	LPS	-.01250	.10021	1.000	-.3471	.3221
	PR	.06000	.10021	.999	-.2746	.3946
	PR-L	.06500	.10021	.998	-.2696	.3996
	AS	-.03417	.10824	1.000	-.3956	.3272
	AS-L	-.17750	.10824	.723	-.5389	.1839
	AY-L	.11000	.10021	.951	-.2246	.4446
AY-L	FBS	-.14750	.10021	.814	-.4821	.1871
	LPS	-.12250	.10021	.916	-.4571	.2121
	PR	-.05000	.10021	1.000	-.3846	.2846
	PR-L	-.04500	.10021	1.000	-.3796	.2896
	AS	-.14417	.10824	.877	-.5056	.2172
	AS-L	-.28750	.10824	.189	-.6489	.0739
	AY	-.11000	.10021	.951	-.4446	.2246

Descriptives – Syntaxn 1A Promoter Activity (Dual Luciferase)

	Mean	Std. Deviation	Std. Error	95% Confidence Interval for Mean		Minimum	Maximum
				Lower Bound	Upper Bound		
FBS	1.0000	.00000	.00000	1.0000	1.0000	1.00	1.00
LPS	.9750	.10247	.05123	.8119	1.1381	.86	1.08
PR	.9025	.06652	.03326	.7967	1.0083	.81	.96
PR-L	.8975	.18804	.09402	.5983	1.1967	.70	1.15
AS	.9967	.14224	.08212	.6433	1.3500	.90	1.16
AS-L	1.1400	.22650	.13077	.5774	1.7026	.90	1.35
AY	.9625	.16091	.08045	.7065	1.2185	.80	1.18
AY-L	.8525	.15305	.07653	.6090	1.0960	.75	1.08
Total	.9590	.14686	.02681	.9042	1.0138	.70	1.35

A.9. Statistical Analysis – SNAP 25 Promoter Activity (Dual Luciferase)

(I) Treatment	(J) Treatment	Mean Difference (I-J)	Std. Error	Sig.	95% Confidence Interval	
					Lower Bound	Upper Bound
FBS	LPS	-.07000	.13047	.999	-.5056	.3656
	PR	.14750	.13047	.943	-.2881	.5831
	PR-L	-.04250	.13047	1.000	-.4781	.3931
	AS	-.09000	.14093	.998	-.5605	.3805
	AS-L	-.07667	.14093	.999	-.5472	.3938
	AY	.00000	.13047	1.000	-.4356	.4356
	AY-L	-.21000	.13047	.740	-.6456	.2256
LPS	FBS	.07000	.13047	.999	-.3656	.5056
	PR	.21750	.13047	.707	-.2181	.6531
	PR-L	.02750	.13047	1.000	-.4081	.4631
	AS	-.02000	.14093	1.000	-.4905	.4505
	AS-L	-.00667	.14093	1.000	-.4772	.4638
	AY	.07000	.13047	.999	-.3656	.5056
	AY-L	-.14000	.13047	.956	-.5756	.2956
PR	FBS	-.14750	.13047	.943	-.5831	.2881
	LPS	-.21750	.13047	.707	-.6531	.2181
	PR-L	-.19000	.13047	.821	-.6256	.2456
	AS	-.23750	.14093	.696	-.7080	.2330
	AS-L	-.22417	.14093	.751	-.6947	.2463
	AY	-.14750	.13047	.943	-.5831	.2881
	AY-L	-.35750	.13047	.163	-.7931	.0781
PR-L	FBS	.04250	.13047	1.000	-.3931	.4781
	LPS	-.02750	.13047	1.000	-.4631	.4081
	PR	.19000	.13047	.821	-.2456	.6256
	AS	-.04750	.14093	1.000	-.5180	.4230
	AS-L	-.03417	.14093	1.000	-.5047	.4363
	AY	.04250	.13047	1.000	-.3931	.4781
	AY-L	-.16750	.13047	.895	-.6031	.2681
AS	FBS	.09000	.14093	.998	-.3805	.5605
	LPS	.02000	.14093	1.000	-.4505	.4905
	PR	.23750	.14093	.696	-.2330	.7080
	PR-L	.04750	.14093	1.000	-.4230	.5180
	AS-L	.01333	.15066	1.000	-.4897	.5163
	AY	.09000	.14093	.998	-.3805	.5605

	AY-L	-.12000	.14093	.988	-.5905	.3505
AS-L	FBS	.07667	.14093	.999	-.3938	.5472
	LPS	.00667	.14093	1.000	-.4638	.4772
	PR	.22417	.14093	.751	-.2463	.6947
	PR-L	.03417	.14093	1.000	-.4363	.5047
	AS	-.01333	.15066	1.000	-.5163	.4897
	AY	.07667	.14093	.999	-.3938	.5472
	AY-L	-.13333	.14093	.977	-.6038	.3372
AY	FBS	.00000	.13047	1.000	-.4356	.4356
	LPS	-.07000	.13047	.999	-.5056	.3656
	PR	.14750	.13047	.943	-.2881	.5831
	PR-L	-.04250	.13047	1.000	-.4781	.3931
	AS	-.09000	.14093	.998	-.5605	.3805
	AS-L	-.07667	.14093	.999	-.5472	.3938
	AY-L	-.21000	.13047	.740	-.6456	.2256
AY-L	FBS	.21000	.13047	.740	-.2256	.6456
	LPS	.14000	.13047	.956	-.2956	.5756
	PR	.35750	.13047	.163	-.0781	.7931
	PR-L	.16750	.13047	.895	-.2681	.6031
	AS	.12000	.14093	.988	-.3505	.5905
	AS-L	.13333	.14093	.977	-.3372	.6038
	AY	.21000	.13047	.740	-.2256	.6456

Descriptives – SNAP 25 Reporter Activity (Dual Luciferase)

	Mean	Std. Deviation	Std. Error	95% Confidence Interval for Mean		Minimum	Maximum
				Lower Bound	Upper Bound		
FBS	1.0000	.00000	.00000	1.0000	1.0000	1.00	1.00
LPS	1.0700	.17493	.08746	.7916	1.3484	.92	1.32
PR	.8525	.04031	.02016	.7884	.9166	.81	.90
PR-L	1.0425	.06994	.03497	.9312	1.1538	.95	1.11
AS	1.0900	.24759	.14295	.4750	1.7050	.90	1.37
AS-L	1.0767	.23352	.13482	.4966	1.6568	.87	1.33
AY	1.0000	.29687	.14844	.5276	1.4724	.75	1.43
AY-L	1.2100	.21726	.10863	.8643	1.5557	.89	1.37
Total	1.0400	.18875	.03446	.9695	1.1105	.75	1.43

A.10. Statistical Analysis – KCNJ11 Promoter Activity (Dual Luciferase)

(I) Treatment	(J) Treatment	Mean Difference (I-J)	Std. Error	Sig.	95% Confidence Interval	
					Lower Bound	Upper Bound
FBS	LPS	-.14000	.15083	.980	-.6436	.3636
	PR	-.14000	.15083	.980	-.6436	.3636
	PR-L	-.15750	.15083	.962	-.6611	.3461
	AS	-.96000*	.16292	.000	-1.5039	-.4161
	AS-L	-.55667*	.16292	.042	-1.1006	-.0127
	AY	.05000	.15083	1.000	-.4536	.5536
	AY-L	.11250	.15083	.994	-.3911	.6161
LPS	FBS	.14000	.15083	.980	-.3636	.6436
	PR	.00000	.15083	1.000	-.5036	.5036
	PR-L	-.01750	.15083	1.000	-.5211	.4861
	AS	-.82000*	.16292	.001	-1.3639	-.2761
	AS-L	-.41667	.16292	.224	-.9606	.1273
	AY	.19000	.15083	.904	-.3136	.6936
	AY-L	.25250	.15083	.703	-.2511	.7561
PR	FBS	.14000	.15083	.980	-.3636	.6436
	LPS	.00000	.15083	1.000	-.5036	.5036
	PR-L	-.01750	.15083	1.000	-.5211	.4861
	AS	-.82000*	.16292	.001	-1.3639	-.2761
	AS-L	-.41667	.16292	.224	-.9606	.1273
	AY	.19000	.15083	.904	-.3136	.6936
	AY-L	.25250	.15083	.703	-.2511	.7561
PR-L	FBS	.15750	.15083	.962	-.3461	.6611
	LPS	.01750	.15083	1.000	-.4861	.5211
	PR	.01750	.15083	1.000	-.4861	.5211
	AS	-.80250*	.16292	.001	-1.3464	-.2586
	AS-L	-.39917	.16292	.267	-.9431	.1448
	AY	.20750	.15083	.859	-.2961	.7111
	AY-L	.27000	.15083	.633	-.2336	.7736
AS	FBS	.96000*	.16292	.000	.4161	1.5039
	LPS	.82000*	.16292	.001	.2761	1.3639
	PR	.82000*	.16292	.001	.2761	1.3639
	PR-L	.80250*	.16292	.001	.2586	1.3464
	AS-L	.40333	.17417	.329	-.1782	.9848
	AY	1.01000*	.16292	.000	.4661	1.5539

	AY-L	1.07250*	.16292	.000	.5286	1.6164
AS-L	FBS	.55667*	.16292	.042	.0127	1.1006
	LPS	.41667	.16292	.224	-.1273	.9606
	PR	.41667	.16292	.224	-.1273	.9606
	PR-L	.39917	.16292	.267	-.1448	.9431
	AS	-.40333	.17417	.329	-.9848	.1782
	AY	.60667*	.16292	.022	.0627	1.1506
	AY-L	.66917*	.16292	.009	.1252	1.2131
AY	FBS	-.05000	.15083	1.000	-.5536	.4536
	LPS	-.19000	.15083	.904	-.6936	.3136
	PR	-.19000	.15083	.904	-.6936	.3136
	PR-L	-.20750	.15083	.859	-.7111	.2961
	AS	-1.01000*	.16292	.000	-1.5539	-.4661
	AS-L	-.60667*	.16292	.022	-1.1506	-.0627
	AY-L	.06250	.15083	1.000	-.4411	.5661
AY-L	FBS	-.11250	.15083	.994	-.6161	.3911
	LPS	-.25250	.15083	.703	-.7561	.2511
	PR	-.25250	.15083	.703	-.7561	.2511
	PR-L	-.27000	.15083	.633	-.7736	.2336
	AS	-1.07250*	.16292	.000	-1.6164	-.5286
	AS-L	-.66917*	.16292	.009	-1.2131	-.1252
	AY	-.06250	.15083	1.000	-.5661	.4411

*. The mean difference is significant at the 0.05 level.

Descriptives – KCNJ11 Promoter Activity (Dual Luciferase)

	Mean	Std. Deviation	Std. Error	95% Confidence Interval for Mean		Minimum	Maximum
				Lower Bound	Upper Bound		
FBS	1.0000	.00000	.00000	1.0000	1.0000	1.00	1.00
LPS	1.1400	.09345	.04673	.9913	1.2887	1.00	1.19
PR	1.1400	.02944	.01472	1.0932	1.1868	1.10	1.17
PR-L	1.1575	.10372	.05186	.9925	1.3225	1.07	1.29
AS	1.9600	.52915	.30551	.6455	3.2745	1.36	2.36
AS-L	1.5567	.41356	.23877	.5293	2.5840	1.20	2.01
AY	.9500	.04320	.02160	.8813	1.0187	.91	1.01
AY-L	.8875	.10372	.05186	.7225	1.0525	.81	1.04
Total	1.1883	.36897	.06736	1.0506	1.3261	.81	2.36

A.11. Statistical Analysis – K_V2.1 Densitometry Analysis

Multiple Comparisons – K_V2.1 Immunoblot Results						
(I) Treatment	(J) Treatment	Mean Difference (I-J)	Std. Error	Sig.	95% Confidence Interval	
					Lower Bound	Upper Bound
FBS	LPS	-1.18626	.46227	.225	-2.7447	.3721
	PR	.08925	.46227	1.000	-1.4692	1.6477
	PR-L	-.66617	.46227	.828	-2.2246	.8922
	AS	-.83989	.49931	.698	-2.5232	.8434
	AS-L	-.82755	.49931	.712	-2.5108	.8557
	AY	-.58265	.49931	.932	-2.2659	1.1006
	AY-L	-.30400	.49931	.998	-1.9873	1.3793
LPS	FBS	1.18626	.46227	.225	-.3721	2.7447
	PR	1.27551	.46227	.162	-.2829	2.8339
	PR-L	.52009	.46227	.943	-1.0383	2.0785
	AS	.34638	.49931	.996	-1.3369	2.0297
	AS-L	.35871	.49931	.995	-1.3246	2.0420
	AY	.60361	.49931	.920	-1.0797	2.2869
	AY-L	.88226	.49931	.647	-.8010	2.5655
PR	FBS	-.08925	.46227	1.000	-1.6477	1.4692
	LPS	-1.27551	.46227	.162	-2.8339	.2829
	PR-L	-.75542	.46227	.726	-2.3138	.8030
	AS	-.92913	.49931	.590	-2.6124	.7541
	AS-L	-.91680	.49931	.605	-2.6001	.7665
	AY	-.67190	.49931	.870	-2.3552	1.0114
	AY-L	-.39325	.49931	.992	-2.0765	1.2900
PR-L	FBS	.66617	.46227	.828	-.8922	2.2246
	LPS	-.52009	.46227	.943	-2.0785	1.0383
	PR	.75542	.46227	.726	-.8030	2.3138
	AS	-.17371	.49931	1.000	-1.8570	1.5096
	AS-L	-.16138	.49931	1.000	-1.8447	1.5219
	AY	.08352	.49931	1.000	-1.5998	1.7668
	AY-L	.36217	.49931	.995	-1.3211	2.0454
AS	FBS	.83989	.49931	.698	-.8434	2.5232
	LPS	-.34638	.49931	.996	-2.0297	1.3369
	PR	.92913	.49931	.590	-.7541	2.6124
	PR-L	.17371	.49931	1.000	-1.5096	1.8570

	AS-L	.01233	.53379	1.000	-1.7872	1.8118
	AY	.25723	.53379	1.000	-1.5423	2.0567
	AY-L	.53588	.53379	.968	-1.2636	2.3354
AS-L	FBS	.82755	.49931	.712	-.8557	2.5108
	LPS	-.35871	.49931	.995	-2.0420	1.3246
	PR	.91680	.49931	.605	-.7665	2.6001
	PR-L	.16138	.49931	1.000	-1.5219	1.8447
	AS	-.01233	.53379	1.000	-1.8118	1.7872
	AY	.24490	.53379	1.000	-1.5546	2.0444
	AY-L	.52355	.53379	.972	-1.2759	2.3230
AY	FBS	.58265	.49931	.932	-1.1006	2.2659
	LPS	-.60361	.49931	.920	-2.2869	1.0797
	PR	.67190	.49931	.870	-1.0114	2.3552
	PR-L	-.08352	.49931	1.000	-1.7668	1.5998
	AS	-.25723	.53379	1.000	-2.0567	1.5423
	AS-L	-.24490	.53379	1.000	-2.0444	1.5546
	AY-L	.27865	.53379	.999	-1.5209	2.0781
AY-L	FBS	.30400	.49931	.998	-1.3793	1.9873
	LPS	-.88226	.49931	.647	-2.5655	.8010
	PR	.39325	.49931	.992	-1.2900	2.0765
	PR-L	-.36217	.49931	.995	-2.0454	1.3211
	AS	-.53588	.53379	.968	-2.3354	1.2636
	AS-L	-.52355	.53379	.972	-2.3230	1.2759
	AY	-.27865	.53379	.999	-2.0781	1.5209

A.12. Statistical Analysis – $Ca_V1.2$ Densitometry Analysis

Multiple Comparisons – $Ca_v1.2$ Immunoblot Results						
(I) Treatment	(J) Treatment	Mean Difference (I-J)	Std. Error	Sig.	95% Confidence Interval	
					Lower Bound	Upper Bound
FBS	LPS	-2.00910*	.39613	.001	-3.3445	-.6737
	PR	-.26765	.39613	.997	-1.6031	1.0678
	PR-L	-.94000	.39613	.306	-2.2754	.3954

	AS	-.66904	.42787	.765	-2.1115	.7734
	AS-L	-.83764	.42787	.531	-2.2801	.6048
	AY	-1.78233*	.42787	.009	-3.2248	-.3399
	AY-L	-1.08091	.42787	.240	-2.5233	.3615
LPS	FBS	2.00910*	.39613	.001	.6737	3.3445
	PR	1.74145*	.39613	.006	.4060	3.0769
	PR-L	1.06910	.39613	.180	-.2663	2.4045
	AS	1.34006	.42787	.081	-.1024	2.7825
	AS-L	1.17146	.42787	.168	-.2710	2.6139
	AY	.22676	.42787	.999	-1.2157	1.6692
	AY-L	.92819	.42787	.409	-.5142	2.3706
PR	FBS	.26765	.39613	.997	-1.0678	1.6031
	LPS	-1.74145*	.39613	.006	-3.0769	-.4060
	PR-L	-.67235	.39613	.689	-2.0078	.6631
	AS	-.40139	.42787	.978	-1.8438	1.0410
	AS-L	-.56999	.42787	.876	-2.0124	.8724
	AY	-1.51468*	.42787	.035	-2.9571	-.0722
	AY-L	-.81326	.42787	.566	-2.2557	.6292
PR-L	FBS	.94000	.39613	.306	-.3954	2.2754
	LPS	-1.06910	.39613	.180	-2.4045	.2663
	PR	.67235	.39613	.689	-.6631	2.0078
	AS	.27096	.42787	.998	-1.1715	1.7134
	AS-L	.10237	.42787	1.000	-1.3401	1.5448
	AY	-.84233	.42787	.524	-2.2848	.6001
	AY-L	-.14091	.42787	1.000	-1.5833	1.3015
AS	FBS	.66904	.42787	.765	-.7734	2.1115
	LPS	-1.34006	.42787	.081	-2.7825	.1024
	PR	.40139	.42787	.978	-1.0410	1.8438
	PR-L	-.27096	.42787	.998	-1.7134	1.1715
	AS-L	-.16860	.45741	1.000	-1.7106	1.3734
	AY	-1.11329	.45741	.278	-2.6553	.4287
	AY-L	-.41187	.45741	.983	-1.9539	1.1302
AS-L	FBS	.83764	.42787	.531	-.6048	2.2801
	LPS	-1.17146	.42787	.168	-2.6139	.2710
	PR	.56999	.42787	.876	-.8724	2.0124
	PR-L	-.10237	.42787	1.000	-1.5448	1.3401
	AS	.16860	.45741	1.000	-1.3734	1.7106
	AY	-.94470	.45741	.467	-2.4867	.5973
	AY-L	-.24328	.45741	.999	-1.7853	1.2988

AY	FBS	1.78233*	.42787	.009	.3399	3.2248
	LPS	-.22676	.42787	.999	-1.6692	1.2157
	PR	1.51468*	.42787	.035	.0722	2.9571
	PR-L	.84233	.42787	.524	-.6001	2.2848
	AS	1.11329	.45741	.278	-.4287	2.6553
	AS-L	.94470	.45741	.467	-.5973	2.4867
	AY-L	.70142	.45741	.781	-.8406	2.2434
AY-L	FBS	1.08091	.42787	.240	-.3615	2.5233
	LPS	-.92819	.42787	.409	-2.3706	.5142
	PR	.81326	.42787	.566	-.6292	2.2557
	PR-L	.14091	.42787	1.000	-1.3015	1.5833
	AS	.41187	.45741	.983	-1.1302	1.9539
	AS-L	.24328	.45741	.999	-1.2988	1.7853
	AY	-.70142	.45741	.781	-2.2434	.8406
*. The mean difference is significant at the 0.05 level.						

A.13. RT-PCR Array Gene List

Gene Symbol	***Alias***	***Refseq #***	***Official Full Name***
Slc2a2	AI266973/Glut-2/Glut2	NM_031197	Solute carrier family 2 (facilitated glucose transporter), member 2
Kcnb1	Kcr1-1/Kv2.1/Shab	NM_008420	Potassium voltage gated channel, Shab-related subfamily, member 1
Abcc8	D930031B21Rik/SUR1/Sur	NM_011510	ATP-binding cassette, sub-family C (CFTR/MRP), member 8
Cacna1c	Cav1.2/Cchl1a1	NM_009781	Calcium channel, voltage-dependent, L type, alpha 1C subunit
Cacna1d	8430418G19Rik/C79217/Cacnl 1a2/Cchl1a/Cchl1a2/D-LTCC	NM_028981	Calcium channel, voltage-dependent, L type, alpha 1D subunit
Kcnj11	Kir6.2/mBIR	NM_010602	Potassium inwardly rectifying channel, subfamily J, member 11
Ins1	Ins-1/Ins2-rs1	NM_008386	Insulin I
Ins2	AA986540/Ins-2/InsII/Mody/Mody4/proinsulin	NM_008387	Insulin II
Hmgcr	HMG-CoAR/MGC103269/Red	NM_008255	3-hydroxy-3-methylglutaryl-Coenzyme A reductase
Dhcr7	AA409147	NM_007856	7-dehydrocholesterol reductase
Fdft1	SQS/SS	NM_010191	Farnesyl diphosphate farnesyl transferase 1
Stx1a	HPC-1	NM_016801	Syntaxin 1A (brain)
Stx4a	Stx4/Syn-4/Syn4	NM_009294	Syntaxin 4A (placental)
Snap25	Bdr/SNAP-25/sp	NM_011428	Synaptosomal-associated protein 25
Snap23	23kDa/AA408749/SNAP-23/Sndt/Syndet	NM_009222	Synaptosomal-associated protein 23
Vamp1	Syb-1/Syb1/VAMP-1/lew	NM_009496	Vesicle-associated membrane protein 1
Vamp2	Syb-2/Syb2/sybII	NM_009497	Vesicle-associated membrane protein 2
Abca1	Abc1	NM_013454	ATP-binding cassette, sub-family A (ABC1), member 1
Ldlr	Hlb301	NM_010700	Low density lipoprotein receptor
Ghrl	2210006E23Rik/MTLRP/MTLR PAP/m46	NM_021488	Ghrelin
Mboat4	GOAT/Gm171	NM_001126314	Membrane bound O-acyltransferase domain containing

			4
Gapdh	Gapd/MGC102544/MGC102546/MGC103190/MGC103191/MGC105239	NM_008084	Glyceraldehyde-3-phosphate dehydrogenase
RTC	RTC	SA_00104	Reverse Transcription Control
PPC	PPC	SA_00103	Positive PCR Control